Journal of Immunology Research

Targeting Innate Immune Cells for Immunotherapy

Guest Editors: Leandro J. Carreño, Pablo González, Rafael Prados-Rosales, Mercedes López, and Andrés Baena

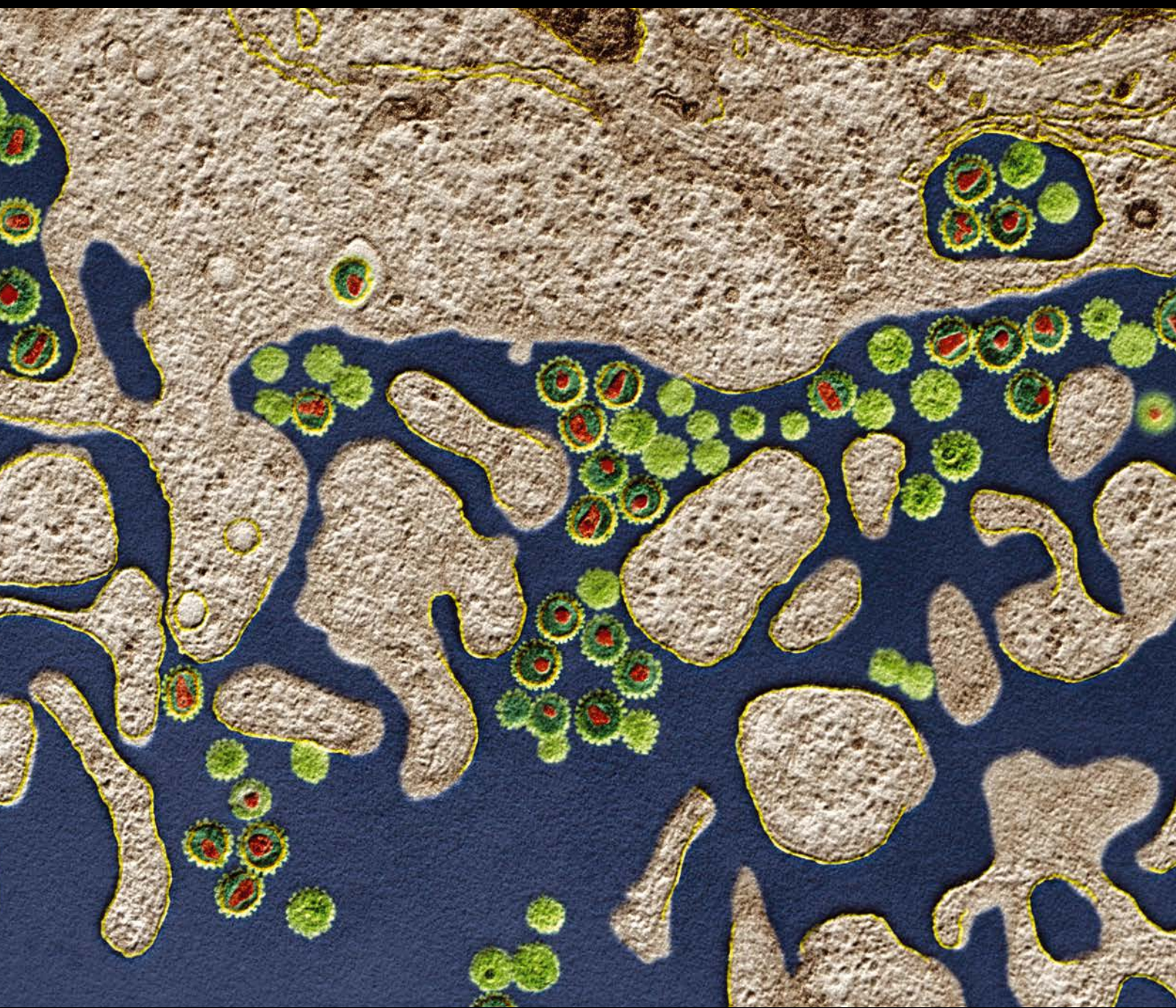

Targeting Innate Immune Cells for Immunotherapy

Journal of Immunology Research

Targeting Innate Immune Cells for Immunotherapy

Guest Editors: Leandro J. Carreño, Rafael Prados-Rosales, Mercedes López, Andrés Baena, and Pablo González

Editorial Board

Contents

Hindawi
Journal of Immunology Research
Volume 2017, Article ID 4271384, 2 pages
https://doi.org/10.1155/2017/4271384

Editorial

Targeting Innate Immune Cells for Immunotherapy

Leandro J. Carreño,[1,2] Rafael Prados-Rosales,[3] Mercedes López,[1,2] Andrés Baena,[4] and Pablo A. González[1,5]

[1]*Millennium Institute on Immunology and Immunotherapy, Santiago, Chile*
[2]*Programa de Inmunología, Instituto de Ciencias Biomédicas, Facultad de Medicina, Universidad de Chile, Santiago, Chile*
[3]*Centro de Investigaciones Cooperativas en Biociencias (CIC bioGUNE), Bilbao, Spain*
[4]*Departamento de Microbiología y Parasitología, Facultad de Medicina, Universidad de Antioquia, Medellín, Colombia*
[5]*Departamento de Genética Molecular y Microbiología, Facultad de Ciencias Biológicas, Pontificia Universidad Católica de Chile, Santiago, Chile*

Correspondence should be addressed to Leandro J. Carreño; leandrocarreno@u.uchile.cl

Received 27 February 2017; Accepted 28 February 2017; Published 5 April 2017

One of the most effective ways to modulate either positively or negatively host immune responses (i.e., to treat cancer and autoimmunity, resp.) is to target effector immune cells, such as B cells, $CD4^+$, and $CD8^+$ T cells, as well as professional antigen-presenting cells, such as dendritic cells (DCs), that promote the activation of the latter two. Frequently, this modulation is aimed at targeting the initiation of the T cell immune response, a process known as T cell priming, which affects not only T cell outcome but also B cell responses that are influenced by the help of $CD4^+$ T cells. At present, several strategies include the optimization of adjuvants and drugs to manipulate the phenotype and function of DCs, frequently with their ex vivo drug treatment and their reintroduction into the host, activating/inhibiting ligands that interact with T cell activation, differentiation, and function. Another strategy consists in ex vivo T cell expansion and reinjection into the host, among others. Although these immunomodulating strategies have shown relatively high success in the clinic with promising therapeutic potential, there are many other strategies that target different immune cell types, especially those associated with the innate immune system, that play crucial roles in immunomodulation. Moreover, it has been evidenced during recent years that cells of the innate immune system can modulate and dictate the inflammatory environment that will take place during T cell priming. Cells of the innate immune system are key players not only at initiating and regulating adaptive immune responses, such as those elicited against pathogens and cancer, but also at modulating tolerance to autoantigens to prevent autoimmune diseases. While some of these cells are considered exclusively innate, as natural killer (NK) cells and innate lymphoid cells (ILCs), others are positioned at the interface of innate and adaptive immune responses, such as DCs, macrophages, monocytes, and natural killer T (NKT) cells. The role of these cells in different immune responses has led to the design of targeted immunotherapies aimed at controlling diseases, such as cancer, autoimmunity, and allergy, as well as potentiating immune responses against pathogens. In this special issue, original studies and review articles are encompassed together to highlight recent discoveries on immunotherapy involving innate immune cells to combat cancer and pathogens.

In the area of cancer immunotherapy, R. Yi et al. analyze how innate immune cell-based immunotherapy combined with classical therapies can improve the outcome of castration-resistant prostate cancer. They perform a meta-analysis aimed at studying the efficacy of the immunotherapeutic vaccine sipuleucel-T combined with regular treatments directed to the androgen receptor (AR). Sipuleucel-T is a cellular immunotherapy which consists in autologous peripheral blood mononuclear cells (PBMCs) incubated with recombinant specific prostatic antigens fused with granulocyte-macrophage colony-stimulating factor. They described that this immunotherapy greatly improved the efficacy of the traditional therapy. Also aiming at cancer, P. G. Lokhov and

E. E. Balashova investigate the efficacy of targeting tumor vasculature antigens and their efficacy against cancer growth. They describe the novel composition called SANTAVAC (Set of All Natural Target Antigens for Vaccination Against Cancer) and their use against tumoral microvasculature. Finally, I. Knippertz et al. used a combined promoter system of adenoviral vectors in order to induce maturation changes in DCs. By targeting the active expression of heat shock factor (mHSF), they induced maturation of human DCs, with a concomitant increase in the expression of proinflammatory cytokines and costimulatory molecules. This approach, combined with specific antigens, could be useful not only in cancer immunotherapy but also in improving immunity against pathogens.

In the area of pathogen immunotherapy, X. Yu et al. constructed a bispecific antibody with the ability to interact with HIV and HIV-infected cells in one direction and with CD89 in the other. This led to the targeting of neutrophils and polymorphic mononuclear cells (PMNs) and resulted in optimal anti-HIV activity. Although this strategy has been described before, in the current work, the authors solved structural limitations of the previous bispecific antibodies, describing two novel structural-modified antibodies that show excellent activity at inhibiting HIV infection and mobilizing innate immune cells. Finally, S. Schülke et al. investigate the adjuvant potential of monophosphoryl lipid A (MPLA) when chemically coupled with protein antigens, using ovalbumin (OVA) as an example. They described that the coupled protein-adjuvant composition is not suitable for allergy treatment, but likely appropriate for other diseases, such as pathogen infections.

Taken together these articles represent novel advances in the field of innate cell-based immunotherapy for cancer and pathogen immunity and may be considered for future clinical studies. Altogether, we are certain that we will see an important increase in the numbers of studies focusing on innate immune cells for immunotherapy in the near future, as these approaches are showing promising results against important diseases.

Acknowledgments

This study is funded by Fondecyt Grant nos. 1160336 and 1140011.

Leandro J. Carreño
Rafael Prados-Rosales
Mercedes López
Andrés Baena
Pablo A. González

Hindawi Publishing Corporation
Journal of Immunology Research
Volume 2016, Article ID 4543861, 10 pages
http://dx.doi.org/10.1155/2016/4543861

Review Article

Sipuleucel-T and Androgen Receptor-Directed Therapy for Castration-Resistant Prostate Cancer: A Meta-Analysis

Renliang Yi,[1] Baoxin Chen,[2] Peng Duan,[2] Chanjiao Zheng,[2] Huanyu Shen,[2] Qun Liu,[2] Chen Yuan,[2] Weilin Ou,[2] and Zhiheng Zhou[3]

[1]*Guangzhou Hospital of Guangzhou Military Region, Guangzhou, China*
[2]*School of Public Health, Guangzhou Medical University, Guangzhou, China*
[3]*Department of Surgery, Massachusetts General Hospital, Harvard Medical School, Boston, MA, USA*

Correspondence should be addressed to Zhiheng Zhou; zhihengz@163.com

Received 11 March 2016; Revised 28 August 2016; Accepted 18 September 2016

Academic Editor: Leandro J. Carreño

New treatments, such as sipuleucel-T and androgen receptor- (AR-) directed therapies (enzalutamide (Enz) and abiraterone acetate (AA)), have emerged and been approved for the management of castration-resistant prostate cancer (CRPC). There are still debates over their efficacy and clinical benefits. This meta-analysis aimed to investigate the efficacy and safety of sipuleucel-T and AR-directed therapies in patients with CRPC. RevMan 5.1 was used for pooled analysis and analysis of publication bias. Seven studies were included in the meta-analysis, with three studies in sipuleucel-T (totally 737 patients, 488 patients in treatment group, and 249 patients in placebo group) and four in AR-directed therapies (totally 5,199 patients, 3,015 patients in treatment group, and 2,184 patients in placebo group). Treatment with sipuleucel-T significantly improved overall survival in patients with CRPC and was not associated with increased risk of adverse event of grade ≥3 ($p > 0.05$). However, treatment with sipuleucel-T did not improve time-to-progression and reduction of prostate-specific antigen (PSA) level ≥50% was not significantly different from that with placebo. AR-directed therapies significantly improved overall survival in patients with CRPC and improved time-to-progression and reduction of PSA level ≥50%. AR-directed therapies did not increase risk of adverse event of grade ≥3 ($p > 0.05$).

1. Introduction

Prostate cancer is one of the most frequently diagnosed cancers in men. Worldwide, in 2015, it is the second most common newly diagnosed cancer and the fourth most common cause of cancer death in men. In the United States, incidence and mortality of prostate cancer ranked first and second, respectively, in men. Over the past few years, incidence of prostate cancer increased steadily, with slowly increased mortality [1–3]. Current treatments for prostate cancer include surgical and medically induced castration and androgen deprivation therapy (ADT) using androgen receptor (AR) antagonists [4]. Despite these treatments, a sizable number of patients will eventually experience disease recurrence and progression [5]. Castrate-resistant prostate cancer (CRPC) is defined as disease progression despite ADT and may present a spectrum of disease ranging from rising prostate-specific antigen (PSA) levels, progression of preexisting disease, or appearance of new metastases [6–8]. CRPC poses a great challenge in the management of prostate cancer.

Docetaxel, approved by the US Food and Drug Administration (FDA) in 2004, is a taxane drug that induces polymerization of microtubules and phosphorylation of Bcl-2 protein. Three weeks of combined docetaxel and prednisone is currently considered the standard of first-line chemotherapy for men with CRPC [9]. The second-line chemotherapy with cabazitaxel has been shown to increased survival time in patients with CRPC. However, severe adverse events have been reported for these treatments [10, 11]. With advances in the understanding of disease pathophysiology, new treatments for CRPC emerge in the recent years that aim to improve both survival and quality-of-life of patients [12]. These treatments include cancer immunotherapy such as sipuleucel-T, AR-directed therapies such as abiraterone

acetate (AA) and enzalutamide (Enz), radium-223, and PROSTVAC [13–18]. Radium-223 is mainly used to manage bone metastases in CRPC [19]. Trials of immunotherapy of PROSTVAC which utilizes recombinant poxviruses to express PSA are ongoing [20]. Phase III clinical trials have been conducted for sipuleucel-T, AA, and Enz and FDA has approved their use in patients with CRPC [21–23]. These new treatments hold great potential as the first-line treatments for patients with CRPC. Finding the optimal regimen is now the major clinical challenge. This meta-analysis aimed to investigate and compare the efficacy and safety of these two treatments and to provide scientific evidence for the management of CRPC.

AA is a steroidal antiandrogen that exerts its effect through inhibiting CYP17A and it also acts as an antagonist of AR [24, 25]. Clinical trials showed significantly improved survival for treatment with AA compared with placebo. It was approved by the FDA in 2011 for patients with CRPC. Enz is a synthetic nonsteroidal pure antiandrogen. It has a strong binding affinity for AR and in addition prevents binding of AR to deoxyribonucleic acid and AR to coactivator proteins [26]. It was approved by the FDA in 2012 for patients with CRPC.

Sipuleucel-T (PROVENGE®) is an autologous vaccine. The antigen presenting cells (APCs) are harvested from individual patient's peripheral blood and later incubated with recombinant fusion protein antigen, which contains both prostatic acid phosphatase and granulocyte-macrophage colony-stimulating factor [27, 28]. This process activates the APCs, which are critical for priming a cytotoxic T-lymphocyte-mediated immune response [27]. These activated APCs are then reinfused into the individual patient. In 2010, sipuleucel-T became the first immune-therapeutic agent approved by the FDA for patients with CRPC, based on consistent observed improvement in overall survival.

This meta-analysis aimed to further determine the clinical efficacy and safety of these two types of treatments, namely, sipuleucel-T and AR-directed therapies (AA and Enz), in the management of CRPC. Survival and disease progression were assessed by overall survival (OS) and time-to-progression (TTP) [29], respectively. Biological endpoint was assessed as a ≥50% reduction of PSA level. Adverse events of grade ≥3 were also reviewed.

2. Methods

2.1. Literature Search and Study Selection. We systematically searched seven literature databases (OVID, Springer, PubMed, Web of Science, ScienceDirect, Medline, and Cochrane Library) from 1966 to October 2015 for all relevant articles by entering terms including "castrate-resistant prostate cancer", "sipuleucel-T", "enzalutamide", and "abiraterone acetate" as key words, title, subject heading, and text word. We also searched for potentially missed articles from the reference list of retrieved articles and from previous narrative reviews on this topic.

Studies were included if they met the following criteria: (1) randomized double-blind place-controlled clinical trials of sipuleucel-T, AA, and Enz presenting original data; (2) patients with CRPC; (3) English articles published before October 2015. In case of duplicated reports, the article presenting the latest and the most comprehensive data on the largest cohorts was selected. Studies were excluded if (1) they were duplicated reports, were of poor quality, were lacking original data, or presented incomplete data; (2) they were review articles, conference abstracts, or commentary. Two authors (Renliang Yi and Baoxin Chen) conducted literature search and study selection independently. Results were compared and discrepancies were resolved by a discussion with another author (Peng Duan).

2.2. Quality Assessment. Full text of articles that fulfilled inclusion and exclusion criteria were retrieved for review. Quality of the included articles was assessed using the Newcastle-Ottawa Scale (NOS) [30], in which a study is judged on three broad perspectives: the selection of the study groups (adequate definition of the cases, representativeness of the cases, selection of controls, and definition of controls), the comparability of the groups (compatibility of cases and controls), and the ascertainment of the outcome of interest (ascertainment of exposure, ascertainment of cases and controls, and nonresponse rate). Total score of NOS is nine, with higher score indicating higher quality. Two authors (Qun Liu and Chen Yuan) conducted quality assessment independently. Results were compared and discrepancies were resolved by a discussion with another author (Weilin Ou).

2.3. Data Extraction. The following outcomes were extracted from each study: OS, TTP, reduction of PSA level ≥50%, and adverse events of grade ≥3. Two authors (Chanjiao Zheng and Huanyu Shen) conducted data extraction independently. Results were compared and discrepancies were resolved by a discussion with corresponding author (Zhiheng Zhou).

2.4. Data Synthesis and Analysis. Review Manager 5.1 software was used for data synthesis and analysis. The hazard ratio (HR) with 95% confidence interval (CI) was calculated for dichotomized data. Quantitative data were expressed as weighted mean difference (WMD) with 95% CI. Heterogeneity analysis was performed using q test with $p > 0.1$ and $I^2 < 50\%$ suggesting homogeneity among studies. For data without significant heterogeneity, fixed-effect models were used for pooled analyses. In case of significant heterogeneity, sensitivity analysis was performed by excluding the study with the highest variance. In the case that no definite cause was found for heterogeneity, random-effect model was used for pooled analyses. The significance of pooled data was further tested and a $p < 0.05$ was considered statistically significant. When enough studies were included, funnel plot was delineated and the publication bias was evaluated.

3. Results

3.1. Study Selection. Our search resulted in 571 articles. A total of 302 articles were excluded after reviewing titles and abstracts, and 80 articles were excluded due to duplicated reports. A total of 182 articles were further excluded after full-text review. Exclusion reasons included review articles

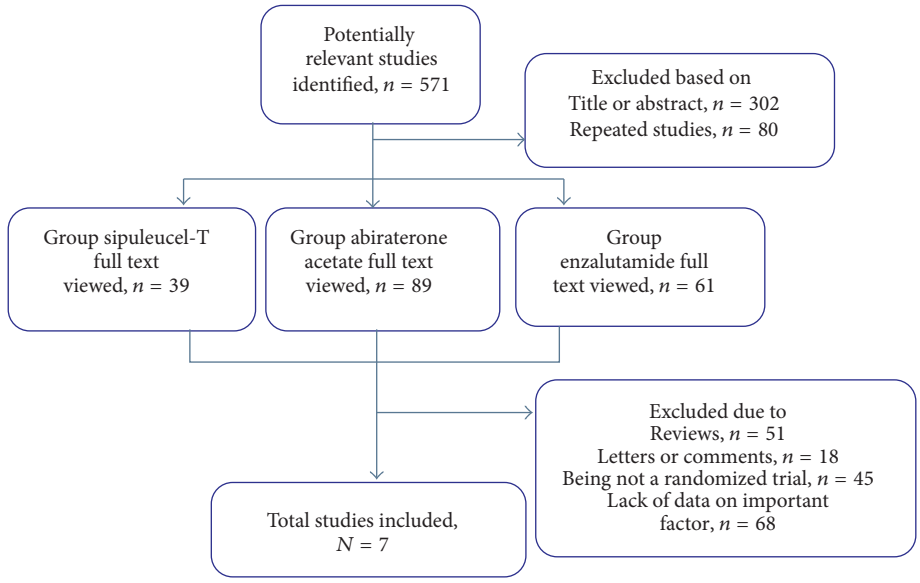

Figure 1: Flow chart of study selection. The summary of the study selection process was shown by flow chart.

Table 1: Quality indicators by Newcastle-Ottawa Scale.

Studies	Selection				Comparability		Exposure			Score
	(1)	(2)	(3)	(4)	(5A)	(5B)	(6)	(7)	(8)	
Beer and Tombal, 2014	Yes	Yes	Yes	Yes	No	Yes	Yes	Yes	Yes	8
Fizazi et al., 2012	Yes	Yes	Yes	Yes	Yes	Yes	Yes	Yes	Yes	9
Higano et al., 2009	Yes	Yes	Yes	Yes	No	Yes	Yes	Yes	Yes	8
Kantoff et al., 2010	Yes	Yes	Yes	Yes	Yes	Yes	Yes	Yes	Yes	9
Rathkopf et al., 2014	Yes	Yes	Yes	Yes	Yes	Yes	Yes	Yes	Yes	9
Scher et al., 2012	Yes	Yes	Yes	Yes	No	Yes	Yes	Yes	Yes	8
Small et al., 2006	Yes	Yes	Yes	Yes	No	Yes	Yes	Yes	Yes	8

(1): case independent validation; (2): representativeness of the cases; (3): community or hospital controls; (4): history of disease; (5A): study controls for the most important factor; (5B): study controls for any additional factor; (6): ascertainment of exposure; (7): was follow-up long enough for outcomes to occur? (8): adequacy of follow-up of cohorts.

and commentary, correspondence, nonrandomized placebo-controlled trials, and lack of complete study outcomes. Seven articles were included for the meta-analysis: three articles on sipuleucel-T, two on AA, and two on Enz, respectively. Figure 1 shows the flow of literature search and study selection.

3.2. Study Characteristics. All seven studies were randomized, double-blind, placebo-controlled clinical trials. Results of quality assessment using NOS for the seven studies are showed in Table 1. The seven studies included a total of 5,936 patients with CRPC. Table 2 shows the main characteristics of the included studies. Regimens used in these studies were as follows: (1) sipuleucel-T: patients were randomly assigned in a 2 : 1 ratio to receive either sipuleucel-T or placebo every two weeks, for a total of three infusions; (2) AA: intervention group received combined AA 1000 mg and prednisone 10 mg daily and placebo group received prednisone 10 mg daily plus placebo; (3) Enz: intervention group received Enz 60 mg daily and placebo group received placebo.

3.3. Overall Survival (OS). All seven studies provided data on survival with follow-up period up to 36 months [29, 31–36]. Analyses of OS were performed in 5,936 patients, with 737 patients for sipuleucel-T (intervention group versus placebo group: 488 versus 249 patients) and 5,199 patients for AR-directed therapies (intervention group versus placebo group: 3,015 versus 2,184 patients). Figure 2 shows the forest plot of analysis of OS. Results showed that, compared with placebo, both sipuleucel-T and AR-directed therapies significantly improved survival of patient with CRPC. Pooled HR for OS was 0.73 for sipuleucel-T (95% CI: 0.61–0.88; $Z = 3.31$; $p < 0.001$) and 0.72 for AR-directed therapies (95% CI: 0.66–0.78; $Z = 7.94$; $p < 0.00001$). Tests for heterogeneity showed insignificant results, indicating homogeneity among studies (both $p > 0.1$ and both $I^2 < 50\%$).

3.4. Time-to-Progression (TTP). Six studies with a total of 5,936 patients reported TTP [29, 31–35], including 737 patients for sipuleucel-T (intervention group versus placebo

Table 2: Main characteristics of included studies.

Study	N	Patients	Design	Interventions	Primary endpoint
Small et al., 2006	127	CRPC	Randomized, double-blind, placebo-controlled	Sipuleucel-T, placebo	OS, TTP, reduction of PSA > 50%, AEs grade ≥ 3
Higano et al., 2009	98	CRPC	Randomized, double-blind, placebo-controlled	Sipuleucel-T, placebo	
Kantoff et al., 2010	512	CRPC	Randomized, double-blind, placebo-controlled	Sipuleucel-T, placebo	
Fizazi et al., 2012	1195	CRPC	Randomized, double-blind, placebo-controlled	Abiraterone acetate, placebo	
Rathkopf et al., 2014	1088	CRPC	Randomized, double-blind, placebo-controlled	Abiraterone acetate, placebo	
Scher et al., 2012	1199	CRPC	Randomized, double-blind, placebo-controlled	Enzalutamide, placebo	
Beer and Tombal, 2014	1717	CRPC	Randomized, double-blind, placebo-controlled	Enzalutamide, placebo	

CRPC: castration-resistant prostate cancer; OS: overall survival; TTP: time-to-progression; PSA: prostate-specific antigen; AEs: adverse events.

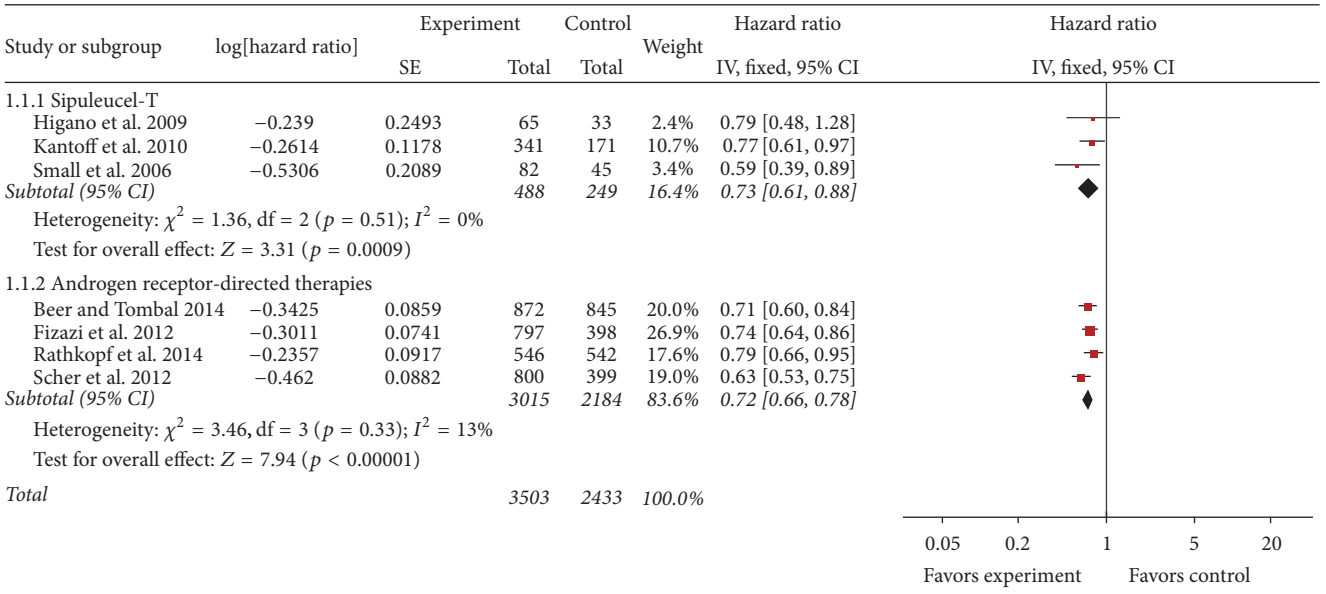

Figure 2: Forest plot of hazard ratio of overall survival of sipuleucel-T and androgen receptor-directed therapies compared with placebo in men with castration-resistant prostate cancer. The bars with squares in the middle represent 95% confidence intervals (95% CIs) and HRs. The central vertical solid line indicates the HRs for null hypothesis. The size of the diamonds represents the weight for the random-effect model in the meta-analysis.

group: 488 versus 249 patients) and 5,199 patients for AR-directed therapies (intervention group versus placebo group: 3,015 versus 2,184 patients). Figure 3 shows the forest plot of analysis of TTP. Compared with placebo, sipuleucel-T showed no significant favorable effect on TTP with pooled HR of 0.88 (95% CI: 0.74–1.06; $Z = 1.35$; $p = 0.18$). Test for heterogeneity was not significant ($p = 0.35$, $I^2 = 4\%$). In contrast, AR-directed therapies showed significant improvement in TTP with pooled HR of 0.59 (95% CI: 0.40–0.88; $Z = 2.59$; $p = 0.009$).

3.5. Reduction of PSA Level ≥50%. Seven studies with a total of 5,936 patients reported reduction of PSA level ≥50% as study outcome [29, 31–36], including 689 patients for sipuleucel-T (intervention group versus placebo group: 458 versus 231 patients) and 4,975 patients for AR-directed therapies (intervention group versus placebo group: 2,928 versus 2,047 patients). Pooled RR showed that sipuleucel-T has no significant effect on reducing PSA level ≥50% (RR: 2.51; 95% CI: 0.65–9.73; $Z = 1.33$; $p = 0.18$). Test for heterogeneity was not significant ($p = 0.5$; $I^2 = 0\%$). In contrast, AR-direct therapies showed significant effect on reducing PSA level ≥50% (RR: 9.82; 95% CI: 1.99–48.46; $Z = 2.89$; $p = 0.004$) (Figure 4).

3.6. Adverse Events (Grade ≥3). To investigate the safety of these treatments, we compared the occurrence of adverse events of grade ≥3, including fatigue, headache, back pain, arthralgia, constipation, and diarrhea, with that in placebo. Pooled RR revealed that, compared with placebo, risk of adverse event was not significantly increased for sipuleucel-T and AR-directed therapies ($p > 0.05$, Table 3 and Figure 5). There were also no significant adverse events related to these two treatments.

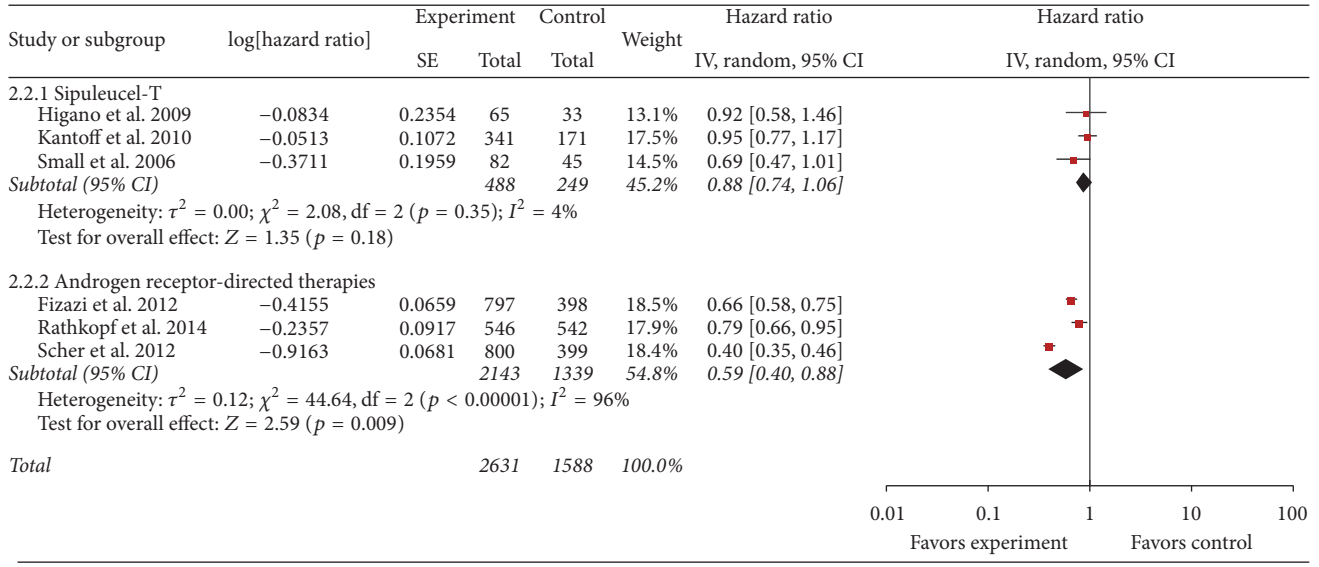

Figure 3: Forest plot of hazard ratio of time-to-progression of sipuleucel-T and androgen receptor-directed therapies compared with placebo in men with castration-resistant prostate cancer. The bars with squares in the middle represent 95% confidence intervals (95% CIs) and HRs. The central vertical solid line indicates the HRs for null hypothesis. The size of the diamonds represents the weight for the random-effect model in the meta-analysis.

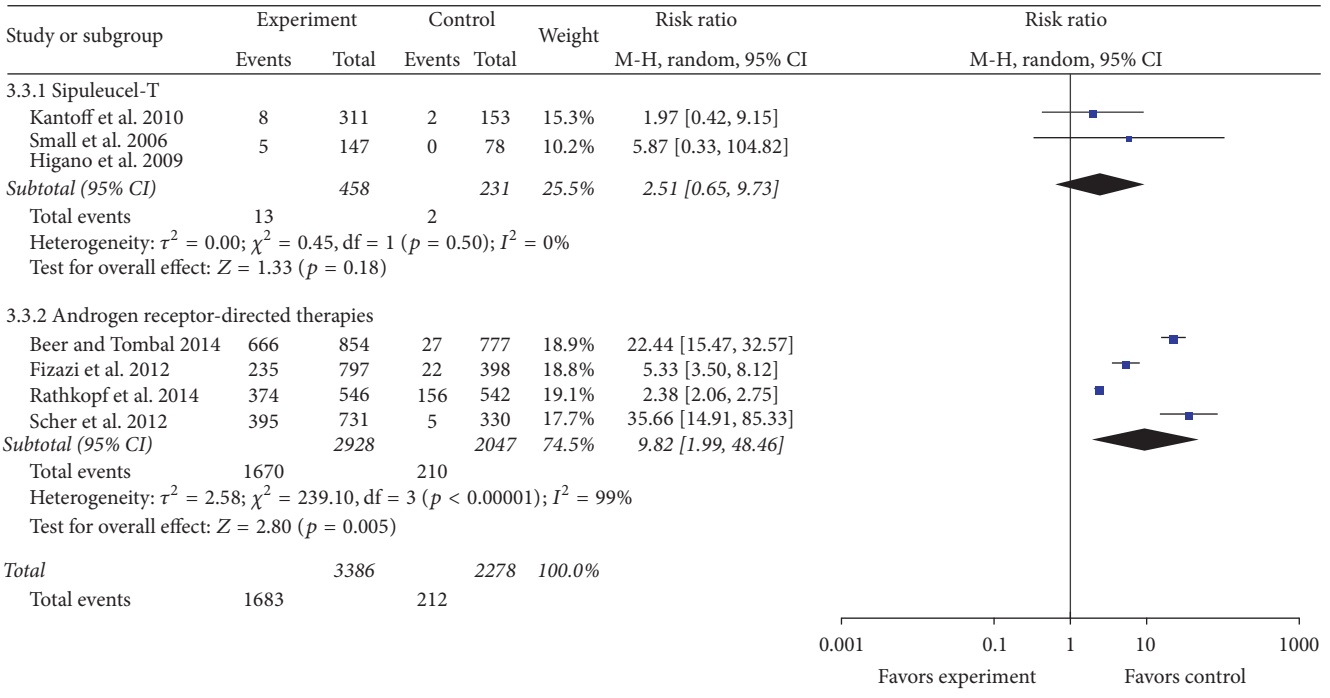

Figure 4: Forest plot of risk ratio of reduction of prostate-specific antigen ≥50% of sipuleucel-T and androgen receptor-directed therapies compared with placebo in men with castration-resistant prostate cancer. The bars with squares in the middle represent 95% confidence intervals (95% CIs) and RRs. The central vertical solid line indicates the RRs for null hypothesis. The size of the diamonds represents the weight for the random-effect model in the meta-analysis.

Study or subgroup	Experiment Events	Experiment Total	Control Events	Control Total	Weight	Risk ratio M-H, fixed, 95% CI
5.10.1 Fatigue: sipuleucel-T						
Higano et al. 2009	1	65	0	33	12.4%	1.55 [0.06, 36.93]
Kantoff et al. 2010	4	338	3	168	75.5%	0.66 [0.15, 2.93]
Small et al. 2006	1	82	0	45	12.1%	1.66 [0.07, 39.99]
Subtotal (95% CI)		*485*		*246*	*100.0%*	*0.89 [0.27, 3.01]*
Total events	6		3			
Heterogeneity: $\chi^2 = 0.42$, df = 2 ($p = 0.81$); $I^2 = 0\%$						
Test for overall effect: $Z = 0.18$ ($p = 0.86$)						
5.10.2 Fatigue: androgen receptor-directed therapies						
Beer and Tombal 2014	16	871	16	844	13.6%	0.97 [0.49, 1.93]
Fizazi et al. 2012	72	791	41	394	45.7%	0.87 [0.61, 1.26]
Rathkopf et al. 2014	13	542	10	540	8.4%	1.30 [0.57, 2.93]
Scher et al. 2012	50	800	29	399	32.3%	0.86 [0.55, 1.34]
Subtotal (95% CI)		*3004*		*2177*	*100.0%*	*0.92 [0.72, 1.18]*
Total events	151		96			
Heterogeneity: $\chi^2 = 0.86$, df = 3 ($p = 0.84$); $I^2 = 0\%$						
Test for overall effect: $Z = 0.68$ ($p = 0.50$)						
5.10.3 Headache: sipuleucel-T						
Higano et al. 2009	2	65	0	33	49.7%	2.58 [0.13, 52.15]
Kantoff et al. 2010	1	338	0	168	50.3%	1.50 [0.06, 36.52]
Small et al. 2006	0	82	0	45		Not estimable
Subtotal (95% CI)		*485*		*246*	*100.0%*	*2.03 [0.23, 17.90]*
Total events	3		0			
Heterogeneity: $\chi^2 = 0.06$, df = 1 ($p = 0.81$); $I^2 = 0\%$						
Test for overall effect: $Z = 0.64$ ($p = 0.52$)						
5.10.4 Headache: androgen receptor-directed therapies						
Beer and Tombal 2014	2	871	3	844	82.0%	0.65 [0.11, 3.86]
Scher et al. 2012	6	800	0	399	18.0%	6.49 [0.37, 114.95]
Subtotal (95% CI)		*1671*		*1243*	*100.0%*	*1.70 [0.44, 6.58]*
Total events	8		3			
Heterogeneity: $\chi^2 = 1.96$, df = 1 ($p = 0.16$); $I^2 = 49\%$						
Test for overall effect: $Z = 0.76$ ($p = 0.45$)						
5.10.5 Back pain: sipuleucel-T						
Higano et al. 2009	2	65	1	33	10.5%	1.02 [0.10, 10.79]
Kantoff et al. 2010	12	338	8	168	84.4%	0.75 [0.31, 1.79]
Small et al. 2006	2	82	0	45	5.1%	2.77 [0.14, 56.50]
Subtotal (95% CI)		*485*		*246*	*100.0%*	*0.88 [0.40, 1.91]*
Total events	16		9			
Heterogeneity: $\chi^2 = 0.71$, df = 2 ($p = 0.70$); $I^2 = 0\%$						
Test for overall effect: $Z = 0.33$ ($p = 0.74$)						
5.10.6 Back pain: androgen receptor-directed therapies						
Beer and Tombal 2014	22	871	25	844	32.2%	0.85 [0.48, 1.50]
Fizazi et al. 2012	56	791	40	394	67.8%	0.70 [0.47, 1.03]
Subtotal (95% CI)		*1662*		*1238*	*100.0%*	*0.75 [0.54, 1.03]*
Total events	78		65			
Heterogeneity: $\chi^2 = 0.33$, df = 1 ($p = 0.56$); $I^2 = 0\%$						
Test for overall effect: $Z = 1.79$ ($p = 0.07$)						
5.10.7 Arthralgia: sipuleucel-T						
Higano et al. 2009	2	65	0	33	8.3%	2.58 [0.13, 52.15]
Kantoff et al. 2010	7	338	5	168	83.7%	0.70 [0.22, 2.16]
Small et al. 2006	1	82	0	45	8.1%	1.66 [0.07, 39.99]
Subtotal (95% CI)		*485*		*246*	*100.0%*	*0.93 [0.35, 2.48]*
Total events	10		5			
Heterogeneity: $\chi^2 = 0.82$, df = 2 ($p = 0.66$); $I^2 = 0\%$						
Test for overall effect: $Z = 0.15$ ($p = 0.88$)						

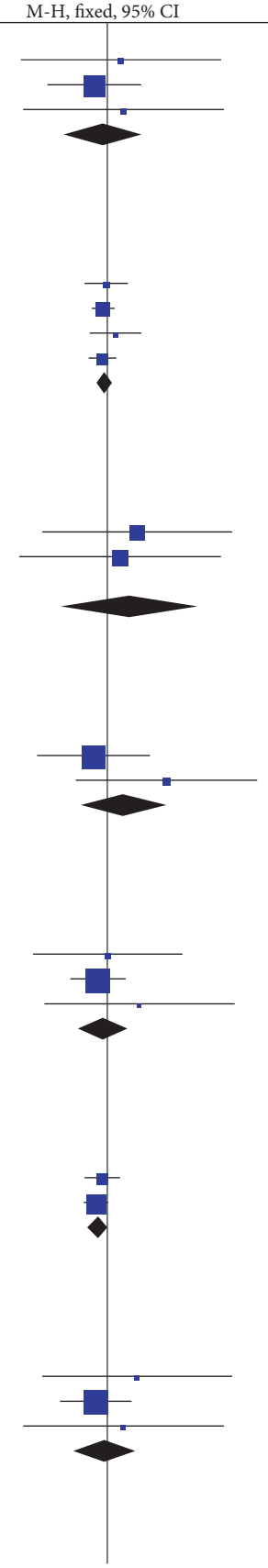

Figure 5: Continued.

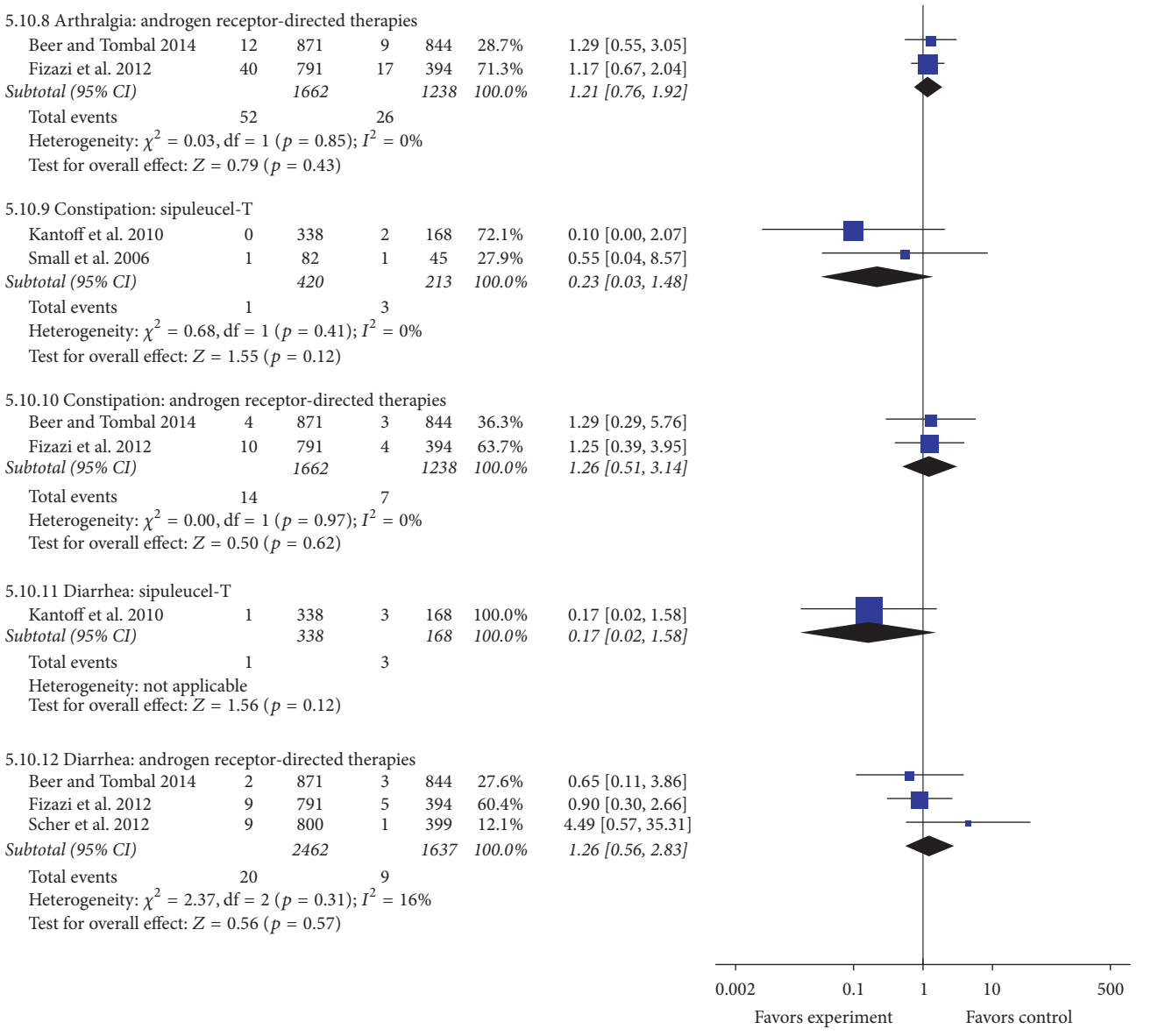

Figure 5: Forest plot of risk ratio of all adverse events of grade ≥3 of sipuleucel-T and androgen receptor-directed therapies compared with placebo in men with castration-resistant prostate cancer. The bars with squares in the middle represent 95% confidence intervals (95% CIs) and RRs. The central vertical solid line indicates the RRs for null hypothesis. The size of the diamonds represents the weight for the random-effect model in the meta-analysis.

3.7. Publication Bias. Funnel plot for publication bias was performed on study outcome of OS. Figure 6 shows symmetry funnel plot, indicating that there was no significant evidence of publication bias.

4. Discussion

Researches on novel treatments for CRPC have gained increasing interest in the past few years, especially those on sipuleucel-T and AR-directed therapies. This meta-analysis investigated the efficacy and safety of sipuleucel-T and AR-directed therapies, providing valuable information that might be useful clinical evidence on the treatments for CRPC. We found that both sipuleucel-T and AR-directed therapies could significantly improve OS in patients with CRPC, with favorable safety. AR-directed therapies appear to have superior effects in improving TTP and in reduction of PSA level. However, there are still debates over the efficacy and optimal regimen of these new treatment methods.

It has been known that traditional chemotherapeutic drugs lacked the selectivity on target tumor cells, which may cause different damage to normal cells, or even serious effects on patients. For example, Lim et al. indicated that adverse effects of docetaxel including edema, neurotoxicity, and hair loss limit its application [37]. Zhou et al. also showed 2.7% of CRPC patients died after docetaxel plus prednisone therapy,

Table 3: Analyses of adverse events (grade ≥ 3).

Adverse events	References	Relative risk(95% confidence interval)	p	Heterogeneity
Sipuleucel-T				
Fatigue	Small et al., 2006 Higano et al., 2009 Kantoff et al., 2010	0.89 (0.27–3.01)	0.86	$p = 0.81$, $I^2 = 0\%$
Headache		2.03 (0.23–17.9)	0.52	$p = 0.81$, $I^2 = 0\%$
Back pain		0.88 (0.4–1.91)	0.74	$p = 0.7$, $I^2 = 0\%$
Arthralgia		0.93 (0.35–2.48)	0.88	$p = 0.66$, $I^2 = 0\%$
Constipation		0.23 (0.03–1.48)	0.12	$p = 0.41$, $I^2 = 0\%$
Diarrhea		0.17 (0.02–1.58)	0.12	—
Androgen receptor-directed therapies				
Fatigue	Fizazi et al., 2012 Scher et al., 2012 Beer and Tombal, 2014 Rathkopf et al., 2014	0.92 (0.49–1.93)	0.5	$p = 0.84$, $I^2 = 0\%$
Headache		1.7 (0.44–6.58)	0.45	$p = 0.16$, $I^2 = 49\%$
Back pain		0.75 (0.54–1.03)	0.07	$p = 0.56$, $I^2 = 0\%$
Arthralgia		1.21 (0.76–1.92)	0.43	$p = 0.85$, $I^2 = 0\%$
Constipation		1.26 (0.51–3.14)	0.62	$p = 0.97$, $I^2 = 0\%$
Diarrhea		1.26 (0.56–2.83)	0.57	$p = 0.31$, $I^2 = 16\%$

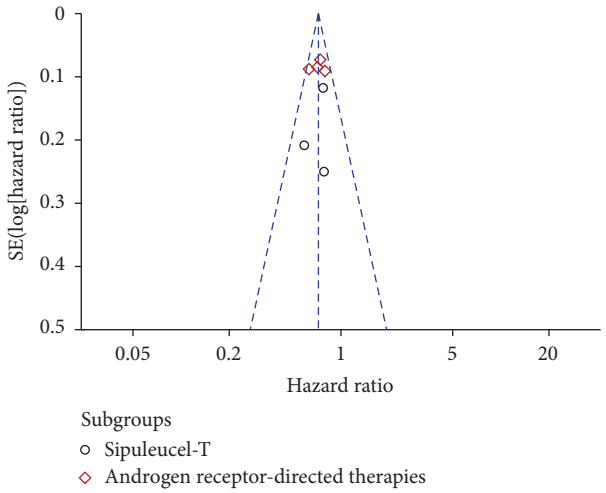

Figure 6: Funnel plot on overall survival for all included studies. The funnel graph plots the log of HR against the standard error of the log of the OR. The circles indicate the individual studies in the meta-analysis. The line in the center represents the meta HR.

58.56% had neutropenia, and 19.82% had leukopenia [38]. Unlike the traditional ones, sipuleucel-T and AR-directed therapies target tumor cells, thus causing little toxic effects on normal cells due to high selectivity. For instance, AA and Enz antagonize androgen receptors to inhibit the activity of tumor cells. Similarly, sipuleucel-T could elicit immune response targeting against antigen prostatic acid phosphatase (PAP) that is highly expressed in most prostate cancer cells [39, 40].

Many results showed that sipuleucel-T and AR-directed therapies improved the overall survival [29, 31–36] by exerting different effects on TTP, PSA level, and AEs. Although surgery, radiotherapy, or chemotherapy had stopped for a period of time before the new drugs clinical trials were given, it is still hard to rule out the possibility of the influence by the former treatments. Therefore, further clinical validation is needed. Beyond that, we paid more attention to the sequela, applicable scopes, and contraindications of these treatments.

All trials had strict selection of patients. To be an eligible case for sipuleucel-T trial, histological confirmation on castrate-resistant prostate cancer, serum testosterone level <50 ng/dL, and a considerable somatic function for expected survival were required. Patients accepted for AA trial should had no more than two previous chemotherapies, at least one previous docetaxel therapy, and mild symptoms or no symptoms (radiographic progression in soft tissue or bone with or without PSA progression, PSA <50 ng/dL, and ECOG performance status of 2 or less). And Enz had similar requirement to AA's.

Upon the drug usage, patients from sipuleucel-T trials were scheduled to undergo leukapheresis procedures every 2 week for a total of three times, and on the second day after each leukapheresis procedure, patients were treated by infusion of sipuleucel-T or placebo. Patients from AA trials received abiraterone acetate 1000 mg once daily plus prednisone 5 mg twice daily by oral or placebo plus prednisone. And in Enz trials patients received enzalutamide 160 mg orally once daily or matched placebo.

We found that in AA trials patients with lower score of ECOG, age ≥ 65 years, and PSA level > or < median had the higher HR. On the contrary, in enzalutamide trials, patients with age ≥ 65 years, higher score of ECOG, and PSA Level > median had the higher HR. While in sipuleucel-T trials, patients with age < median, psa < or > median, and higher score of ECOG had the higher HR. Such differences may be related to the characteristics of different individuals. Drake 2012 indicated that the subgroup of patients aged less than 65 years did not favor sipuleucel-T. Another observation by them was the potential harm from the IMPACT study interventions, because, to some extent, sipuleucel-T broke the immune balance [41].

Challenges remain in finding the optimal regimen for sipuleucel-T and AR-directed therapies. Combined sipuleucel-T, AA, and prednisone formula has been proposed as a novel treatment diagram in CRPC. Research has shown that concurrent administration of AA and prednisone did not blunt immunologic effects or alter immune parameters that correlate with sipuleucel-T's clinical benefits [42]. Cumulative APC activation, cumulative APC number, total nucleated cell counts, and immune responses to sipuleucel-T were not affected by coadministration of AA and prednisone. Such combination of treatments was well tolerated, with no new risk marker emerging. Sipuleucel-T is recommended as the first-line treatment for patients with CRPC by the National Comprehensive Cancer Network [43] and it is recommended as early use in asymptomatic CRPC or patients with mild symptoms. Comparatively, treatments with AA and Enz could induce symptomatic disease progression. Badrising et al. 2014 reported that tolerance could be built up when combining Enz and AA [44]. This was possibly a result of mutation of AR induced by prednisone, which will subsequently impact the effect of Enz on AR. Therefore, it appears that there is limited clinical benefit for combination or sequential use of Enz and AA [45–48].

Competing Interests

The authors declared no competing interests.

Authors' Contributions

Renliang Yi, Baoxin Chen, and Zhiheng Zhou conceived and designed the research. Renliang Yi, Baoxin Chen, Peng Duan, and Chen Yuan carried out literature search. Chanjiao Zheng and Huanyu Shen carried out data extraction. Qun Liu and Weilin Ou carried out quality assessment. Baoxin Chen and Zhiheng Zhou carried out manuscript preparation. Chanjiao Zheng, Huanyu Shen, and Zhiheng Zhou carried out manuscript revision. Renliang Yi and Baoxin Chen contributed equally to this work.

Acknowledgments

The authors thank Dr. Zining Lei for her helpful suggestions and advice on this paper. This work was supported by The Healthcare Project of the Health Department of the General Logistics Department of the Chinese People's Liberation Army (Renliang Yi: 14BJZ34), the National Natural Science Foundation of China (Zhiheng Zhou: 81473001), and the Training Project of Outstanding Young College Teachers in Guangdong Province, China (Zhiheng Zhou: Yq2013138).

References

[1] World Health Organization, Programmes and projects: Cancer, http://www.who.int/cancer/en/.

[2] J. Ferlay, E. Steliarova-Foucher, J. Lortet-Tieulent et al., "Cancer incidence and mortality patterns in Europe: estimates for 40 countries in 2012," *European Journal of Cancer*, vol. 49, no. 6, pp. 1374–1403, 2013.

[3] R. L. Siegel, K. D. Miller, and A. Jemal, "Cancer statistics, 2015," *CA: A Cancer Journal for Clinicians*, vol. 65, no. 1, pp. 5–29, 2015.

[4] G. L. Plosker, "Sipuleucel-T: in metastatic castration-resistant prostate cancer," *Drugs*, vol. 71, no. 1, pp. 101–108, 2011.

[5] Ö. Acar, T. Esen, and N. A. Lack, "New therapeutics to treat castrate-resistant prostate cancer," *The Scientific World Journal*, vol. 2013, Article ID 379641, 8 pages, 2013.

[6] S. M. Geary, C. D. Lemke, D. M. Lubaroff, and A. K. Salem, "Proposed mechanisms of action for prostate cancer vaccines," *Nature Reviews Urology*, vol. 10, no. 3, pp. 149–160, 2013.

[7] C. R. Pound, A. W. Partin, M. A. Eisenberger, D. W. Chan, J. D. Pearson, and P. C. Walsh, "Natural history of progression after PSA elevation following radical prostatectomy," *Journal of the American Medical Association*, vol. 281, no. 17, pp. 1591–1597, 1999.

[8] D. L. Suzman and E. S. Antonarakis, "Castration-resistant prostate cancer: latest evidence and therapeutic implications," *Therapeutic Advances in Medical Oncology*, vol. 6, no. 4, pp. 167–179, 2014.

[9] R. Petrioli, E. Francini, and G. Roviello, "Is there still a place for docetaxel rechallenge in prostate cancer?" *World Journal of Clinical Oncology*, vol. 6, no. 5, pp. 99–103, 2015.

[10] S. Badrising, V. van der Noort, I. M. van Oort et al., "Clinical activity and tolerability of enzalutamide (MDV3100) in patients with metastatic, castration-resistant prostate cancer who progress after docetaxel and abiraterone treatment," *Cancer*, vol. 120, no. 7, pp. 968–975, 2014.

[11] C.-H. Ohlmann, "Chemotherapy of prostate cancer," *Urologe*, vol. 54, no. 10, pp. 1461–1470, 2015.

[12] C. Printz, "New prostate cancer drugs hold promise," *Cancer*, vol. 119, no. 2, pp. 247–248, 2013.

[13] D. Lorente, J. Mateo, R. Perez-Lopez, J. S. de Bono, and G. Attard, "Sequencing of agents in castration-resistant prostate cancer," *The Lancet Oncology*, vol. 16, no. 6, pp. e279–e292, 2015.

[14] R. M. Bambury and D. E. Rathkopf, "Novel and next-generation androgen receptor–directed therapies for prostate cancer: beyond abiraterone and enzalutamide," *Urologic Oncology: Seminars and Original Investigations*, vol. 34, no. 8, pp. 348–355, 2016.

[15] L. T. Dauer, M. J. Williamson, J. Humm et al., "Radiation safety considerations for the use of 223RaCl2 de in men with castration-resistant prostate cancer," *Health Physics*, vol. 106, no. 4, pp. 494–504, 2014.

[16] R. Iacovelli, A. Palazzo, G. Procopio, P. Gazzaniga, and E. Cortesi, "Abiraterone acetate in castration-resistant prostate cancer," *Anti-Cancer Drugs*, vol. 23, no. 3, pp. 247–254, 2012.

[17] S. Bhattacharya, M. Hirmand, D. Phung, and S. van Os, "Development of enzalutamide for metastatic castration-resistant prostate cancer," *Annals of the New York Academy of Sciences*, vol. 1358, no. 1, pp. 13–27, 2015.

[18] S. Lebdai, V. Basset, J. Branchereau et al., "What do we know about treatment sequencing of abiraterone, enzalutamide, and chemotherapy in metastatic castration-resistant prostate cancer?" *World Journal of Urology*, vol. 34, no. 5, pp. 617–624, 2016.

[19] C. Parker, S. Nilsson D Heinrich, S. I. Helle et al., "Alpha emitter radium-223 and survival in metastatic prostate cancer," *New England Journal of Medicine*, vol. 369, no. 3, pp. 213–223, 2013.

[20] P. W. Kantoff, T. J. Schuetz, B. A. Blumenstein et al., "Overall survival analysis of a phase II randomized controlled trial of a poxviral-based PSA-targeted immunotherapy in metastatic

castration-resistant prostate cancer," *Journal of Clinical Oncology*, vol. 28, no. 7, pp. 1099–1105, 2010.

[21] P. G. Kluetz, Y.-M. Ning, V. E. Maher et al., "Abiraterone acetate in combination with prednisone for the treatment of patients with metastatic castration-resistant prostate cancer: U.S. food and drug administration drug approval summary," *Clinical Cancer Research*, vol. 19, no. 24, pp. 6650–6656, 2013.

[22] Y. M. Ning, W. Pierce, V. E. Maher et al., "Enzalutamide for treatment of patients with metastatic castration-resistant prostate cancer who have previously received docetaxel: U.S. foodand drugadministrationdrug approval summary," *Clinical Cancer Research*, vol. 19, no. 22, pp. 6067–6073, 2013.

[23] M. A. Cheever and C. S. Higano, "PROVENGE (sipuleucel-T) in prostate cancer: the first FDA-approved therapeutic cancer vaccine," *Clinical Cancer Research*, vol. 17, no. 11, pp. 3520–3526, 2011.

[24] W. Kim and C. J. Ryan, "Quo vadis: advanced prostate cancer-clinical care and clinical research in the era of multiple androgen receptor-directed therapies," *Cancer*, vol. 121, no. 3, pp. 361–371, 2015.

[25] B. A. Gartrell and F. Saad, "Abiraterone in the management of castration-resistant prostate cancer prior to chemotherapy," *Therapeutic Advances in Urology*, vol. 7, no. 4, pp. 194–202, 2015.

[26] J. B. Aragon-Ching, "Further analysis of PREVAIL: enzalutamide use in chemotherapy-naïve men with metastatic castration-resistant prostate cancer," *Asian Journal of Andrology*, vol. 16, no. 6, pp. 803–804, 2014.

[27] P. A. Burch, J. K. Breen, J. C. Buckner et al., "Priming tissue-specific cellular immunity in a phase I trial of autologous dendritic cells for prostate cancer," *Clinical Cancer Research*, vol. 6, no. 6, pp. 2175–2182, 2000.

[28] C. J. Paller and E. S. Antonarakis, "Sipuleucel-T for the treatment of metastatic prostate cancer: promise and challenges," *Human Vaccines & Immunotherapeutics*, vol. 8, no. 4, pp. 509–519, 2012.

[29] E. J. Small, P. F. Schellhammer, C. S. Higano et al., "Placebo-controlled phase III trial of immunologic therapy with sipuleucel-T (APC8015) in patients with metastatic, asymptomatic hormone refractory prostate cancer," *Journal of Clinical Oncology*, vol. 24, no. 19, pp. 3089–3094, 2006.

[30] G. A. Wells, B. Shea, D. O'Connell et al., "The Newcastle-Ottawa Scale (NOS) for assessing the quality of nonrandomised studies in meta-analyses," http://www.ohri.ca/programs/clinical_epidemiology/oxford.htm.

[31] C. S. Higano, P. F. Schellhammer, E. J. Small et al., "Integrated data from 2 randomized, double-blind, placebo-controlled, phase 3 trials of active cellular immunotherapy with sipuleucel-T in advanced prostate cancer," *Cancer*, vol. 115, no. 16, pp. 3670–3679, 2009.

[32] P. W. Kantoff, C. S. Higano, N. D. Shore et al., "Sipuleucel-T immunotherapy for castration-resistant prostate cancer," *The New England Journal of Medicine*, vol. 363, no. 5, pp. 411–422, 2010.

[33] K. Fizazi, H. I. Scher, A. Molina et al., "Abiraterone acetate for treatment of metastatic castration-resistant prostate cancer: final overall survival analysis of the COU-AA-301 randomised, double-blind, placebo-controlled phase 3 study," *The Lancet Oncology*, vol. 13, no. 10, pp. 983–992, 2012.

[34] D. E. Rathkopf, M. R. Smith, J. S. De Bono et al., "Updated interim efficacy analysis and long-term safety of abiraterone acetate in metastatic castration-resistant prostate cancer patients without prior chemotherapy (COU-AA-302)," *European Urology*, vol. 66, no. 5, pp. 815–825, 2014.

[35] H. I. Scher, K. Fizazi, F. Saad et al., "Increased survival with enzalutamide in prostate cancer after chemotherapy," *The New England Journal of Medicine*, vol. 367, no. 13, pp. 1187–1197, 2012.

[36] T. M. Beer and B. Tombal, "Enzalutamide in metastatic prostate cancer before chemotherapy," *The New England Journal of Medicine*, vol. 371, no. 18, pp. 1755–1756, 2014.

[37] H. Lim, K. M. Kim, S. Jeong, E. K. Choi, and J. Jung, "Chrysin increases the therapeutic efficacy of docetaxel and mitigates docetaxel-induced edema," *Integrative Cancer Therapies*, 2016.

[38] T. Zhou, S.-X. Zeng, D.-W. Ye et al., "A multicenter, randomized clinical trial comparing the three-weekly docetaxel regimen plus prednisone versus mitoxantone plus prednisone for Chinese patients with metastatic castration refractory prostate cancer," *PLoS ONE*, vol. 10, no. 1, Article ID e0117002, 2015.

[39] N. Agarwal, G. Di Lorenzo, G. Sonpavde, and J. Bellmunt, "New agents for prostate cancer," *Annals of Oncology*, vol. 25, no. 9, Article ID mdu038, pp. 1700–1709, 2014.

[40] E. Anassi and U. A. Ndefo, "Sipuleucel-T (Provenge) injection the first immunotherapy agent (Vaccine) for hormone-refractory prostate cancer," *P and T*, vol. 36, no. 4, pp. 197–202, 2011.

[41] C. G. Drake, "Re: interdisciplinary critique of sipuleucel-T as immunotherapy in castration-resistant prostate cancer," *Journal of the National Cancer Institute*, vol. 104, no. 18, p. 1422, 2012.

[42] E. J. Small, R. S. Lance, T. A. Gardner et al., "A randomized phase II trial of sipuleucel-T with concurrent versus sequential abiraterone acetate plus prednisone in metastatic castration-resistant prostate cancer," *Clinical Cancer Research*, vol. 21, no. 17, pp. 3862–3869, 2015.

[43] J. Mohler, A. Armstrong, R. Bahnson et al., *NCCN Clinical Practice Guidelines in Oncology: Prostate Cancer, V.4*, 2013, https://www.nccn.org/.

[44] S. Badrising, V. Van Der Noort, I. M. Van Oort et al., "Clinical activity and tolerability of enzalutamide (MDV3100) in patients with metastatic, castration-resistant prostate cancer who progress after docetaxel and abiraterone treatment," *Cancer*, vol. 120, no. 7, pp. 968–975, 2014.

[45] Y. Loriot, D. Bianchini, E. Ileana et al., "Antitumour activity of abiraterone acetate against metastatic castration-resistant prostate cancer progressing after docetaxel and enzalutamide (MDV3100)," *Annals of Oncology*, vol. 24, no. 7, pp. 1807–1812, 2013.

[46] K. L. Noonan, S. North, R. L. Bitting, A. J. Armstrong, S. L. Ellard, and K. N. Chi, "Clinical activity of abiraterone acetate in patients with metastatic castration-resistant prostate cancer progressing after enzalutamide," *Annals of Oncology*, vol. 24, no. 7, pp. 1802–1807, 2013.

[47] A. A. Azad, B. J. Eigl, R. N. Murray, C. Kollmannsberger, and K. N. Chi, "Efficacy of enzalutamide following abiraterone acetate in chemotherapy-naive metastatic castration-resistant prostate cancer patients," *European Urology*, vol. 67, no. 1, pp. 23–29, 2015.

[48] A. J. Schrader, M. Boegemann, C.-H. Ohlmann et al., "Enzalutamide in castration-resistant prostate cancer patients progressing after docetaxel and abiraterone," *European Urology*, vol. 65, no. 1, pp. 30–36, 2014.

Hindawi Publishing Corporation
Journal of Immunology Research
Volume 2016, Article ID 5031529, 7 pages
http://dx.doi.org/10.1155/2016/5031529

Research Article

Allogeneic Antigen Composition for Preparing Universal Cancer Vaccines

Petr G. Lokhov[1,2] and Elena E. Balashova[1,2]

[1] *Department of Proteomic Research and Mass Spectrometry, Institute of Biomedical Chemistry, Moscow, Russia*
[2] *BioBohemia Ltd., Moscow, Russia*

Correspondence should be addressed to Petr G. Lokhov; lokhovpg@rambler.ru

Received 15 February 2016; Revised 8 June 2016; Accepted 28 August 2016

Academic Editor: Mercedes López

Recently it was demonstrated that tumors induce specific changes to the surface of human endothelial cells thereby providing the basis for designing endothelial cell-based vaccines that directly target antigens expressed by the tumor endothelium. The present report extends these studies *in vitro* by investigating the efficacy of allogeneic antigens with regard to their ability to target immune responses against the tumor vasculature since alloantigens simplify vaccine development and implementation in clinical practice. We demonstrated that allogeneic SANTAVAC (Set of All Natural Target Antigens for Vaccination Against Cancer), which presents a specifically prepared composition of cell surface antigens from tumor-stimulated endothelial cells, allows targeting of the tumor vasculature with efficacy of 17, where efficacy represents the killing rate of target cells before normal cells are adversely affected, and efficacy of 60, where efficacy represents the fold decrease in the number of target cells and directly relates to tumor growth arrest. These data suggest that allogeneic SANTAVAC may be considered an antigenic composition that following administration in the presence of respective adjuvants may be clinically tested as a therapeutic or prophylactic universal cancer vaccine without adverse side effects to the normal vasculature.

1. Introduction

Vaccination using antigens expressed by endothelial cells lining the tumor vasculature represents the most attractive vaccination strategy because immunization using this approach may prevent the growth of any solid tumor [1]. Therefore, endothelial cells can be used as a source of antigens used in the development of a universal cancer vaccine (UCV). However, autoimmune-mediated damage to microvessels, the primary targets of anticancer endothelial cell-based vaccination strategies, may lead to side effects, namely, autoimmune-mediated damage of microvessels in healthy tissues [2, 3]. Therefore, antigen compositions constituting a UCV that are distinct from antigens expressed by endothelial cells in normal tissues need to be designed to prevent the elicitation of undesired autoimmunity.

Recently we described the interactions between tumor-induced endothelial cell surface heterogeneity and endothelial cell escape from cell-mediated immune responses [4, 5]. These data sets suggested that an efficient autologous vaccine could be designed utilizing surface antigens expressed by cultured human microvascular endothelial cells (HMEC) if their tumor-induced cell surface profile and the profile of target HMEC were similar. In this scenario, the efficacy of the autologous vaccine would exceed 18 (i.e., 18 tumor endothelial cells will be destroyed before 1 endothelial cell in normal tissue is destroyed) [5]. Antigen compositions intended for vaccination were based on a specifically derived set of HMEC natural cell surface antigens distinguished by the abbreviation SANTAVAC (Set of All Natural Target Antigens for Vaccination Against Cancer) [6]. Although the design of these studies was mainly intended to describe an autologic type of SANTAVAC, it was found that alloantigen compositions also may be efficiently used for anticancer vaccination. In one case, the killing rate of target HMEC using allogeneic surface antigens related directly to the *in vitro* design of the allogeneic universal vaccine with efficacy of targeting equal to 4 [6]. This efficacy provides a therapeutic

window where tumor HMEC could be killed before HMEC of normal tissues are adversely affected. Unfortunately, the efficacy of the allogeneic SANTAVAC in these studies was characterized by a limited number of experiments. To fill this gap, additional cytotoxicity assays (CTA) were performed in the present study to complement the UCV design based on the SANTAVAC. The possibility of excluding a patient's own biomaterial from the vaccine preparation simplifies the development activities and increases the value of the allogeneic SANTAVAC vaccines.

2. Materials and Methods

2.1. Cell Culture. Two abdominal subcutaneous adipose tissue biopsies were obtained from female patients (40–50 years old) undergoing open abdominal surgical procedures at the National Medico-Surgical Center (Moscow, Russia). The protocol was approved by the Research Ethics Committee and the patients provided written informed consent. The biopsy specimens were transported to the laboratory, and endothelial primary cultures were established using magnetic beads coated with anti-CD31 monoclonal antibody (Dynabeads CD31 Endothelial Cells, Invitrogen, Life Technologies, Carlsbad, CA, USA) as described previously [4]. Culture media (Medium MCDB 131 and Microvascular Growth Supplement, Gibco, Thermo Fisher Scientific, Waltham, MA, USA) supplemented with 10% FBS (fetal bovine serum) (PAA Laboratories, Dartmouth, MA, USA), 50 μg/mL streptomycin, 50 U/mL penicillin, 2 mM glutamine (Gibco), and 12 U/mL heparin (Sigma-Aldrich, St. Louis, MO, USA) were changed every 2-3 days and after the first passage. Cells were grown to 65% confluence and used in future experiments. To obtain HMEC with tumor-induced phenotypes, cell cultures were incubated for 4 days in culture medium (MCDB 131, FBS, streptomycin-penicillin, glutamine, and heparin) supplemented with 5%, 15%, and 25% of tumor-conditioned medium. Cells were visualized using a Leica DM5000B microscope (Leica Microsystems, Buffalo Grove, IL, USA).

Primary fibroblast cultures were established from an adult skin biopsy (45-year-old woman; donor provided written informed consent) as described by Rittié and Fisher [7]. Primary cultures were cultured in DMEM (Gibco) supplemented with 10% FBS, 5 μg/mL streptomycin, 5 U/mL penicillin, and 2 mM glutamine at 5% CO_2 at 37°C and third passage cells were used to obtain fibroblast-associated antigens (FAA).

2.2. Tumor-Conditioned Medium. Tumor-conditioned medium was collected from HepG2 (human hepatocellular carcinoma cells, ATCC, Manassas, VA, USA; cell lines have been authenticated by cell proteomic footprinting [8]) as described by Folkman et al. [9]. Media were conditioned for 48 h, collected, centrifuged for 10 min at 600 ×g, and filter-sterilized (0.2 μm). Tumor-conditioned medium was then concentrated 10x using Centriplus Centrifugal Filter Devices YM-3 (Millipore, Merck KGaA, Darmstadt, Germany) and used in experiments.

In order to determine the optimal concentration of tumor-conditioned medium required to provide different tumor-induced stimuli to HMEC, the 10x tumor-conditioned medium was added to HMEC seeded in the wells of a 96-well plate at different concentrations (0, 10, 20, 30, 40, and 50% in MCDB 131 medium supplemented with streptomycin-penicillin, glutamine, and heparin). After 3 days in culture, cells were counted in wells using trypan blue staining to determine the concentration of tumor-conditioned medium that induced weak (stimuli just a little higher than in the control), moderate (half of the maximum), and strong (a little more than related to maximum) stimulation.

2.3. FACS Analysis. Endothelial cells were stained with phycoerythrin- (PE-) conjugated mouse anti-hVEGFR-2 IgG1 (clone 89106, R&D Systems, Minneapolis, MN, USA) or PE-conjugated mouse anti-human CD62E IgG1 (clone 68-5H11, BD Pharmingen, Becton Dickinson, San Jose, CA, USA). For isotype control, cells were stained with PE-conjugated mouse IgG1 (R&D Systems, clone 11711, or BD Pharmingen, clone MOPC-21, resp.). Flow cytometry was performed on a BD FACSCalibur flow cytometry system (Becton Dickinson) and the data analyzed using Cell Quest software (Becton Dickinson).

2.4. Preparation of SANTAVAC and FAA. HMEC or fibroblasts grown to 65% confluence were washed 5x with HBSS before being treated with 0.2 μg/mL trypsin (15,000 U/mg, Promega, Madison, WI, USA) in HBSS. A 0.5 mL trypsin solution was added to each well of a 6-well plate, incubated for 20 min at 37°C in saturated humidity, then collected again, and centrifuged (600 ×g for 5 min). The resulting supernatant contained cell surface targets and was considered a solution of SANTAVAC or fibroblast-associated antigens (FAA), respectively.

2.5. Preparation of SANTAVAC-Loaded DC. Monocyte-derived dendritic cells (DC) were generated as described previously [10]. Briefly, fresh peripheral blood mononuclear cells (PBMCs) from healthy donors were isolated using Ficoll-Hypaque (PanEco, Moscow, Russia) gradient centrifugation and were then allowed to adhere to 12-well culture plates for 1 h. Nonadherent cells were collected and centrifuged, and cell pellets were mixed with autologous serum containing 10% DMSO and stored in liquid nitrogen. Cryopreserved, nonadherent PBMCs, which also are considered as peripheral blood lymphocytes, were later used as a source of effector cells (cytotoxic T lymphocytes, CTL) for cytotoxicity assays. The adherent cell fraction was cultured in RPMI-1640 (Gibco) supplemented with 10% FBS, streptomycin-penicillin, and glutamine in the presence of 0.075 μg/mL granulocyte macrophage colony-stimulating factor (Neostim, 1.67×10^6 ME, FDS FARMA, UK) and 1000 U/mL interleukin-4 (Sigma-Aldrich). After 6 d in culture, SANTAVAC (0.5 mL) or FAA (0.5 mL) were added to each well of a 12-well culture plate with immature DC (3×10^5 cells/well in 1 mL of culture medium) and DC were matured with 1000 U/mL tumor necrosis factor-α (Sigma-Aldrich) for

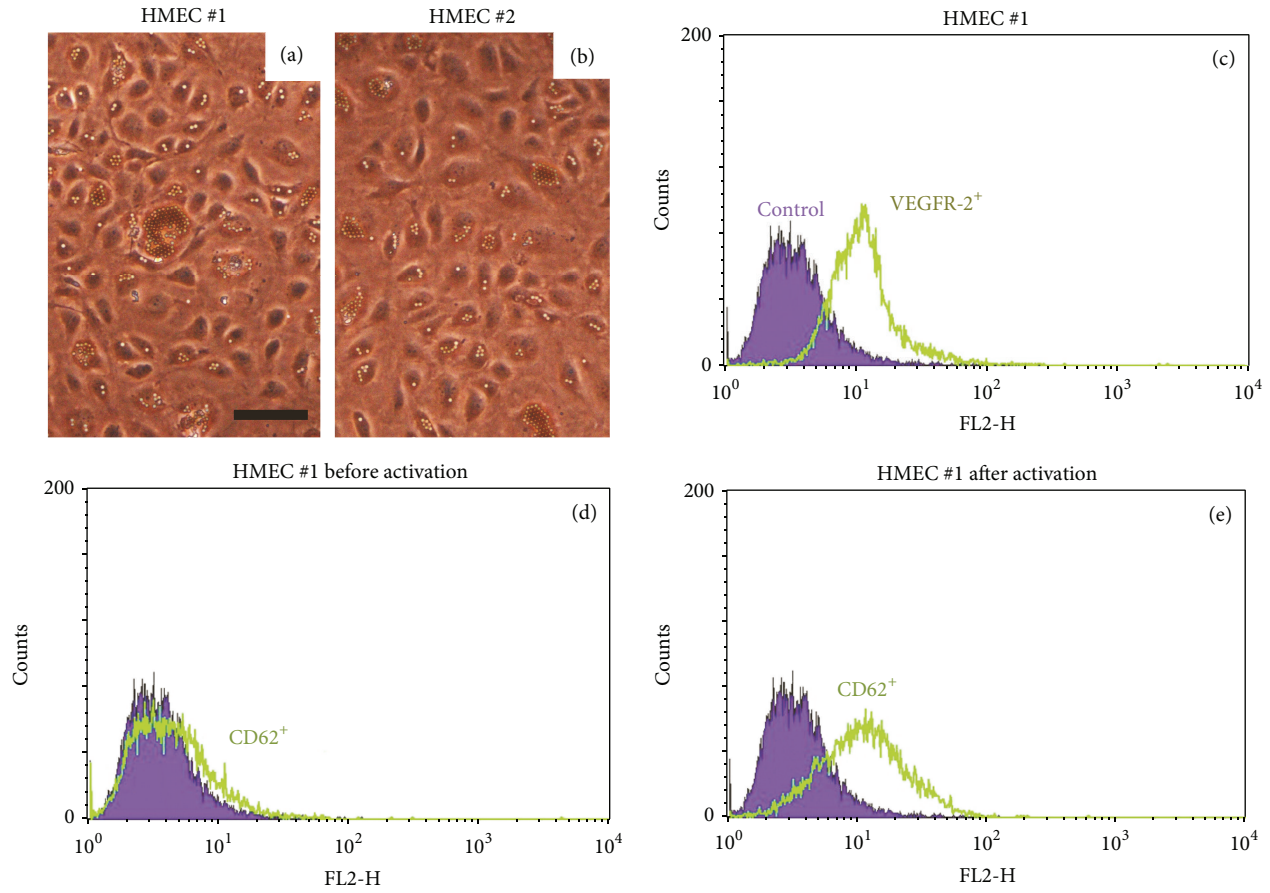

FIGURE 1: Primary HMEC cultures. A representative HMEC primary culture from donor 1 (a) and donor 2 (b). Images were obtained using a Leica DM5000B microscope (scale bar, 50 μm). Flow cytometric analysis of HMEC from donor 1 before activation (c, d) and after activation (e). Cells were stained with PE-conjugated monoclonal mouse anti-hVEGFR-2 or anti-human CD62E antibodies (labeled as "VEGFR-2$^+$" or "CD62$^+$"). For isotype control, cells were stained with PE-conjugated mouse IgG1 (labeled as "*control*").

48 h. Matured, SANTAVAC-loaded or FAA-loaded DC were then used to stimulate CTL.

2.6. Stimulation of CTL. SANTAVAC-loaded DC (3×10^5 cells/well) in 12-well culture plates were combined with 6×10^6 autologous nonadherent PBMCs (1 : 20) in 1 mL of RPMI-1640 medium (containing 10% FBS, streptomycin-penicillin, and glutamine) supplemented with 30 U/mL of clinical grade human interleukin-2 (Ronkoleukin, Biotech, St. Petersburg, Russia). The culture medium supplemented with interleukin-2 was replaced every third day. After incubation for nine days, nonadherent PBMCs containing stimulated CTL were washed by centrifugation and used as effector CTL in cytotoxicity assays.

2.7. Cytotoxicity Assays. HMEC (5×10^3 cells/well) were seeded into 48-well plates, which yielded 3×10^4 cells/well after 72 h. Effector CTL were then added to HMEC at an effector : target ratio of 20 : 1. On the third day, target HMEC were washed to remove CTL and attached HMEC were trypsinized and viability detected using trypan blue exclusion [11]. Cell counts were averaged over 3 measurements. The number of nonstimulated and tumor-stimulated HMEC in the presence or absence of effector CTL stimulated with FAA-loaded DC was used as controls. CTA data were used to calculate the *in vitro* efficacy of the allogeneic SANTAVAC formulation, namely, efficacy type I, denoted as "efficacy I" and calculated as a ratio of the number of *nonstimulated cells in control wells* (*i.e.*, HMEC$^{0\%}$) to the number of tumor-stimulated cells in experimental wells, and efficacy type II, denoted as "efficacy II" and calculated as a ratio of the number *of tumor-stimulated cells in control wells* (*i.e.*, HMEC$^{5\%}$, HMEC$^{15\%}$, or HMEC$^{25\%}$) to tumor-stimulated cells in experimental wells.

3. Results

3.1. Primary HMEC Cultures. Anti-CD31 beads were used to isolate HMEC from a fat biopsy. Figures 1(a) and 1(b) show primary HMEC cultures isolated from fat biopsies obtained from donors 1 and 2, respectively. Adipose tissue-derived HMEC presented with typical cobblestone-like morphology. FACS analysis (Figure 1(c) for HMEC donor 1; data for

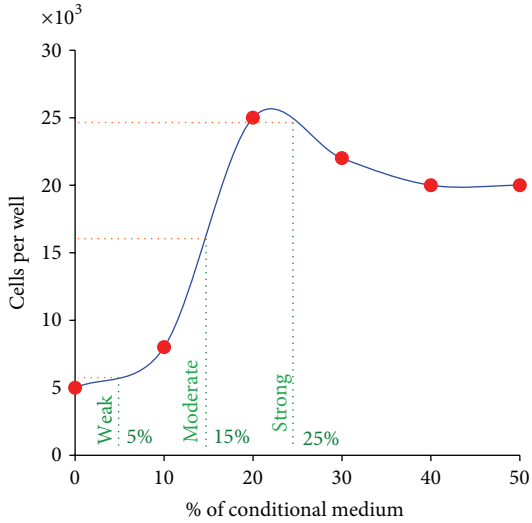

Figure 2: Dose determination of tumor-conditioned medium used to prepare HMEC with tumor-induced cell surface profiles. HMEC cultures were incubated with 0, 10, 20, 30, 40, or 50% tumor-conditioned medium. After 3 days in culture, cells were counted (red points) in wells using trypan blue exclusion. Cell numbers were approximated using a curve used to determine the concentrations of tumor-conditioned medium that elicited either *weak* (stimuli just a little higher than in the control), *moderate* (half of the maximum), or *strong* (maximum) stimulation of HMEC cultures (green lines). Green lines represent percentage selected for CTA.

donor 2 are not shown) revealed that the VEGFR-2 endothelial cell marker is associated with almost 90% of the cells during the first passage following isolation. No growth of contaminating fibroblasts or mesothelial cells was detected, demonstrating that primary HMEC cultures were successfully established. Additionally, FACS analysis of CD62 confirmed the endothelial nature of the primary cultures after activation using tumor-conditioned medium (Figures 1(d) and 1(e)).

3.2. Tumor-Induced Stimulation. The optimal concentration of tumor-conditioned medium required to provide HMEC stimulation was determined next. HMEC were cultured for 3 days in the presence of different concentrations of tumor-conditioned medium. Culture medium containing tumor-conditioned volumes of 5%, 15%, or 25% elicited weak (stimuli just a little higher than in the control), moderate (half of the maximum), or strong (a little more than related to maximum) levels of HMEC stimulation, respectively (Figure 2).

3.3. Cytotoxicity Assays. The immunologic properties of respective SANTAVAC compositions were evaluated by loading DC with corresponding SANTAVAC as a means of activating and stimulating human cytotoxic T lymphocytes (CTL) against target HMEC. CTL stimulated with fibroblast-associated antigen- (FAA-) loaded DC incubated in the presence of target HMEC were used as controls. On day 3, surviving target HMEC were identified using trypan blue exclusion.

A subtle improvement in cytotoxicity was observed when CTL were stimulated with FAA-loaded DC. DC loaded with HMEC and stimulated with 15% or 25% tumor-conditioned medium elicited effective immune responses measured by high death rates of target HMEC (Figure 3). Notably, CTL stimulated with DC loaded with antigens from $HMEC^{15\%}$ (superscript represents the percentage of tumor-conditioned medium used to stimulate HMEC) was also most effective against $HMEC^{15\%}$ target cells (in this case almost all target cells were dead). The target $HMEC^{25\%}$ were most efficiently killed by CTL stimulated with DC loaded with antigens from $HMEC^{25\%}$. SANTAVAC efficacy I indicates that *in vitro* modeled vaccine safety was 17.3, achieved using antigens derived from $HMEC^{15\%}$ and $HMEC^{15\%}$ used as targets. SANTAVAC efficacy II indicates that the *in vitro* modeled capacity to arrest tumor growth was ~60, also achieved by $SANTAVAC^{15\%}$▶$HMEC^{15\%}$ (hereinafter [*$SANTAVAC^{x\%}$ is SANTAVAC generated from $HMEC^{x\%}$ for CTA*]▶[*$HMEC^{y\%}$ used as target cells in same CTA*]).

4. Discussion

4.1. SANTAVAC: The Antigenic Composition of a Universal Endothelial Cell-Based Cancer Vaccine. Development of cell-based vaccines focuses on the elicitation of immune responses against target cells expressing native antigens [12, 13]. Cell surface targets are prioritized for vaccine design [14, 15] and are accessible to proteases whose byproducts could be isolated following *in vitro* proteolytic cleavage. Previously, it was shown that the "antigenic essence" of cells, which may be used in cell-based vaccines in contrast to whole cells, could be prepared by proteolytic cleavage of cell surface targets [16, 17]. The composition of this "antigenic essence," which was established by the proteomic footprinting [8, 18], directly defined target cell killing rates in CTA that represent an *in vitro* anticancer vaccination model [4]. The "antigenic essence" prepared for vaccines designed to target the tumor vasculature gave rise to the name SANTAVAC [6]. SANTAVAC formulations can be mixed with different adjuvants and their immunogenicity and safety tested *in vivo* as UCV.

4.2. Allogeneic SANTAVAC. The present study expanded on the selection of alloantigens used in the preparation of SANTAVAC vaccines. The primary benefit of utilizing alloantigens as vaccine components is the possibility of excluding the patient's biomaterial from the vaccine preparation, thereby simplifying vaccine development, lowering the cost, and facilitating translation into clinical practice. Although autogenic SANTAVAC induced much higher target cell killing rates in CTA than alloantigens, alloantigens may also be highly efficient. Alloantigen compositions that induced low tumor killing rates also exhibited low killing rates of healthy tissues providing the required therapeutic window for their application. From the perspective of estimating vaccine

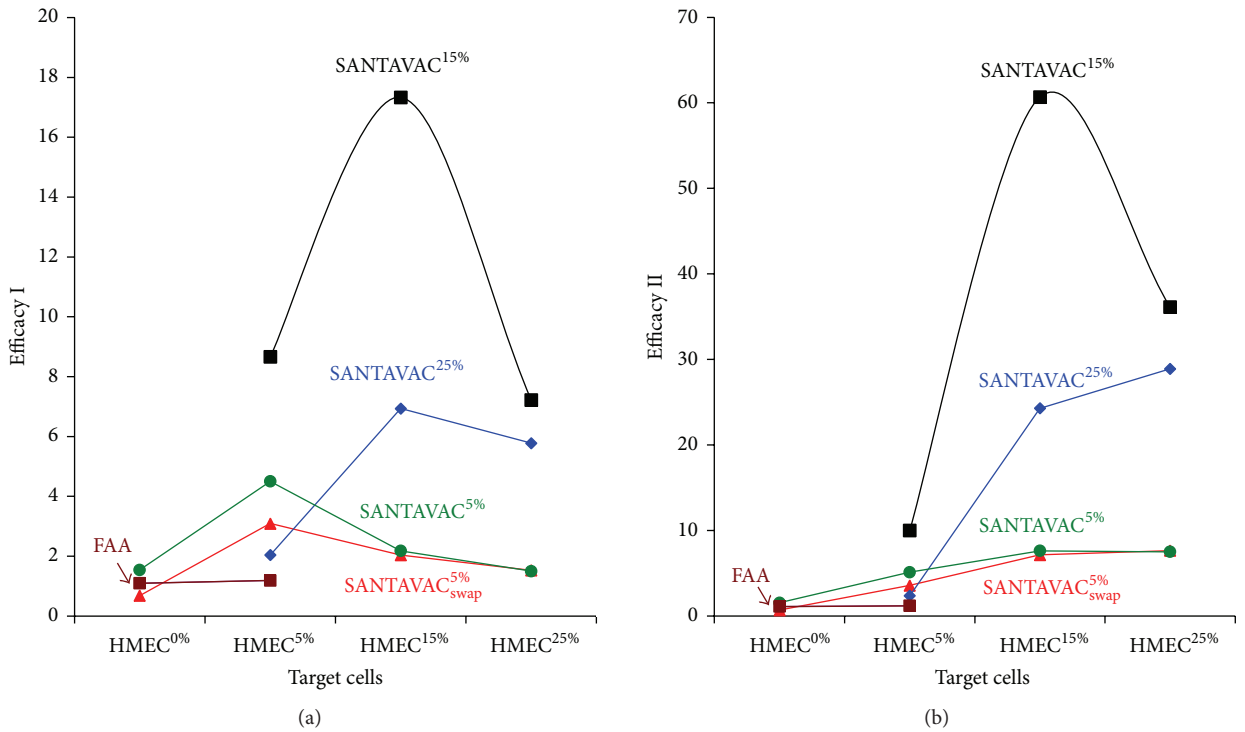

Figure 3: Efficacy I (a) and efficacy II (b) of target cell killing by SANTAVAC in CTA. Target HMEC were incubated in the presence of effector CTL at a 1 : 20 ratio. After 3 days, CTL were removed, target cells were carefully washed, and target cell viability was determined. Data is expressed as efficacy I (a) or efficacy II (b) of target cell killing by SANTAVAC. Efficacy I was calculated as a ratio of the number of *nonstimulated cells in control wells* (*i.e.*, $HMEC^{0\%}$) to the number of tumor-stimulated cells in experimental wells. Efficacy II was calculated as a ratio of the number *of tumor-stimulated cells in control wells* (*i.e.*, $HMEC^{5\%}$, $HMEC^{15\%}$, or $HMEC^{25\%}$) to the number of tumor-stimulated cells in experimental wells; that is, the percentage of tumor-conditioned medium in control wells was the same as in the experimental wells. Efficacy I allows *in vitro* estimation of the SANTAVAC efficacy by demonstrating how many endothelial cells in the tumor vasculature will be destroyed before 1 endothelial cell in normal tissue is destroyed (used to predict vaccine safety). Efficacy II allows *in vitro* estimation of the SANTAVAC efficacy by demonstrating the degree of HMEC proliferation suppression in the tumor vasculature and is used to establish the degree by which the vaccine can arrest tumor growth (predicted vaccine therapeutic effect). For efficacy calculation, the data representing the mean value of 3 independent measurements was used. "FAA" indicates the data related to the control (■) in CTA where fibroblast-associated antigens were used to simulate CTL. "*swap*" indicates CTA data where primary cell cultures used to generate antigens and primary cell cultures which were used as target cells were swapped (it was done to demonstrate the reproducibility of the CTA results at defined percentages of the tumor-conditioned medium used to stimulate HMEC). Percentage values indicated in the superscript correspond to the percentage of tumor-conditioned medium used to stimulate target HMEC or HMEC used to generate SANTAVAC for targeting immune response in CTA.

efficacy (defined by target cell destruction in the absence of damage to healthy tissues), the immune response elicited by alloantigens was safer and may have broader applications in the medical field.

To prepare allogeneic SANTAVAC, the following previously discovered observations relating to endothelial cell heterogeneity were considered: (i) the tumor influence on HMEC was not specific to the tumor type and HMEC heterogeneity was a result of differences in strength of this influence; (ii) there was a linear dependence between target cell killing rates and the similarity of cell surface profiles of target cells and cells used to generate surface antigens for targeting the immune response; and (iii) the increase in tumor-induced changes at the HMEC surface led to decreased immunogenicity of HMEC surface antigens [4]. In addition, one particular observation from previous experiments suggested that the strongest changes to the HMEC surface were induced by HepG2 cells. This research was therefore designed to measure target cell killing rates in CTA where alloantigens were derived from HMEC stimulated to grow following stimulation by HepG2 that possessed a different signal strength (from weak to strong stimuli) [4]. It was therefore expected that the CTA experiments would reveal the maximum efficacy of allogeneic SANTAVAC *in vitro*.

Figure 2 showed how tumor stimuli strength was selected to provide HMEC with the diversity of tumor-induced surface profiles. Weak stimuli corresponded to the tumor-conditioned medium that induced an HMEC proliferation rate slightly higher compared to proliferation of control HMEC. Moderate stimuli corresponded to the percentage of tumor-conditioned medium which provided HMEC proliferation at half the maximum rate. Strong stimuli corresponded to the percentage of tumor-conditioned medium used which provided HMEC the stimuli to proliferate at a high rate.

4.3. Cytotoxicity Assays (CTA). CTA revealed that HMEC with tumor-induced surface changes may be efficiently targeted by allogeneic SANTAVAC. This phenomenon was consistent with previously published data describing HMEC heterogeneity that established the foundation for the development of the SANTAVAC. Tumor cells induced unidirectional changes to the HMEC surface profiles resulting in a more similar antigen profile between target cell surface antigens and the surface antigen profile of cells used to generate antigens needed to target the immune response. As a consequence, the observed efficacy of SANTAVAC generated from $HMEC^{15\%}$ and $HMEC^{25\%}$ (i.e., $SANTAVAC^{15\%}$ and $SANTAVAC^{25\%}$, resp.) was sufficiently higher than the efficacy observed for control cells (*i.e.*, $HMEC^{0\%}$) and $SANTAVAC^{5\%}$. The high similarity between antigens present in SANTAVAC and the cell surface antigens expressed by target cells explains this observation.

The fact that target cell killing of $SANTAVAC^{15\%} \blacktriangleright HMEC^{15\%}$ was sufficiently higher than that of $SANTAVAC^{25\%} \blacktriangleright HMEC^{25\%}$ can be explained by one above-mentioned statement: that immunogenicity decreases with increasing tumor-induced changes to the HMEC antigen surface profile. Therefore, moderate tumor-induced changes to HMEC surface antigens would be preferable in the context of vaccine design resulting in efficacy I equal to 17.3 (safety) and efficacy II equal to 60 (capacity to arrest tumor growth). In this report two types of efficacy were described in relation to the allogeneic SANTAVAC vaccine. Efficacy I allowed for an *in vitro* estimation of the number of tumor vasculature endothelial cells that would be destroyed before one normal tissue endothelial cell would be destroyed. Efficacy II allowed for an *in vitro* estimation of the vaccine efficacy in the context of suppression of HMEC proliferation of the tumor vasculature and primarily is a reflection of the potential for the vaccine to arrest tumor growth; that is, it describes the vaccine's therapeutic effect.

It should be noted that stimuli of different strengths would be expected *in vivo* due to gradual diminishing growth stimuli in relation to increasing distance from the tumor cells. Therefore, it can be expected that HMEC with different target surface profiles, including profiles related to $HMEC^{15\%}$, will also be present in the tumor-associated vasculature.

5. Conclusion

Future studies in the field of vaccine development using allogeneic SANTAVAC are required; however, *in vitro* data presented in this report demonstrated that the allogeneic SANTAVAC was a perfect candidate for the development of a UCV with outstanding efficacy and safety. The SANTAVAC formulation described achieved efficacy equal to 17 and 60 in relation to *in vitro* prediction of vaccine safety and capacity to arrest tumor growth, respectively. Criteria critical to the development of such efficient allogeneic SANTAVAC are defined in this paper and may be used for preparing UCV for clinical trials.

Abbreviations

HMEC:	Human microvascular endothelial cells
DC:	Dendritic cells
SANTAVAC:	Set of All Natural Target Antigens for Vaccination Against Cancer
UCV:	Universal cancer vaccine
CTA:	Cytotoxicity assays
FAA:	Fibroblast-associated antigens
CTL:	Cytotoxic T lymphocytes.

Competing Interests

Petr G. Lokhov declares that he has patents relating to work described in this report in the context of cancer vaccine preparation.

Acknowledgments

This work was funded by BioBohemia Ltd. (Moscow, Russia).

References

[1] Y. Okaji, N. H. Tsuno, S. Saito et al., "Vaccines targeting tumour angiogenesis-a novel strategy for cancer immunotherapy," *European Journal of Surgical Oncology*, vol. 32, no. 4, pp. 363–370, 2006.

[2] M. N. Hart, K. L. Sadewasser, P. A. Cancilla, and L. E. DeBault, "Experimental autoimmune type of vasculitis resulting from activation of mouse lymphocytes to cultured endothelium," *Laboratory Investigation*, vol. 48, no. 4, pp. 419–427, 1983.

[3] M. Matsuda, "Experimental glomerular tissue injury induced by immunization with cultured endothelial cell plasma membrane," *Acta Pathologica Japonica*, vol. 38, no. 7, pp. 823–829, 1988.

[4] P. G. Lokhov and E. E. Balashova, "Tumor-induced endothelial cell surface heterogeneity directly affects endothelial cell escape from a cell-mediated immune response in vitro," *Human Vaccines & Immunotherapeutics*, vol. 9, no. 1, pp. 198–209, 2013.

[5] P. G. Lokhov and E. E. Balashova, "Universal cancer vaccine: an update on the design of cancer vaccines generated from endothelial cells," *Human Vaccines and Immunotherapeutics*, vol. 9, no. 7, pp. 1549–1552, 2013.

[6] P. G. Lokhov and E. E. Balashova, "Design of universal cancer vaccines using natural tumor vessel-specific antigens (SANTAVAC)," *Human Vaccines and Immunotherapeutics*, vol. 11, no. 3, pp. 689–698, 2015.

[7] L. Rittié and G. J. Fisher, "Isolation and culture of skin fibroblasts," *Methods in Molecular Medicine*, vol. 117, pp. 83–98, 2005.

[8] P. Lokhov, E. Balashova, and M. Dashtiev, "Cell proteomic footprint," *Rapid Communications in Mass Spectrometry*, vol. 23, no. 5, pp. 680–682, 2009.

[9] J. Folkman, C. C. Haudenschild, and B. R. Zetter, "Long-term culture of capillary endothelial cells," *Proceedings of the National Academy of Sciences of the United States of America*, vol. 76, no. 10, pp. 5217–5221, 1979.

[10] N. Romani, S. Gruner, D. Brang et al., "Proliferating dendritic cell progenitors in human blood," *The Journal of Experimental Medicine*, vol. 180, no. 1, pp. 83–93, 1994.

[11] C. O. Yun, K. F. Nolan, E. J. Beecham, R. A. Reisfeld, and R. P. Junghans, "Targeting of T lymphocytes to melanoma cells through chimeric anti-GD3 immunoglobulin t-cell receptors," *Neoplasia*, vol. 2, no. 5, pp. 449–459, 2000.

[12] C. L.-L. Chiang, F. Benencia, and G. Coukos, "Whole tumor antigen vaccines," *Seminars in Immunology*, vol. 22, no. 3, pp. 132–143, 2010.

[13] T. D. De Gruijl, A. J. M. Van Den Eertwegh, H. M. Pinedo, and R. J. Scheper, "Whole-cell cancer vaccination: from autologous to allogeneic tumor- and dendritic cell-based vaccines," *Cancer Immunology, Immunotherapy*, vol. 57, no. 10, pp. 1569–1577, 2008.

[14] M. A. Cheever, J. P. Allison, A. S. Ferris et al., "The prioritization of cancer antigens: a National Cancer Institute pilot project for the acceleration of translational research," *Clinical Cancer Research*, vol. 15, no. 17, pp. 5323–5337, 2009.

[15] J. M. Lang, A.-C. Andrei, and D. G. McNeel, "Prioritization of cancer antigens: keeping the target in sight," *Expert Review of Vaccines*, vol. 8, no. 12, pp. 1657–1661, 2009.

[16] E. E. Balashova and P. G. Lokhov, "Proteolytically-cleaved fragments of cell-surface proteins from live tumor cells stimulate anti-tumor immune response in vitro," *Journal of Carcinogenesis & Mutagenesis*, vol. 1, article 103, 2010.

[17] E. E. Balashova and P. G. Lokhov, "Proteolytically-cleaved fragments of cell surface proteins stimulate a cytotoxic immune response against tumoractivated endothelial cells in vitro," *Journal of Cancer Science & Therapy*, vol. 2, no. 5, pp. 126–131, 2010.

[18] E. E. Balashova, M. I. Dashtiev, and P. G. Lokhov, "Proteomic footprinting of drug-treated cancer cells as a measure of cellular vaccine efficacy for the prevention of cancer recurrence," *Molecular & Cellular Proteomics*, vol. 11, no. 2, 2012.

Hindawi Publishing Corporation
Journal of Immunology Research
Volume 2016, Article ID 6078473, 17 pages
http://dx.doi.org/10.1155/2016/6078473

Research Article

Transcriptional Targeting of Mature Dendritic Cells with Adenoviral Vectors via a Modular Promoter System for Antigen Expression and Functional Manipulation

Ilka Knippertz,[1] Andrea Deinzer,[1] Jan Dörrie,[2] Niels Schaft,[2] Dirk M. Nettelbeck,[3] and Alexander Steinkasserer[1]

[1]*Department of Immune Modulation at the Department of Dermatology, Universitätsklinikum Erlangen, Hartmannstrasse 14, 91052 Erlangen, Germany*
[2]*Department of Dermatology, Universitätsklinikum Erlangen, Hartmannstrasse 14, 91052 Erlangen, Germany*
[3]*German Cancer Research Center, Im Neuenheimer Feld 280, 69120 Heidelberg, Germany*

Correspondence should be addressed to Ilka Knippertz; ilka.knippertz@uk-erlangen.de

Received 17 March 2016; Accepted 29 May 2016

Academic Editor: Pablo González

To specifically target dendritic cells (DCs) to simultaneously express different therapeutic transgenes for inducing immune responses against tumors, we used a combined promoter system of adenoviral vectors. We selected a 216 bp short Hsp70B′ core promoter induced by a mutated, constitutively active heat shock factor (mHSF) 1 to drive strong gene expression of therapeutic transgenes MelanA, BclxL, and IL-12p70 in HeLa cells, as well as in mature DCs (mDCs). As this involves overexpressing mHSF1, we first evaluated the resulting effects on DCs regarding upregulation of heat shock proteins and maturation markers, toxicity, cytokine profile, and capacity to induce antigen-specific $CD8^+$ T cells. Second, we generated the two-vector-based "modular promoter" system, where one vector contains the mHSF1 under the control of the human CD83 promoter, which is specifically active only in DCs and after maturation. mHSF1, in turn, activates the Hsp70B′ core promotor-driven expression of transgenes MelanA and IL-12p70 in the DC-like cell line XS52 and in human mature and hence immunogenic DCs, but not in tolerogenic immature DCs. These *in vitro* experiments provide the basis for an *in vivo* targeting of mature DCs for the expression of multiple transgenes. Therefore, this modular promoter system represents a promising tool for future DC-based immunotherapies *in vivo*.

1. Introduction

Dendritic cells (DCs) function as sentinels at the interface of the innate and the adaptive immune system, thereby inducing highly potent and antigen-specific immune responses triggered by "danger" signals. As master antigen-presenting cells (APCs), they not only express proinflammatory cytokines (particularly IL-12) but also capture, process, and present antigens on major histocompatibility (MHC) molecules to naïve T cells, leading to an adaptive T cell-mediated immune response [1]. Importantly, DCs possess the unique feature to cross-present typical MHC class II restricted antigens via MHC class I, thereby inducing cytotoxic $CD8^+$ cell (CTL) responses and enhancing antitumor humoral responses [2, 3]. In this context, DCs have been shown to have a significant impact on oncogenesis, tumor progression, and response to therapy in various preclinical tumor models and preclinical studies [4]. Additionally, the discovery of immune checkpoint blockers (e.g., monoclonal antibody [mAb] to CTLA-4; mAb to PD-1) and their possible combination with DC vaccination has made cancer immunotherapy one of the most exciting topics in the oncology field recently [5, 6]. The main DC-based anticancer interventions developed so far comprise various *ex vivo* and *in vivo* immune manipulating strategies. *Ex vivo*, DCs were loaded with different tumor associated antigens (TAAs) using various strategies including (i) peptide or protein pulsing, (ii) loading with complete tumor lysate or (iii) tumor apoptotic bodies, and (iv) RNA transfection

or (v) viral transduction [7]. *In vivo*, cancer antigens can be delivered to DCs by fusing them to monoclonal antibodies specifically targeting DC surface receptors such as mannose receptor, C type 1 (MRC1), CD209 (DC-SIGN), or DEC-205 [7–10]. Another strategy is to incorporate TAAs, DNA, RNA, or toll-like receptor ligands into DC-targeting immunoliposomes, nanoparticles, or viral vectors for delivery [11–14].

In recent years, viral vectors like lentiviruses or adenoviruses (Ads) have been widely used in clinical trials for many different types of inherited or acquired disorders with Ad vectors being the ones most commonly used for cancer gene therapy [15, 16]. Adenoviruses have many advantages as they (i) can be grown into high titer stable stocks, (ii) infect nondividing and dividing cells of different types, (iii) are maintained in cells as an episome, and (iv) have been proven safe and well tolerated while also being therapeutically active [16]. Most Ad vectors are genetically modified versions of Ad5 and can be either replication-defective or replication-competent. Replication-defective Ad vectors are effectively used as gene delivery vehicles and have the essential E1A, E1B, and E3 genes deleted and replaced by an expression cassette encoding for foreign therapeutic transgenes up to ~6.5 kb in size [16]. Specific targeting of a cell (e.g., a DC) can be achieved by transductional or transcriptional targeting or a combination of both. Transductional targeting involves chemically or genetically modifying an adenovirus to redirect its tropism from its natural binding partner CAR (coxsackie and adenovirus receptor) to a new target expressed preferentially on the target cell like, for example, DC-SIGN or DEC-205 for DCs [17]. Transcriptional targeting, on the other hand, involves using tissue-specific promoters to genetically limit expression of the introduced gene to distinct tissues [17].

However, there was no cell type- and maturation-specific promoter available for DCs until recently. In 2013, we identified and characterized a tripartite promoter complex specifically regulating human CD83 expression in mature immunogenic DCs. We found that it consisted of a 261 bp core promoter flanked by (i) a 164 bp upstream regulatory element and (ii) a 185 bp downstream enhancer separated from the promoter by a 500 bp noncoding spacer sequence [18]. All three elements were shown to be essential for transcriptional activation in mature immunogenic DCs, while not mediating this specific activation in tolerogenic immature DCs (iDCs), or other CD83-positive cell types, such as subsets of activated B or T cells. Thus, this promoter complex shows great potential for the transcriptional targeting of mature DCs and thereby the development of new immunotherapeutic approaches.

Despite the successes of DC-based immunotherapy in individual patients, the immunogenic potential to induce effective antitumor CTL responses is still considered suboptimal [19]. Furthermore, the *ex vivo* generation of DC-vaccines is laborious and expensive. Hence, new vaccination strategies involving *in vivo* targeting of DCs for antigen expression and functional manipulation should be addressed. To do this, we developed a combined promoter system to transcriptionally target human DCs to express several therapeutic transgenes at the same time, the "modular promoter (MP)" system. Due to the limited space for foreign DNA in adenoviral vectors, it is problematic to use large, cell-specific promoters for several transgenes. Therefore, we combined the cell type- and maturation-specific CD83 promoter, which has a size of 1.2 kb [18], with another short and induction-specific promoter in a two-vector system. In this system, the transgenes in one vector are under the control of a short inducible promoter, which is activated by a factor, expressed from the larger, highly specific CD83 promotor in the second vector. As a short, inducible promoter we chose the short heat shock protein (Hsp) 70B′ promoter, which has been reported before to mediate specifically heat-dependent transgene expression in replication-deficient adenoviruses [20]. The *hsp70B′* gene, along with *hsp70(A)-1*, *hsp70(A)-2,* and *hsp70B,* belongs to the *hsp70* gene family, all regulated by the heat shock transcription factor 1 (HSF1) [20–23]. HSF1 is a highly conserved transcription factor that coordinates stress-induced transcription and directs versatile physiological processes in eukaryotes [24]. Upon induction, it undergoes trimerization, as well as phosphorylation, followed by nuclear translocation and DNA binding to heat shock promoters [25].

For our MP system we used a mutated, constitutively active HSF1 (mHSF1) [26] whose expression is controlled here by the DC- and maturation-specific human CD83 promoter [18]. In turn, mHSF1 then binds to the short heat shock response element Hsp70B′ driving the simultaneous expression of multiple therapeutic transgenes. Concomitantly, mHSF1 also binds to endogenous heat shock promoters of targeted DCs. We have shown previously that exposure of human DCs to thermal stress leads to an upregulation of Hsp70A, costimulatory molecules, and proinflammatory cytokines, as well as a markedly improved capacity to prime autologous naïve $CD8^+$ T cells *in vitro* [27]. Therefore, in the present study we also analyzed the effects of mHSF1 overexpression on DCs.

Our results demonstrate that the newly generated MP system allows, for the first time, specific and simultaneous expression of different therapeutic transgenes in human mature DCs *in vitro*, representing a promising tool to improve future DC-based immunotherapies. Moreover, we found no effects regarding the viability, maturation, and function of DCs by overexpressing mHSF1.

2. Methods

2.1. Human Dendritic Cells and $CD8^+$ T Cells. Generation of human monocyte-derived dendritic cells (DCs) was performed as previously described [28]. In brief, peripheral blood mononuclear cells (PBMCs) were prepared from leukoreduction system chambers (LRSCs) of healthy donors by density centrifugation, followed by plastic adherence on tissue culture dishes (BD Falcon, MA, US). The nonadherent fraction was stored at −80°C for isolation of autologous $CD8^+$ T cells, while the adherent cell fraction was cultured for 4 days in DC-medium consisting of RPMI 1640 (Lonza, Basel, Switzerland) supplemented with 1% (vol/vol) of heat-inactivated human serum type AB (Lonza), 1% Penicillin/Streptomycin/L-Glutamine (Sigma-Aldrich, St. Louis, MO, US), and 10 mM Hepes (Lonza) as well as

800 IU/mL (day 0) or 400 IU/mL (day 3) recombinant human granulocyte macrophage colony-stimulating factor (GM-CSF) and 250 IU/mL (day 0 and 3) recombinant IL-4 (both Miltenyi, Bergisch-Gladbach, Germany). On day 4, immature DCs (iDCs) were used for further experiments. Maturation of DCs was induced by the addition of a maturation cocktail (MC) consisting of 200 U/mL IL-1β, 1000 U/mL IL-6 (both CellGenix, Freiburg, Germany), 10 ng/mL TNF-α (Beromun; Boehringer Ingelheim, Germany), and 1 μg/mL PGE_2 (Prostin E_2, Pfizer, NY, US) for 24 or 48 hours or by 0.1 ng/mL lipopolysaccharide (LPS; Sigma-Aldrich) for 20 hours. For the isolation of autologous $CD8^+$ T cells the nonadherent fraction was thawed and $CD8^+$ T cells were isolated using anti-CD8 MACS beads (Miltenyi) according to the manufacturer's instructions. Afterwards cells were cultured in RPMI 1640 (Lonza) medium additionally containing 10% (vol/vol) of heat-inactivated human serum type AB (Lonza), 1% L-Glutamine (Sigma-Aldrich), 20 mg/L gentamycin, 10 mM Hepes (Lonza), 1 mM sodium pyruvate (Lonza), and 1% MEM nonessential aa (PAN Biotech, Aidenbach, Germany). Cryopreservation and thawing of $CD8^+$ T cells were performed as described elsewhere [29]. Cell counting was performed by using a Neubauer counting chamber and Trypan Blue for exclusion of dead cells. Whenever relevant, HLA-$A0201^+$ donor material was used.

2.2. Approvals and Legal Requirements. For the generation of PBMCs, moDCs, and $CD8^+$ T cells from LRSCs of healthy donors, the positive vote from the local ethics committee was obtained (ethics vote number 4556).

2.3. Cell Lines. HeLa cells were cultured in Dulbecco's Modified Eagle Medium (DMEM; Lonza) supplemented with 10% (vol/vol) FCS (PAA/GE Healthcare, Little Chalfont, UK) and 1% (vol/vol) Penicillin/Streptomycin/L-Glutamine (Sigma-Aldrich). XS52 cells, kindly provided by A. Takashima (University of Texas Southwestern Medical Center, Dallas, TX, US), were cultured in Iscove's Modified Dulbecco's Medium (IMDM; Lonza) supplemented with 10% (vol/vol) FCS, 1% (vol/vol) Penicillin/Streptomycin/L-Glutamine, 1% (vol/vol) sodium pyruvate (Lonza), 10% (vol/vol) NS47 supernatant, and 10 ng/mL murine GM-CSF. 293 (Quantum) cells were cultured in RPMI 1640 (Lonza) supplemented with 10% (vol/vol) FCS and 1% (vol/vol) Penicillin/Streptomycin/L-Glutamine.

2.4. Plasmid Vectors. The promoterless pGL3-Basic luciferase reporter vector (Promega, WI, US) was used for determination of vector-related background activity and to generate pHsp70B$'_{-29/-489}$ and pHsp70B$'_{-29/-242}$ by digesting the human *hsp70B* gene 5$'$-region (according to GenBank accession no. X13229) with HindIII/BamHI or HindIII/SmaI, respectively. pHsp70B$'_{-29/-242}$ was then used to generate pMelA, pBclxL, and pIL-12 by replacing the luciferase gene by the open reading frame sequences of either MelanA/MART-1, Bcl-xL, or the human single-chain of IL-12(p70) [30] (kindly provided by F. Schnieders, Provecs Medical GmbH, Hamburg, Germany). The vector pMelA/BclxL/IL-12 was then generated by the sequential connection of the expression cassettes Hsp70B$'_{-29/-242}$-MelanA/, Hsp70B$'_{-29/-242}$-BclxL/, and Hsp70B$'_{-29/-242}$-IL-12(p70). Plasmids expressing mHSF1 under the control of the human CD83 promoter (P-510) were manufactured by replacing the luciferase gene by the open reading frame sequence of mHSF1 [26] (kindly provided by R. Voellmy, HSF Pharmaceuticals, Fribourg, Switzerland) of pGL3-CD83 promoter constructs described before [18], resulting in pP-510/mHSF1, pEs/P-510/mHSF1, and pEas/P-510/mHSF1. All constructs were generated by standard cloning procedures.

The pGL3-Promoter vector (Promega), containing a SV40 promoter, was used as a positive control and to determine transfection efficacy.

All plasmids for transient transfection experiments were purified by standard endo-free anion-exchange columns (Qiagen, Hilden, Germany) and verified by DNA sequencing (MWG Biotech, Ebersberg, Germany).

2.5. Recombinant Adenoviruses. Ad5MelA/BclxL/IL-12, Ad5-MP2, Ad5mHSF1, Ad5P-510/mHSF1, Ad5Es/P-510/mHSF1, Ad5Eas/P-510/mHSF1, Ad5MelA, Ad5Luc1, and Ad5TL are first generation, E1- and E3-deleted, replication-deficient adenoviral vectors. Ad5mHSF1 contains mHSF1 [26] under the control of a CMV promoter, kindly provided by R. Voellmy (HSF Pharmaceuticals, Fribourg, Switzerland). Ad5Luc1 contains a CMV-firefly luciferase cassette and Ad5TL contains both a CMV-firefly luciferase cassette and a CMV-GFP cassette (both kindly provided by D. T. Curiel, Washington University School of Medicine, MO, US). All other replication-deficient adenoviruses were cloned as follows: a gene cassette containing either a Hsp70B$'_{-29/-242}$-MelanA/Hsp70B$'_{-29/-242}$-BclxL/Hsp70B$'_{-29/-242}$-IL-12(p70)-, a Hsp70B$'_{-29/-242}$-MelanA/Hsp70B$'_{-29/-242}$-IL-12(p70)- (MP2), a P-510-mHSF1-, Es/P-510-mHSF1-, Eas/P-510-mHSF1-, or a CMV-MelanA sequence was inserted into pShuttle. Virus genomes were obtained by homologous recombination of the corresponding shuttle plasmids containing the different expression cassettes indicated above with pAdEasy-1 in *E. coli* BJ5183 as described before [31]. Adenovirus particles were produced by transfection of the different PacI-digested pAd vectors into 293 cells using Lipofectamine (Invitrogen/Life Technologies, CA, US). All viruses were amplified in 293 cells and purified by two rounds of CsCl equilibrium density gradient ultracentrifugation. Verification of viral genomes and exclusion of wild-type contamination were performed by PCR. Physical particle concentration [viral particles (vp)/mL] was determined by OD_{260} reading and infectious particle concentration was determined by $TCID_{50}$ assay on 293 cells.

2.6. Transfection of Cell Lines. For transfection of HeLa cells, 5×10^4 or 8×10^4 cells were seeded in a 24-well or 12-well plate (BD Falcon) in a final volume of 500 μL or 1 mL growth medium per well, respectively. The next day, HeLa cells were transfected using *Lipofectamine*™ LTX with *Plus*™ reagent (Invitrogen/Life Technologies) according to the manufacturer's protocol with a total amount of 0.5 μg (24-well) or 0.7 μg (12-well) DNA. Twenty-four hours later, cells

were transduced with adenoviruses at 300 $TCID_{50}$/cell in a final volume of 200 μL DMEM (Lonza) containing 2% FCS (PAA/GE Healthcare). After 1.5 hours of incubation at room temperature on a rocker, 800 μL (24-well) or 2 mL (12-well) growth medium was added. Cells were harvested for further experiments one day after transduction.

For transfection of XS52 cells, 5×10^5 cells were seeded in a 6-well plate (BD Falcon) in a final volume of 2 mL cell growth medium per well. The following day, cells were transduced using X-tremeGENE™ HP DNA Transfection Reagent (Roche, Basel, Switzerland) according to the manufacturer's instructions with 2 μg DNA and 6 μL transfection reagent in a final volume of 200 μL Opti-MEM I Reduced Serum Medium (Gibco/ThermoFisher Scientific, MA, US). Four hours after transfection, 2 mL of growth medium was added and cells were incubated for another 24 hours at 37°C/5% CO_2 before they were used for further analyses.

2.7. Adenoviral Transduction of Dendritic Cells. Immature d4 DCs were seeded in 12-well tissue culture plates (BD Falcon) at a concentration of 1×10^6 cells/well in 250 μL medium supplemented with either 800 U/mL GM-CSF and 500 U/mL IL-4 (for iDCs) or the maturation cocktail consisting of 400 U/mL IL-1β, 2000 U/mL IL-6, 20 ng/mL TNF-α, and 2 μg/mL PGE_2, in addition to IL-4 and GM-CSF (for mDCs). When indicated, 0.1 ng/mL LPS were used instead of the cytokine cocktail, which was added to the cell culture after the transduction. Adenovirus was added to the cells at 500 $TCID_{50}$/cell in a final volume of 250 μL medium without cytokines. For cotransduction of two adenoviruses, the final volume was halved to 125 μL medium without cytokines, also resulting in a final infection volume of 500 μL. After 1.5 hours of incubation at room temperature, 2 mL of growth medium replenished with cytokines as described before was added per well. To determine transduction efficacy, cells were transduced with Ad5TL and the percentage of living green fluorescent cells was assessed by flow cytometric analysis with a FACScan cell analyzer (BD Biosciences, NJ, US). Only experiments that yielded transduction efficiencies of more than 70% were evaluated and are shown.

2.8. Transfection and Peptide Pulsing of Dendritic Cells. Immature DCs were transduced with Ad5Luc1 or Ad5mHSF1 or medium-treated in the presence of the cytokine maturation cocktail as described above. The next day, transfection of mature DCs with MelanA/MART-1 RNA was performed using the nonlipid cationic reagent Transmessenger™ transfection kit (Qiagen) following an adapted protocol from Liao et al. [32] as described previously in detail by Schaft et al. [33]. For peptide pulsing, mature DCs were incubated with 10 μg/mL of the MelanA-derived HLA-A2-binding analogue peptide ELAGIGILTV in DC cell culture medium for 1 hour at 37°C/5% CO_2.

2.9. Priming and Tetramer Staining of $CD8^+$ T Cells. MelanA RNA-transfected or MelanA peptide-loaded mature DCs were used to stimulate autologous MACS-sorted $CD8^+$ T cells at a ratio of 1 : 10 for one week at 37°C/5% CO_2. Fresh T cell medium was added when necessary and on days 2 and 4 1000 IU/mL IL-2 (Novartis, Nürnberg, Germany) and 10 ng/mL IL-7 were supplemented. On day 7, cells were harvested and stained with a HLA-A2-MelanA/iTag MHC class I-tetramer (Beckmann Coulter, Krefeld, Germany) in combination with an anti-CD8-PC7 antibody (Beckmann Coulter). Finally, cells were analyzed using a FC500 cytofluorometer (Beckmann Coulter).

2.10. Flow Cytometric Analyses. Cells were stained with specific mAb or appropriate isotype controls for 30 min at 4°C in FACS buffer (Dulbecco's PBS [Lonza] containing 2% FCS [PAA/GE Healthcare]), washed twice, and finally resuspended in cold FACS buffer containing 0.1 μg/mL propidium iodide (PI) (Carl Roth, Karlsruhe, Germany). Stained cells were immediately analyzed with a FACScan cell analyzer (BD Biosciences). Cell debris and dead cells were excluded from the analyses by gating on proper forward and sideward light scatter and on PI negative cells. Also, percentages of PI positive cells were calculated using this gating strategy. A minimum of 10^4 living cells was measured for each sample and results were analyzed using FCS Express 4 Flow Cytometry Software (De Novo Software, CA, US). The following monoclonal antibodies (all from BD Biosciences) were used to determine the phenotype of DCs: PE-labeled mouse anti-human CD25 (M-A251), CD80 (L307.4), CD83 (HB15e), CD86 (IT2.2), HLA-ABC (G46-2.6), and HLA-DR (G46.6). Isotype mAb controls (all from BD Biosciences) used but not shown were IgG1-PE (MOPC-21), IgG2a-PE (G155-178), and IgG2b-PE (27-35).

2.11. Cytometric Bead Array. Inflammatory cytokines secreted by DCs into the supernatant were assessed using the Human Inflammatory Cytokine Cytometric Bead Array (CBA; BD Biosciences) according to the manufacturer's protocol.

2.12. ELISA. IL-12p40 and IL-12p70 concentrations in cell culture supernatants were determined by standard two-site sandwich BD OptEIA™ Human IL-12 (p70) and Human IL-12 (p40) ELISA Kits (BD Biosciences) according to the manufacturer's manual.

2.13. BCA Protein Assay. Protein concentrations of cell lysates for SDS-PAGE and luciferase reporter assays were determined by Pierce™ Protein Assay Kit (ThermoFisher Scientific, MA, US) according to the manufacturer's protocol.

2.14. SDS-PAGE and Western Blotting. Whole cell extracts for SDS-PAGE were generated as follows: 1×10^6 DCs or XS52 cells were washed with ice-cold PBS and then resuspended in 50 μL lysis buffer mixed with $NaVO_3$, NaF, and PMSF. Afterwards, protein concentrations were determined by the BCA protein assay described above. To prepare sample proteins, they were boiled in the presence of a loading dye mixed with SDS and 2-mercaptoethanol for 10 min at 95°C. Then, 20 to 30 μg of total protein per sample was separated on a 12.5% polyacrylamide gel and afterwards transferred onto nitrocellulose filters (Schleicher & Schüll/GE Healthcare, UK) with a pore size of 0.2 μm with the wet blotting

device "Mini-Protean II Cell and System" (BioRad, CA, US). Membranes were incubated with primary antibodies (Abs) diluted 1 : 1000–1 : 100 against HSF1, Hsp40, Hsp70A (C92F3A-5), Hsp70B′, Hsp90 (AC-88), Grp94 (9G10) all from Stressgen (distributed by Biomol, Hamburg, Germany), BclxL (2H12; Calbiochem/Merck-Millipore, Darmstadt, Germany), MelanA (A103; Sigma-Aldrich), or *beta*-actin (AC-74; Sigma-Aldrich), followed by HRP-conjugated horse anti-mouse IgG, goat anti-rabbit IgG, or goat anti-rat IgG Abs (all Cell Signaling Technology, UK) diluted 1 : 10000–1 : 2000. Detection was performed with the chemiluminescent Pierce ECL Western Blotting Substrate (ThermoFisher Scientific) on a high performance chemiluminescence film (GE Healthcare).

2.15. Luciferase Reporter Assay. Luciferase activity was measured using the luciferase assay system (Promega) according to the manufacturer's instructions, but utilizing 50 μL of luciferase assay reagent and 10 μL of cell lysate. Relative luminescence units (RLUs) were obtained with a Wallac Victor plate reader (PerkinElmer, MA, US). RLUs were normalized to the protein concentration as determined using the Pierce BCA™ Protein Assay Kit (ThermoFisher Scientific).

2.16. Statistical Analyses. The significance of differences was determined by using either one-way ANOVA or two-way ANOVA and Bonferroni's Multiple Comparison *post hoc* test; P values < 0.05 were considered statistically significant.

3. Results

3.1. The "Modular Promoter" System. We considered two aspects to be important for the development of a combined promoter system, the so-called modular promoter (MP) system, to transcriptionally target DCs. On the one hand, the system should be highly specific for the targeted DC and on the other hand, the therapeutic transgenes should be expressed very efficiently. As there is only limited space for foreign DNA in plasmid and especially viral vectors, we envisioned a dual vector system, in which one vector expresses a mutated, constitutively active heat shock factor (mHSF) 1 [26] under the control of the human mDC-specific CD83 promoter [18] (Figure 1(a)). The mHSF1, in turn, will then induce simultaneous expression of different therapeutic transgenes contained in the second vector, such as tumor antigens, proinflammatory cytokines, or apoptosis inhibitors, by binding to the short heat shock response elements (HRE; Figure 1(a)). We hypothesized that the expression of tumor antigens in combination with different therapeutic proteins will subsequently enhance the capacity of these modified DCs to induce improved and potent antitumoral immune responses.

Of note, mHSF1 may also induce the expression of different endogenous heat shock proteins, such as Hsp70 or Hsp90, by binding to the cellular HRE (Figure 1(b)). Therefore, it was indispensable to examine the resulting effects of an overexpression of mHSF1 on DCs, especially regarding (i) expression of phenotypic cell surface maturation markers, (ii) toxicity, and (iii) function.

3.2. Specific Induction of the Short pHsp70B′$_{-29/-242}$ Promoter in HeLa Cells. To develop a new and efficient dual promoter-based transcriptional DC-targeting strategy, we initially compared the activity of two different promoter fragments derived from the 5′ region of the human *hsp70B* gene. In 1985, Richard Voellmy isolated and characterized a 450 bp BamHI/HindIII fragment of a 70,000-dalton heat shock protein segment (Hsp70) involved in the control of transcription and translation of heat shock proteins [34]. Later, Schiller and colleagues reported this copy of the *hsp70* gene as the *hsp70B* gene [35]. Four cis-acting heat shock regulatory sequences (HSE 1–4) were described, which were supposed to contribute to the Hsp70B promoter activity. Additionally, HSE 1–3 (within a short fragment of ~200 bp in the 5′ nontranscribed region) were shown to be sufficient for optimal activity in human HeLa cells. To determine if the shorter element is sufficient, we cloned a −29/−489 bp and a −29/−242 bp fragment of the human *hsp70B* gene 5′ region (according to GenBank accession no. X13229) into the pGL3-Basic luciferase reporter vector resulting in pHsp70B$_{-29/-489}$ and pHsp70B$_{-29/-242}$, respectively (Figure 2(a)). Afterwards, plasmids were used to transfect HeLa cells. As a control we used the promoterless pGL3-Basic ("Basic") and the pGL3-SV40-Promoter ("SV40") vector. The next day, transcriptional activity was induced by the transduction of HeLa cells with an adenovirus encoding for a mutant constitutively active HSF1 (Ad5mHSF1). Transduction with Ad5Luc1 or Mock treatment served as controls. Twenty-four hours later, a luciferase reporter assay was performed and results were normalized relative to the respective pGL3-SV40-Promoter control. As shown in Figure 2(b), the Hsp70B$_{-29/-489}$ and Hsp70B$_{-29/-242}$ promoter were exclusively induced by Ad5mHSF1 up to 16-fold relative to the SV40 promoter, whereas there was no induction in the Mock sample or by the control virus. Furthermore, neither Ad5Luc1 nor Ad5mHSF1 influenced the transcriptional activity of the SV40 promoter and the Basic vector. Interestingly, there was no difference in the promoter activity when directly comparing the long Hsp70B$_{-29/-489}$ with the short Hsp70B$_{-29/-242}$ promoter, but looking closely at the Mock-treated versus the Ad5mHSF1-transduced cells for each promoter, we found an increase of up to 40 times for the longer promoter fragment and up to 64 times for the shorter one. Finally, the Hsp70B$_{-29/-242}$ promoter was listed as the Hsp70B′ (HSPA6) promoter in the GenBank (accession no. NM_002155) in 2004.

Thus, we identified the Hsp70B′$_{-29/-242}$ promoter to be highly and specifically induced in HeLa cells and for this reason it was used in the following experiments to generate the "modular promoter" system.

3.3. Multiple Therapeutic Transgenes Can Be Simultaneously Expressed under the Control of the Hsp70B′$_{-29/-242}$ Promoter. In order to prove our concept that mHSF1 can induce not only the expression of single transgenes but also the simultaneous expression of several transgenes under the control of the Hsp70B′$_{-29/-242}$ promoter, we generated plasmid vectors containing either a Hsp70B′$_{-29/-242}$-MelA/MART-1 ("pMelA"), a Hsp70B′$_{-29/-242}$-BclxL ("pBclxL"),

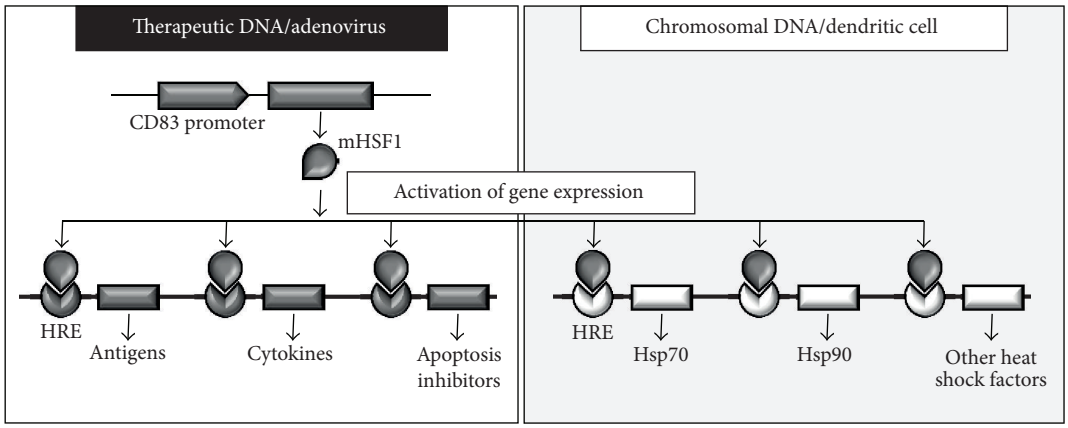

Figure 1: Schematic representation of the therapeutic DNA/adenovirus strategy and the effects of mHSF1 overexpression on endogenous heat shock response elements. (a) A constitutively active mutant heat shock factor 1 (mHSF1) will be expressed under the control of the human mDC-specific CD83 promoter. In turn mHSF1 binds to short heat shock response elements (HRE) of a second vector-encoded DNA driving expression of therapeutic transgenes (e.g., antigens, cytokines, or apoptosis inhibitors). (b) By overexpressing mHSF1 in the target cell, also endogenous HRE will become activated resulting in the expression of different heat shock proteins (Hsp), such as Hsp70 or Hsp90.

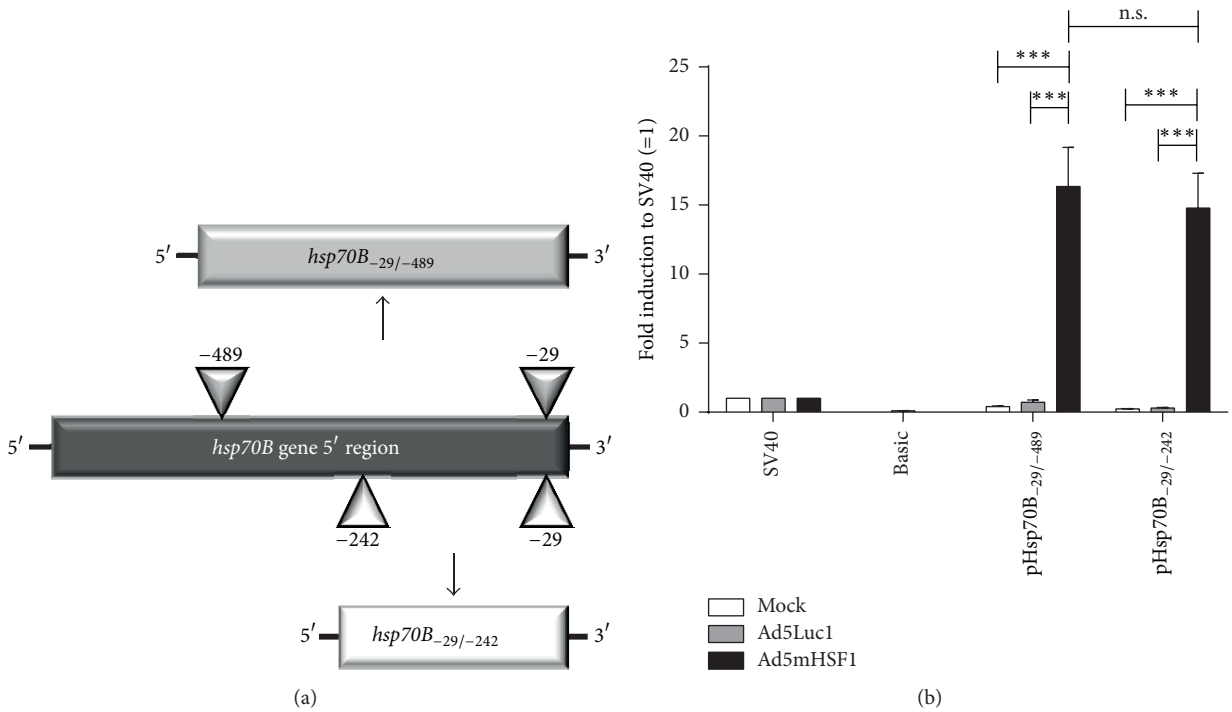

Figure 2: Generation and evaluation of two different Hsp70B heat shock response elements. (a) Plasmid vectors containing $Hsp70B_{-29/-489}$ and $Hsp70B_{-29/-242}$ were generated by digesting the human *hsp70B* gene 5′-region with HindIII/BamHI or HindIII/SmaI, respectively, followed by ligation into the pGL3Basic vector. (b) HeLa cells were transfected with 0.5 μg of plasmid DNA of pGL3-SV40-promoter vector ("SV40"), promoterless pGL3-Basic vector ("Basic"), $pHsp70B_{-29/-489}$, or $pHsp70B_{-29/-242}$. The next day, cells were either left untreated ("Mock") or transduced with adenoviruses Ad5Luc1 or Ad5mHSF1 at 300 $TCID_{50}$/cell. Twenty-four hours later, cells were harvested and analyzed by luciferase reporter assays. Results are shown as fold induction relative to the individual pGL3-SV40-promoter control containing no virus, Ad5Luc1 or Ad5mHSF1. Data are mean ± SEM of three independent experiments. $^{***}P < 0.001$, n.s.: not significant ($P > 0.05$); bars without annotation are not significant ($P > 0.05$); two-way ANOVA with Bonferroni's Multiple Comparison *post hoc* test.

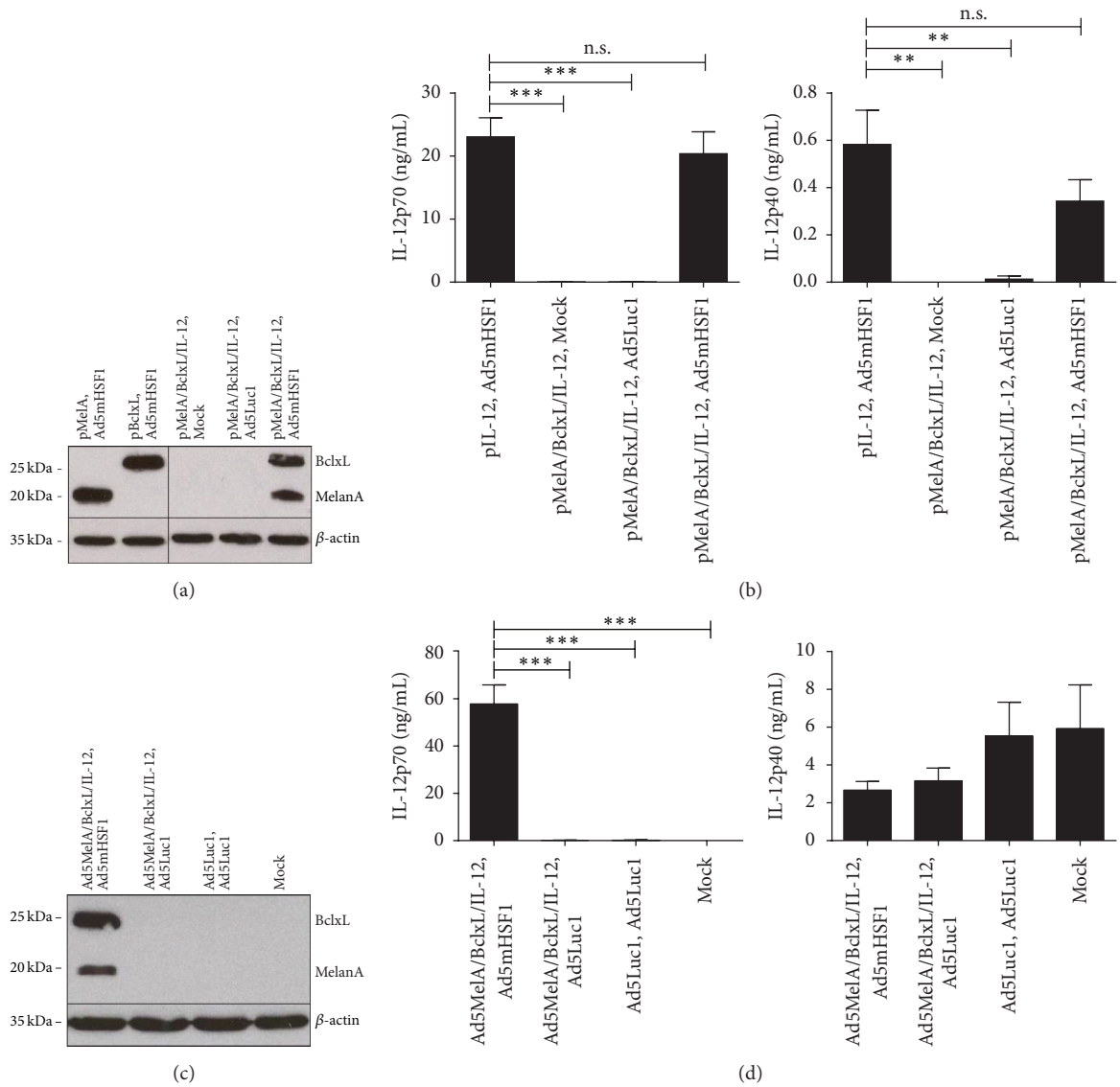

FIGURE 3: The constitutively active mHSF1 induces specific transgene expression in HeLa cells and human DCs. (a, b) HeLa cells were transfected with 0.7 μg DNA of plasmid vectors expressing MelanA/MART-1 ("MelA"), BclxL or/and IL-12 under the control of the Hsp70B$'_{-29/-242}$ heat shock response element as indicated. The next day, cells were either left untreated ("Mock") or transduced with adenoviruses Ad5Luc1 or Ad5mHSF1 at 300 $TCID_{50}$/cell. (c, d) Human immature DCs were cotransduced in the presence of the maturation cytokine cocktail with adenoviruses as indicated at a total amount of 500 $TCID_{50}$/cell. (a–d) Twenty-four hours later, cell lysates were analyzed for BclxL and MelanA expression by Western Blot (a, c) and cell culture supernatants for content of IL-12p40 and IL-12p70 by ELISA (b, d). (a and c) Showing one representative experiment out of three; (b and d) data are mean ± SEM of three independent experiments with different donors. $^{**}P < 0.01$, $^{***}P < 0.001$, and n.s.: not significant ($P > 0.05$); bars without annotation are not significant ($P > 0.05$); one-way ANOVA with Bonferroni's Multiple Comparison *post hoc* test.

a Hsp70B$'_{-29/-242}$-IL-12 ("pIL-12"), or the triple Hsp70-B$'_{-29/-242}$-MelA-Hsp70B$'_{-29/-242}$-BclxL-Hsp70B$'_{-29/-242}$-IL-12 ("pMelA/BclxL/IL-12") expression cassette. HeLa cells were transfected with the above-mentioned vectors followed by transduction with Ad5mHSF1, Ad5Luc1, or Mock the next day. Twenty-four hours later cells were harvested, lysed, and separated by SDS-PAGE followed by Western Blotting using specific antibodies for MelanA/MART-1, BclxL, and beta-actin expression. As shown in Figure 3(a), MelanA and BclxL were highly expressed only after specific HSP70B$'$ promoter activation by Ad5mHSF1. Of note, the MelanA and BclxL proteins were equally well expressed from the triple plasmid pMelA/BclxL/IL-12. For the determination of the IL-12 concentration in the cell culture supernatants of cells analyzed in (a), IL-12p70- and IL-12p40- specific ELISA were performed (Figure 3(b)). Again, IL-12 production after transfection with pIL-12 or pMelA/BclxL/IL-12 was induced by Ad5mHSF1. Transduced HeLa cells secreted high amounts of the immunologic active IL-12p70 (23.06 ng/mL and 20.39 ng/mL, resp.) and much lower amounts of the

homodimer IL-12p40 (0.58 ng/mL and 0.34 ng/mL, resp.). Moreover, there was almost no difference in the quantity of either IL-12p70 or IL-12p40 expressed from pIL-12 or pMelA/BclxL/IL-12, respectively.

Regarding our aim to insert the MP system into an adenoviral vector, we next generated Ad5MelA/BclxL/IL-12 containing an Hsp70B$'_{-29/-242}$-MelanA/Hsp70B$'_{-29/-242}$-BclxL/Hsp70B$'_{-29/-242}$-IL-12 expression cassette. Adenovirus vectors contain several promoters within their own genome, for example, the early transcripts E1A-E4, as well as multiple recognition sites within these promoters for transcription factors. They often represent cis-acting DNA sequences that increase transcription, independent of their orientation and distance relative to the RNA start site [36]. To exclude the possible interference of these viral enhancers and upstream regulatory elements with the Hsp70B$'$ promoter of our system, we cotransduced human iDCs with Ad5MelA/BclxL/IL-12, Ad5mHSF1 or control virus Ad5Luc1 in the presence of a cytokine maturation cocktail. As a control, cells were matured in absence of an adenoviral vector ("Mock"). Twenty-four hours later, lysates of DCs were generated to perform Western Blot analyses to assess MelanA, BclxL, and beta-actin expression (Figure 3(c)). In addition, cell culture supernatants were analyzed by ELISA for the content of IL-12p70 and IL-12p40 (Figure 3(d)). As depicted there, only the cotransduction of Ad5MelA/BclxL/IL-12 with Ad5mHSF1 induced a specific transgene expression of MelanA, BclxL, and high amounts of secreted IL-12p70 (57.84 ng/mL). Furthermore, DCs transduced with Ad5MelA/BclxL/IL-12 produced less of the homodimer IL-12p40 in comparison to Mock or only Ad5Luc1 treated DCs (2.67 and 3.16 ng/mL versus 5.93 and 5.54 ng/mL, resp.).

In summary, we showed that the expression of multiple therapeutic transgenes under the control of the Hsp70B$'$ promoter can specifically be induced in HeLa cells, as well as in primary human DCs. Moreover, we demonstrated that the Hsp70B$'$ promoter acts in a highly specific manner, not only in a plasmid-based vector system, but particularly also in an adenoviral context.

3.4. Overexpression of mHSF1 Induces Expression of Heat Shock Proteins and Does Not Impair DC Function. As overexpression of mHSF1 is also expected to induce the activation of endogenous heat shock proteins thereby inducing a heat shock response of Ad5mHSF1 treated DCs, we addressed the influence of mHSF1 overexpression on DCs as follows. Immature DCs were transduced with Ad5mHSF1 or control virus Ad5Luc1 or Mock-treated either in the presence (mDC) or absence (iDC) of the maturation cocktail. Twenty-four and 48 hours later, analyses of DCs were conducted. First, regulation of heat shock proteins HSF1, Hsp40, Hsp70A, Hsp70B$'$, Hsp90, and Grp94 was determined in cell lysates of DCs by SDS-PAGE followed by Western Blotting (Figure 4(a)). Here, a clear increase in expression of heat shock proteins Hsp40 and Hsp70A was observed for iDCs and mDCs, whereas Hsp70B$'$ and Hsp90 was only induced in mDCs after Ad5mHSF1 treatment in comparison to Ad5Luc1 or Mock controls. HSF1 was only increased in Ad5Luc1 transduced mDCs, while mHSF1 was only found in DCs treated with Ad5mHSF1. Expression of Grp94 was unaffected by any treatment. Next, we examined the expression of typical cell surface activation markers including CD25, CD80, CD83, CD86, HLA-ABC (MHCI), and HLA-DR (MHCII) by FACS analyses (Figure 4(b)). As expected, all maturation markers of DCs treated with the cytokine cocktail ("mDC") for 24 as well as 48 hours were upregulated in comparison to iDCs. Notably, treatment with any type of adenoviral vectors did not induce maturation of iDCs when compared to the Mock control. Furthermore, when DCs were matured during transduction (mDC), the adenoviral vectors did not influence the expression of the assessed surface markers. In addition to their activation status, DCs were also analyzed by FACS for their viability using propidium iodide (PI) staining. As shown in Figure 4(c), there was only a slight increase in the percentage of dead cells induced by the adenovirus treatment. The percentage of PI positive iDCs increased from 5.68% (Mock, 24 h) and 7.10% (Mock, 48 h) to 9.98% (Ad5Luc1, 24 h) and 11.90% (Ad5Luc1, 48 h) or 13.20% (AdmHSF1, 24 h) and 18.43% (AdmHSF1, 48 h), respectively. Matured DCs remained almost uninfluenced when compared with noninfected cells (2.20% and 1.55% PI$^+$ cells after 24 h or 48 h, resp.). Transduction with Ad5Luc1 resulted in 2.55% (24 h) or 1.78% (48 h) and with Ad5mHSF1 in 4.68 (24 h) or 5.13% (48 h) PI positive DCs.

Next, we assayed the functionality of these DCs by evaluating their capacity to secrete proinflammatory cytokines including IL-1β, IL-6, IL-8, IL-12p70, and TNF-α, as well as the anti-inflammatory cytokine IL-10, by cytometric bead array 24 and 48 hours after treatment (Figure 4(d)). As the maturation cocktail contains IL-1β, IL-6, and TNF-α, Mock-treated DCs served as a control and yielded the background of the corresponding cytokine indicated by a red line in the graph. Interestingly, 24 and *48* hours after infection, Ad5mHSF1-transduced mDCs showed a superior secretion of IL-1β (2381/*2451* pg/mL), IL-6 (13965/*16740* pg/mL), IL-8 (41154/*43674* pg/mL), IL-12p70 (35/*34* pg/mL), and TNF-α (5176/*5005* pg/mL) to Mock-treated mDCs (1443/*1877* pg/mL, 8993/*11063* pg/mL, 27581/*32420* pg/mL, 10/*7* pg/mL, and 2757/*1546* pg/mL, resp.). This was not the case for Ad5Luc1 transduced mDCs, where (with the exception of IL-12p70 and TNF-α) only a slight increase of cytokine production for IL-1β (1710/*1775* pg/mL), IL-6 (11038/*11519* pg/mL), and IL-8 (33398/*34201* pg/mL) could be observed either 24 or *48* hours after transduction. Interleukin-10 is only secreted at very low amounts but slightly enhanced at both time points in supernatants of Ad5mHSF1 (65/*49* pg/mL) treated mDCs, but not of Ad5Luc1 (37/*24* pg/mL) treated ones, in comparison to the Mock control (34/*24* pg/mL). Immature DCs secreted almost no cytokines, independent of the treatment and time point at which they were analyzed. Finally, we assessed the functional ability of Ad5mHSF1 transduced mature DCs to prime autologous naïve CD8$^+$ T cells. Therefore, iDCs were transduced with Ad5Luc1 or Ad5mHSF1 or were Mock-treated in the presence of the cytokine maturation cocktail the day before they were transfected with MelanA RNA or peptide-loaded with MelanA. Subsequently, DCs were cocultured with MACS-sorted CD8$^+$ T cells for seven days and afterwards

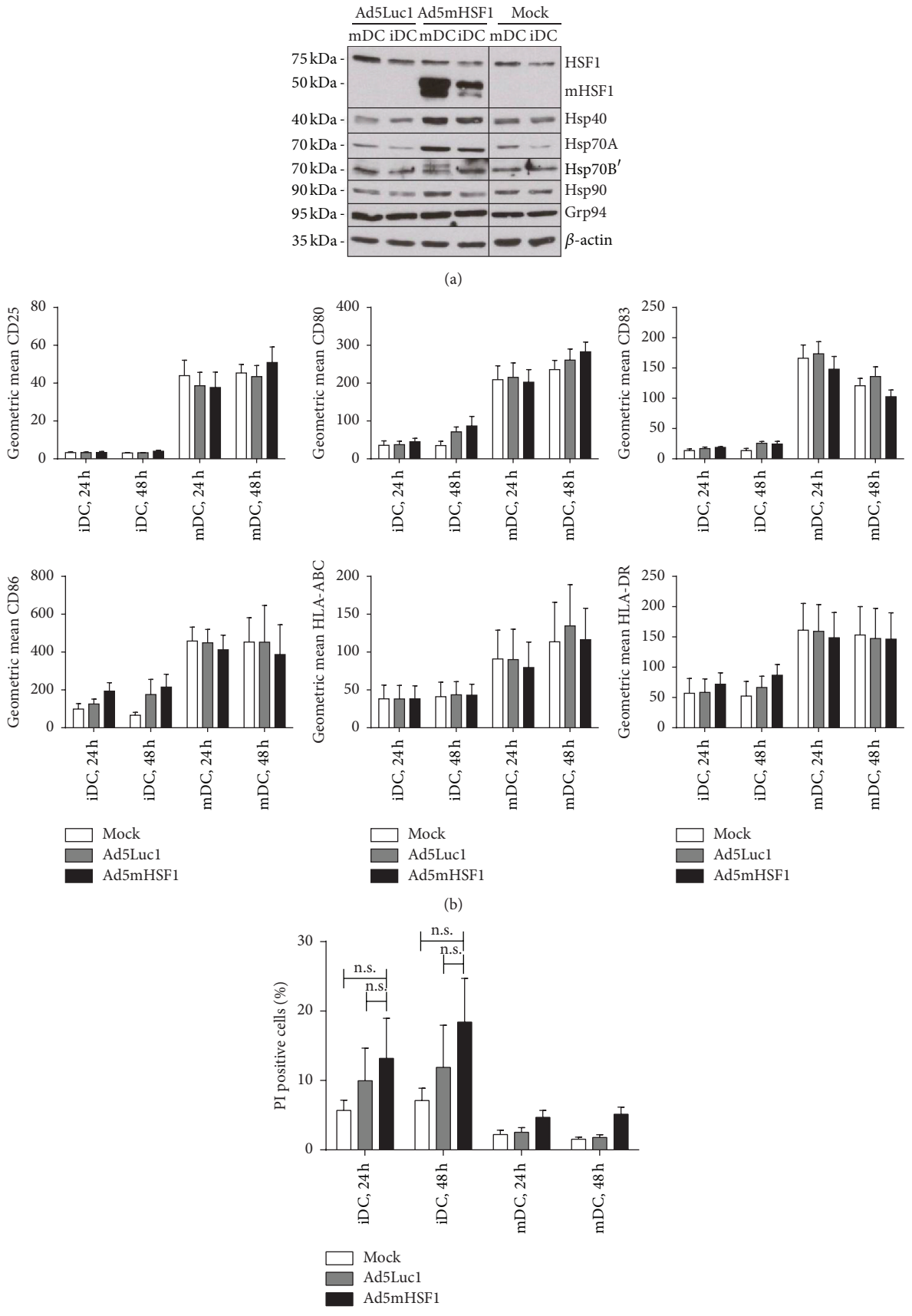

Figure 4: Continued.

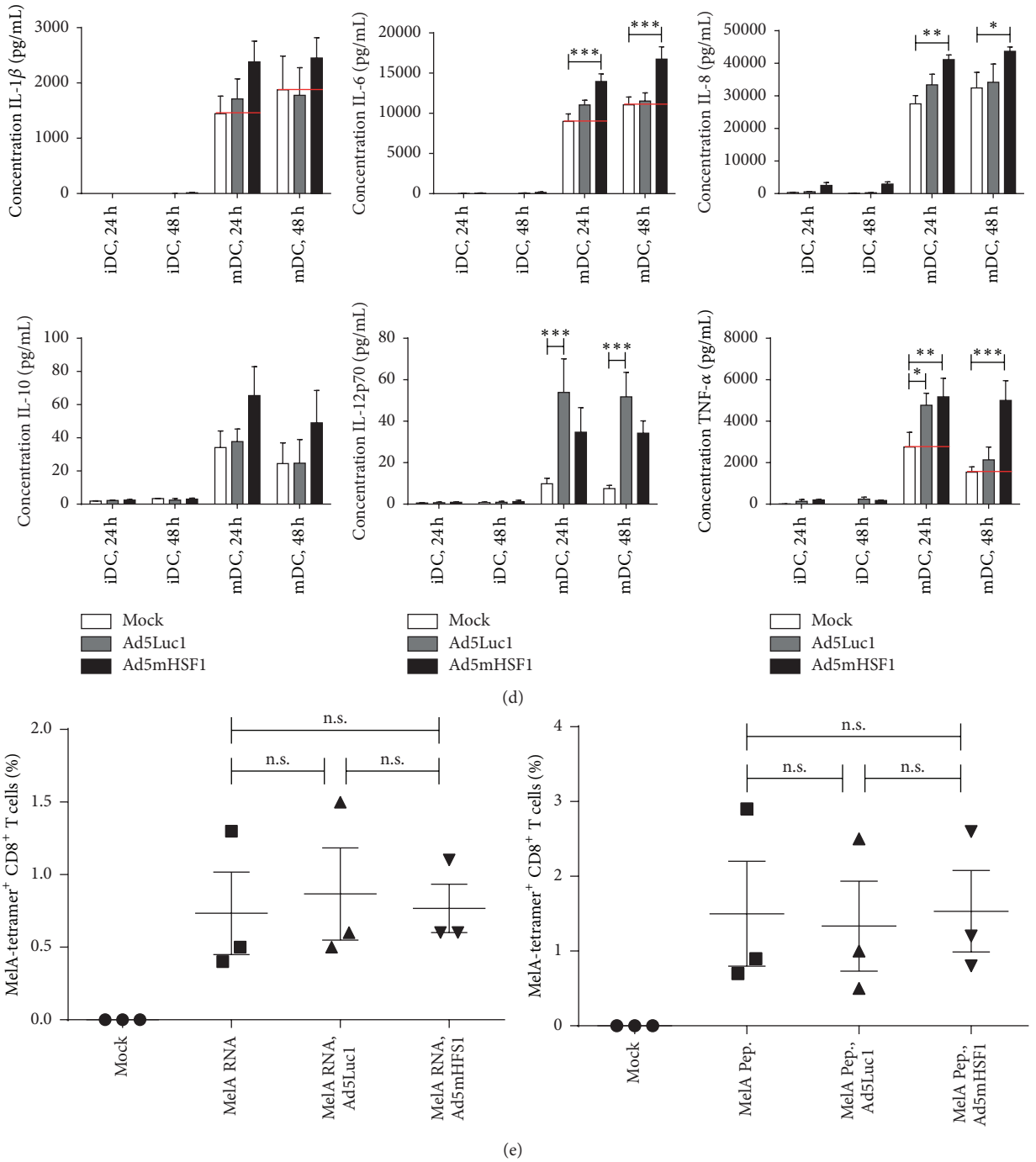

Figure 4: Overexpression of mHSF1 does not impair the phenotype and function of immature and mature DCs. Immature DCs were transduced with Ad5Luc1 or Ad5mHSF1 at 500 $TCID_{50}$/cell or Mock-treated and were either left immature ("iDC") or were matured ("mDC") with a maturation cytokine cocktail (IL-1β, IL-6, TNF-α, and PGE_2). (a) Western Blot analyses of cell lysates harvested 24 h after transduction on HSF1, mHSF1, Hsp40, Hsp70A, Hsp70B′, Hsp90, Grp94, and beta-actin protein expression. One representative experiment out of three is shown. (b, c) Flow cytometric analyses of iDCs and mDCs on CD25, CD80, CD83, CD86, HLA-ABC, and HLA-DR (b) as well as PI (c) 24 h and 48 h after transduction. Data are mean ± SEM of four independent experiments with DCs derived from different donors. (d) Cell culture supernatants derived from experiments shown in (b and c) were analyzed by cytometric bead array for the content of IL-1β, IL-6, IL-8, IL-10, IL-12p70, and TNF-α. The red line in (d) indicates background levels of respective cytokines derived from the cytokines present in the maturation cocktail. Data are mean ± SEM of three independent experiments. (e) Twenty-four hours after adenoviral transduction accompanied by maturation of DCs, cells were either transfected with wild-type MelanA RNA (left panel) or loaded with MelanA analogue peptide (right panel). Antigen-loaded DCs were cocultured with MACS-sorted autologous $CD8^+$ T cells for seven days. Induction of antigen-specific CTLs was determined by HLA-A2-MelanA/iTag MHC class I-tetramer and anti-CD8-PC7 staining using a FC500 cytofluorometer. Data are mean ± SEM of three independent experiments with different donors. (b–e) $^*P < 0.05$, $^{**}P < 0.01$, $^{***}P < 0.001$, and n.s.: not significant ($P > 0.05$); bars without annotation are not significant ($P > 0.05$), one-way, (e) or two-way ANOVA (b–d) with Bonferroni's Multiple Comparison *post hoc* test.

analyzed by staining with a HLA-A2-MelanA/iTag MHC class I-tetramer and an anti-CD8 antibody followed by flow cytometry. As shown in Figure 4(e), only antigen-loaded DCs induced the proliferation of MelanA-specific $CD8^+$ T cells with analogue peptide-loaded DCs (1.5%) being twofold more potent than wild-type RNA-transfected (0.73%) DCs. Moreover, transduction with neither the control adenovirus (RNA: 0.87%, Pep: 1.34%) nor Ad-mediated overexpression of mHSF1 (RNA: 0.77%, Pep: 1.53%) impaired the capacity of antigen-loaded DCs to induce specific CTL responses, independent of the route of delivery.

From these data we conclude that neither transduction with the used adenoviral vectors *per se* nor the overexpression of mHSF1 interfered with the function of DCs. However, transduction with Ad5mHSF1 resulted in the upregulation of various heat shock proteins and proinflammatory cytokines by mDCs.

3.5. Specific Targeting of Mature DCs by a Combined CD83-Hsp70B′ Promoter System. To realize our final goal of transcriptionally targeting human mature DCs, we created new vectors where the expression of mHSF1 is driven by the human CD83 promoter, recently characterized by our group [18]. This tripartite promoter complex, consisting of a 510 bp upstream plus core promoter element ("P-510") and a 185 bp enhancer ("E") fragment, was shown to act in a cell type- and maturation-specific manner. To assess this, also in the context of the modular promoter system, we generated plasmid vectors (Figure 5(a)) containing mHSF1 and only the P-510 CD83 promoter ("pP-510/mHSF1") or the P-510 plus the enhancer in either the sense or antisense direction ("pEs/P-510/mHSF1" or "pEas/P-510/mHSF1"). These were cotransfected into the murine DC-like cell line XS52 with plasmid vectors expressing MelanA/MART-1 and IL-12 under the control of the $Hsp70B'_{-29/-242}$ HRE ("pMP2"; Figures 5(a)–5(c)). As a control pMP2 was replaced by (i) a vector comprising only the $Hsp70B'_{-29/-242}$ promoter or (ii) the empty pLG3-Basic vector ("Basic") (Figures 5(a) and 5(b)). Twenty-four hours later, cells were lysed for SDS-PAGE and Western Blotting for MelanA and beta-actin detection, while cell culture supernatants were analyzed by ELISA for the content of IL-12p70 and IL-12p40. As depicted in Figure 5(b), only cotransfection of pMP2 with pEs/P-510/mHSF1 or pEas/P-510/mHSF1 resulted in a strong and robust MelanA expression, while pP-510/mHSF1 without the enhancer showed only weak transgene expression. Accordingly, IL-12p70 secretion was not detectable in controls, at low levels in the context of pMP2 plus pP-510/mHSF1 transfected cells (1.07 ng/mL) and in large amounts by the combination of pMP2 with pEs/P-510/mHSF1 (4.08 ng/mL) or pEas/P-510/mHSF1 (4.79 ng/mL) (Figure 5(c)). Interleukin-12p40, however, was only detectable in supernatants derived from pMP2 plus pEs/P-510/mHSF1 (0.01 ng/mL) or pEas/P-510/mHSF1 (0.434 ng/mL) transfected XS52 cells.

Finally, we generated corresponding adenoviral vectors, that is, Ad5MP2, Ad5P-510/mHSF1, Ad5Es/P-510/mHSF1, and Ad5Eas/P-510/mHSF1. These were used together with Ad5Luc1 (negative control), Ad5MelA (positive control), or Ad5mHSF1 to cotransduce immature human DCs. DCs were then either left immature ("iDC") or were matured with LPS for 20 hours ("mDC") because this maturation stimulus induced the highest expression of the CD83 promoter ([18] and unpublished results). Afterwards, cell lysates were analyzed for expression of MelanA and beta-actin by Western Blot and supernatants by IL-12p70 and IL-12p40 ELISA. Clearly, MelanA expression was specifically induced only in mDCs after cotransduction of Ad5MP2 with adenoviruses containing the CD83 promoter-mHSF1 cassette (Figure 5(d)). Positive controls Ad5MP2 plus Ad5mHSF1, as well as Ad5MelA plus Ad5Luc1, revealed expression of the transgene in iDCs and mDCs, while negative controls did not show a signal for either. Similar results were obtained for cytokine-matured DCs (data not shown). Regarding IL-12p70, LPS-matured DCs, in contrast to cocktail-matured DCs, produced higher amounts in general (Figure 5(e)). Interestingly, in comparison to controls, that is, Ad5MP2 plus Ad5Luc1 (19.05 ng/mL) or Ad5MelA plus Ad5Luc1 (16.1 ng/mL), the amount of IL-12p70 expressed doubled when Ad5MP2 was cotransduced with Ad5P-510/mHSF1 (35.87 ng/mL), Ad5Es/P-510/mHSF1 (41.46 ng/mL), or Ad5Eas/P-510/mHSF1 (57.56 ng/mL). Cocktail-matured DC (data not shown) showed a lower, but specific, IL-12p70 production upon cotransduction of Ad5MP2 with Ad5P-510/mHSF1 (9.83 ng/mL), Ad5Es/P-510/mHSF1 (16.78 ng/mL), or Ad5Eas/P-510/mHSF1 (16.83 ng/mL). In comparison to LPS-matured DCs, immature DCs showed a lower expression of IL-12p70 (max. 8.93 ng/mL), while in the positive control (Ad5MP2 plus Ad5mHSF1), higher amounts of IL-12p70 were detected for both LPS-matured (52.3 ng/mL) and immature DCs (80.96 ng/mL). In contrast, IL-12p40 was mainly secreted by control-transduced LPS-matured DCs (max. 29.54 ng/mL), whereas LPS-matured DCs transduced with the MP adenoviruses showed less (max. 13.05 ng/mL) and iDCs no IL-12p40 irrespective of the adenovirus used.

Taken together, we have here demonstrated our modular promoter system to specifically target human immunogenic mature DCs to efficiently induce the expression of different therapeutic transgenes.

4. Discussion

One big challenge facing cancer immunotherapy is the generation of cell-specific treatment strategies. For *in vivo* DC-targeting, the restriction of transgene expression to this specific cell type is the main interest. Adenoviruses display several advantages for this targeted delivery of therapeutic transgenes such as tumor antigens and immune stimulatory proteins. They permit an extended expression of full length antigens within the transduced DC. In contrast to other targeting strategies, where peptides, proteins, or mRNAs are used, the cancer-proteins are synthesized over a longer period and processed by the DCs' own antigen-presentation machinery. As a consequence, long-lasting antigen-presentation to T cells is ensured without generating concerns regarding the breakdown of peptide/MHC complexes [37].

Melanoma is viewed as an "immunogenic" tumor type which is why here Ad-based and other strategies to improve

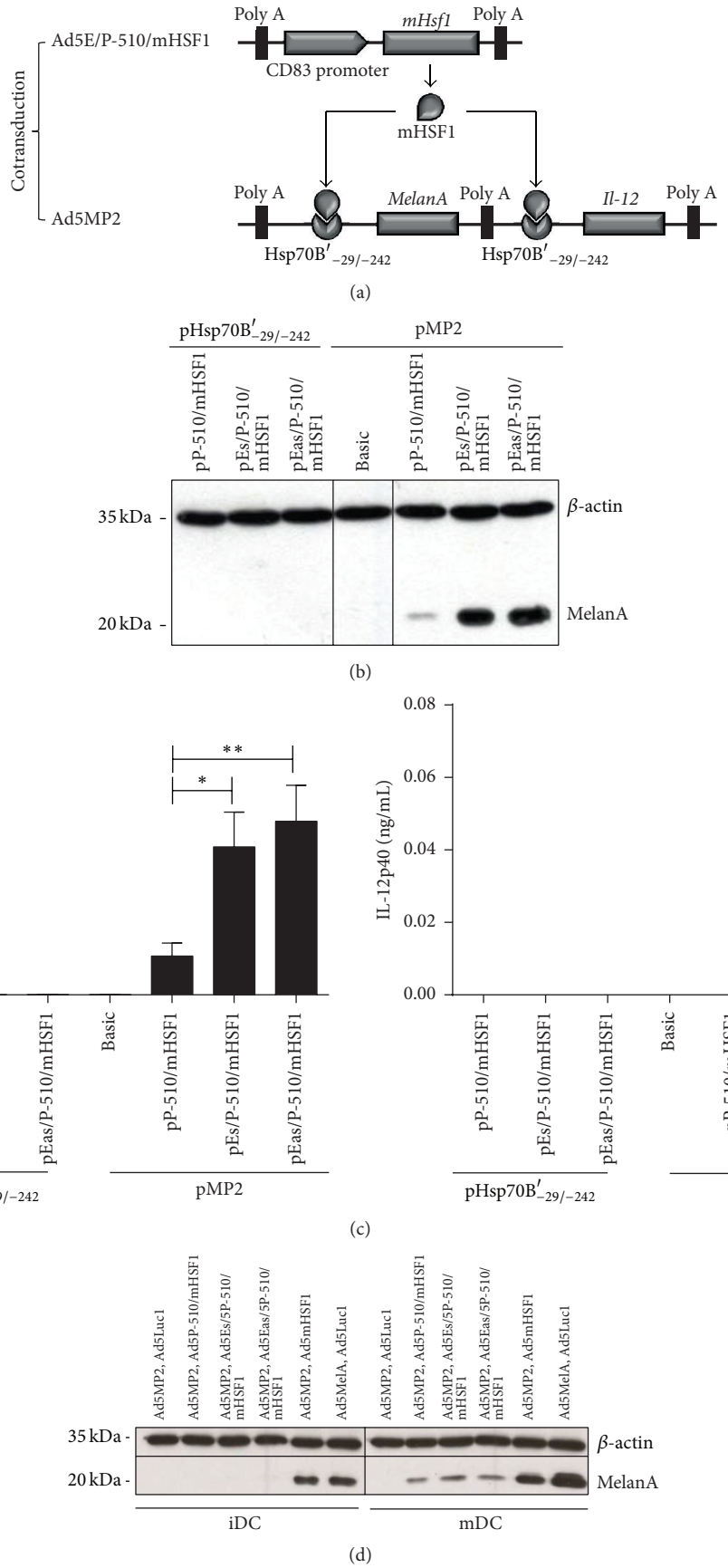

Figure 5: Continued.

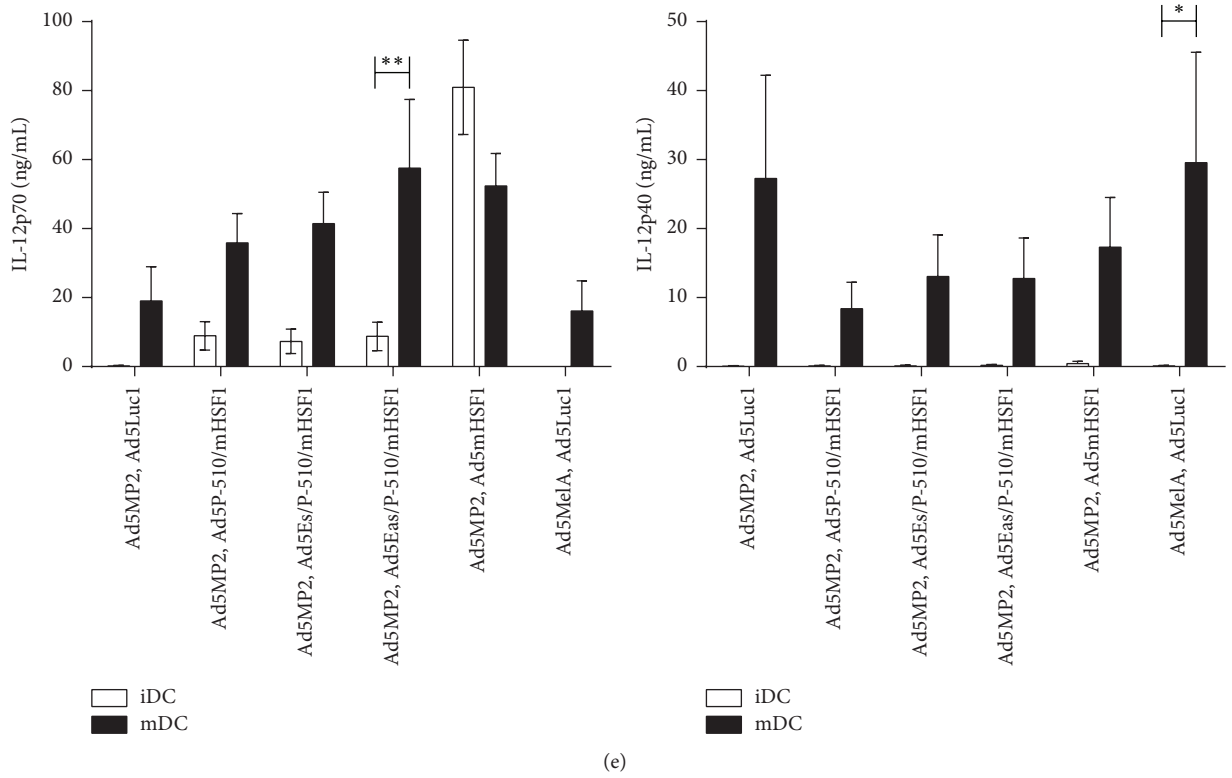

(e)

FIGURE 5: The "modular promoter (MP)" system enables highly efficient and specific expression of therapeutic transgenes in mature DCs. (a) Schematic outline of the dual vector "modular promoter" system. Ad5E/P-510/mHSF1 drives expression of mHSF1 under the control of the cell type- and maturation-specific human CD83 promoter, which in turn induces specific induction of therapeutic transgenes MelanA and Il-12 by binding to the $Hsp70B'_{-29/-242}$ HRE encoded by Ad5MP2. (b, c) XS52 cells were cotransfected with a total amount of 2 μg of plasmid vectors pP-510/mHSF1, pEs/P-510/mHSF1, or pEas/P-510/mHSF1 in combination with plasmid vectors encoding the HRE alone ("$pHsp70B'_{-29/-242}$") or the modular promoter system ("pMP2"). As a control, the empty pGL3-Basic vector ("Basic") was used. (d, e) Human immature DCs were cotransduced with Ad5MP2 or Ad5MelA in combination with Ad5Luc1, Ad5mHSF1, Ad5P-510/mHSF1, Ad5Es/P-510/mHSF1, or Ad5Eas/P-510/mHSF1. Cells were either left immature or were matured by adding 0.1 ng/mL LPS. (b–e) Twenty hours after transfection, cell lysates were analyzed by Western Blot for expression of MelanA and beta-actin (b, d) and cell culture supernatants by ELISA for content of IL-12p40 and IL-12p70 (c, e). Either one representative (b, d) or data mean ± SEM from three independent experiments (c, e) is shown. $^{*}P < 0.05$; $^{**}P < 0.01$; bars without annotation are not significant ($P > 0.05$), one-way ANOVA (c) or two-way ANOVA (e) with Bonferroni's Multiple Comparison *post hoc* test.

DC-mediated immunotherapies have been used for the treatment of this disease. Moreover, malignant melanoma is the most common cause of mortality from skin cancer worldwide. It is refractory to irradiation and chemotherapy in late phases but rather amenable to immunological approaches [38]. Although great efforts have been made in recent years, antitumor DC-based vaccines rarely exceeded 15% of the objective clinical responses [39]. Hence, there is still a high medical need to develop new strategies to improve DC vaccination.

In this study, we present *in vitro* experiments using a combined CD83-Hsp70B′ promoter system ("modular promoter [MP]" system; Figures 1 and 5(a)) to specifically target mature DCs for the simultaneous expression of different therapeutic transgenes in the context of malignant melanoma. Therefore, we expressed a mutated HSF1 (mHSF1) with a deletion between amino acid positions 202–316 of wild-type HSF1, which has been shown to be constitutively active even in the absence of stress [26], under the control of the DC- and maturation-specific human CD83 promoter [18]. In turn, mHSF1 is used to drive simultaneous Hsp70B′-dependent therapeutic transgene expression. Heat shock promoters, particularly Hsp70 promoters, have often been used for gene therapy in the past and the Hsp70B′ promoter displays several advantages. First, it is induced only after severe stress, resulting in a lower basal expression compared to other *hsp70* genes [40, 41]. This is in accordance with our data, as these demonstrated the Hsp70B′ promoter to be induced only by mHSF1 and not to be sensitive to stress factors induced by lipofection (Figure 2(b)) or adenoviral transduction (Figure 3). Second, the moderate expression of Hsp70B′ was reported to be restricted to white blood cells like DCs, monocytes, and NK cells especially but to be nearly absent in other blood cells and tissues [42]. Third, the core Hsp70B′ promoter element is very short (213 bp) and showed a promoter activity 16 times higher than the strong

SV40 promoter (Figure 2(b)). In addition, (m)HSF1 is not immunogenic as it is an ubiquitously expressed protein.

Interestingly, overexpression of mHSF1 did not influence the maturation status, the survival of immature and mature DCs, or their capability to prime naïve $CD8^+$ T cells in an antigen-specific manner whereas heat treatment of these DCs did result in the upregulation of maturation markers and increased capability to prime naïve $CD8^+$ T cells [27]. However, mHSF1 overexpression or adenoviral transduction of mDCs per se induced elevated levels of proinflammatory cytokines including IL-1β, IL-6, IL-8, IL-12p70, and TNF-α in cell culture supernatants. We also found Hsp40 and Hsp70A to be upregulated in cell lysates of iDCs and mDCs, whereas Hsp70B′ and Hsp90 were only induced in mDCs. Heat shock proteins such as Hsp40 and Hsp70 have been described to act as chaperones and be involved in the proper folding of proteins as well as in the prevention of the formation of nascent protein aggregations thereby keeping the proteins in a substrate-grabbable state. Others, like Hsp90, have been demonstrated to contribute to antigen-presentation on MHC I [43–45]. In this regard, heat shock proteins also became the focus of attention in the vaccine research area. Exogenous Hsp70 and Hsp90 have been reported to induce secretion of cytokines like GM-CSF, IL-1β, IL-6, IL-12, and TNF-α and to upregulate cell surface maturation markers CD83, CD86, or CD40 as well as to enhance the migratory capacity of DCs [46–48]. Induction of heat shock proteins, on the other hand, is ensued by the induction of HSF1 [49]. Besides its role as a transcription factor in stressed cells, HSF1 is involved in a multitude of physiological processes such as cell metabolism, gametogenesis, aging, insulin signaling, and cancer progression [24, 25]. Regarding the latter, HSF1 was shown to act on cancer development by regulating tumor cell proliferation, antiapoptosis, epithelial-mesenchymal transition (EMT), migration, invasion, and metastasis [50]. Interestingly, almost nothing is known about the influence of HSF1 or mHSF1 overexpression on human DCs. Thus, at least to our knowledge, this is the first study indicating that overexpression of mHSF1 does not impair DC maturation and function, although varying reports on the DC's responsiveness to heat shock were published [27, 51–53]. Solely Ostberg and colleagues reviewed that effects such as the induction of maturation or stimulation of T cells, induced by mild thermal stress, are not dependent on HSF1-mediated transcriptional events in murine bone marrow derived DCs [54]. The mHSF1 used in the present study however was also overexpressed by Xia and colleagues in HeLa cells [55]. As a consequence, HeLa cells, which are normally relatively insensitive to Fas-mediated killing, became sensitive to Fas-induced apoptosis, thereby providing a new target for Fas-based antitumor vaccines.

Encouraged by these results, we generated the modular promoter system to transcriptionally target mature DCs. To perform first proof of principle, we successfully expressed several therapeutic transgenes under the control of the core Hsp70B′ promoter element, which we could specifically induce with CMV promoter-driven mHSF1 both in HeLa cells by plasmid transfection and in primary mature human DCs by adenoviral vectors (Figure 3). In a second step, we developed a two-vector-based system, where we set mHSF1 under the control of the human DC- and maturation-specific CD83 promoter to express MelanA and IL-12p70 (Figure 5(a)). The advantage of MelanA is its widespread expression on melanocytic cells and its ubiquitin-mediated proteasome-dependent degradation leading to the presentation of the antigen via MHC class I [56]. Interleukin-12p70, on the other hand, enhances the cytotoxic activity of $CD8^+$ CTLs and NK cells [57]. Moreover, exogenous expression of IL-12p70 is able to overcome the inhibitory effect of PGE_2 on IL-12p70 production of DCs matured with the standard cytokine maturation cocktail used not only *in vitro* but also *in vivo* in clinical trials [58]. Of note, the combined CD83-Hsp70B′ promoter system not only facilitated specific transcriptional targeting of mature immunogenic DCs but also guaranteed high expression of the respective transgenes (Figure 5) without affecting endogenous CD83 expression in maturing DCs (data not shown).

To date, only very few promoter systems have been proven suitable for the transcriptional targeting of DCs. The group of Ross et al., for instance, demonstrated the promoter of the cytoskeletal fascin protein to induce specific transgene expression in mature murine DCs after gene gun-mediated DNA immunization [59]. Similar results were also reported by Sudowe et al. to induce type 1 immune responses [59, 60]. In the context of a lentiviral vector system, Dresch and colleagues described the 5′ untranslated region from the *DC-STAMP* gene as a suitable promoter region to yield long-term and cell-selective transgene expression in murine DCs *in vivo* [61]. Several cell type-specific promoters have been reported in the past to target murine DCs *in vitro* and *in vivo;* however here we report the first promoter system allowing the specific targeting of mature human DCs. Regarding its future prospects for cancer therapy, the CD83-Hsp70B′ promoter system offers several interesting features. Due to its modular composition, the system is highly flexible and hence not restricted to a specific tumor entity or therapeutic application. On the one hand, the therapeutic transgenes encoded by one adenoviral vector could be replaced by any gene of interest, even mutated cancer- and patient-specific TAAs. On the other hand, it would be possible to use an even more specific promoter or one with different cell-specificity, for the expression of the mHSF1 within the other vector. This modular composition would in theory allow the *in vivo* targeting of any combination of transgenes to any cell type although this requires substantial additional preparatory experiments. Moreover, by combining transductional targeting of adenoviruses to dendritic cells via bispecific diabodies or single-chain antibodies incorporated into the virus capsid, a further increase of targeting specificity might be achieved.

Finally, since CD83 is not expressed by immature but is highly induced in mature DCs, the applied CD83 promoter complex represents an ideal candidate for transcriptional targeting of mature DCs *in vivo* and could set the stage for next generation *in situ* vaccination strategies. This should be particularly effective and safe, as it assures selective antigen expression in mDCs while avoiding expression in tolerogenic iDCs for the first time. These promising perspectives,

however, need to first be analyzed and explored in further preclinical investigations.

5. Conclusions

In this study, we present the initial *in vitro* experiments showing that a combined two-vector CD83-Hsp70B′ promoter system is able to transcriptionally target human mature DCs for the first time with a highly specific and effective expression of a panel of potential therapeutic transgenes. Moreover, we first demonstrate that overexpression of mHSF1 does not interfere with DC maturation, viability, and function. Hence, this study provides valuable new insights for the development of a safe, modular, highly flexible, and hence patient-tailored vaccination protocol for *in vivo* targeting of DCs, but also other efficient genetic therapies in the future.

Competing Interests

The authors declare that there are no competing interests regarding the publication of this paper.

Acknowledgments

This work was supported by the Deutsche Forschungsgemeinschaft (DFG) via the CRC643 (Projects B13 and C1) and the ELAN-Fonds of the Universitätsklinikum Erlangen. The authors thank A. Takashima (University of Texas Southwestern Medical Center, TX, US), F. Schnieders (Provecs Medical GmbH, Hamburg, Germany), R. Voellmy (HSF Pharmaceuticals, Fribourg, Switzerland), and D. T. Curiel (Washington University School of Medicine, MO, US) for kindly providing research material and Vera E. Assmann (Universitätsklinikum Erlangen, Erlangen, Germany) for proofreading the paper.

References

[1] J. Datta, E. Berk, J. A. Cintolo, S. Xu, R. E. Roses, and B. J. Czerniecki, "Rationale for a multimodality strategy to enhance the efficacy of dendritic cell-based cancer immunotherapy," *Frontiers in Immunology*, vol. 6, article 271, 2015.

[2] I. Caminschi and K. Shortman, "Boosting antibody responses by targeting antigens to dendritic cells," *Trends in Immunology*, vol. 33, no. 2, pp. 71–77, 2012.

[3] W. R. Heath and F. R. Carbone, "Cross-presentation, dendritic cells, tolerance and immunity," *Annual Review of Immunology*, vol. 19, pp. 47–64, 2001.

[4] N. Bloy, J. Pol, F. Aranda et al., "Trial watch: dendritic cell-based anticancer therapy," *OncoImmunology*, vol. 3, no. 11, Article ID e963424, 2014.

[5] A. Makkouk and G. J. Weiner, "Cancer immunotherapy and breaking immune tolerance: new approaches to an old challenge," *Cancer Research*, vol. 75, no. 1, pp. 5–10, 2015.

[6] K. Palucka and J. Banchereau, "Dendritic-cell-based therapeutic cancer vaccines," *Immunity*, vol. 39, no. 1, pp. 38–48, 2013.

[7] J. Constantino, C. Gomes, A. Falcão, M. T. Cruz, and B. M. Neves, "Antitumor dendritic cell-based vaccines: lessons from 20 years of clinical trials and future perspectives," *Translational Research*, vol. 168, pp. 74–95, 2016.

[8] R. M. Steinman, "Decisions about dendritic cells: past, present, and future," *Annual Review of Immunology*, vol. 30, pp. 1–22, 2012.

[9] G. Schreibelt, L. J. J. Klinkenberg, L. J. Cruz et al., "The C-type lectin receptor CLEC9A mediates antigen uptake and (cross-) presentation by human blood BDCA3+ myeloid dendritic cells," *Blood*, vol. 119, no. 10, pp. 2284–2292, 2012.

[10] V. Apostolopoulos, T. Thalhammer, A. G. Tzakos, and L. Stojanovska, "Targeting antigens to dendritic cell receptors for vaccine development," *Journal of Drug Delivery*, vol. 2013, Article ID 869718, 22 pages, 2013.

[11] P. J. Tacken, I. S. Zeelenberg, L. J. Cruz et al., "Targeted delivery of TLR ligands to human and mouse dendritic cells strongly enhances adjuvanticity," *Blood*, vol. 118, no. 26, pp. 6836–6844, 2011.

[12] A. Garu, G. Moku, S. K. Gulla, and A. Chaudhuri, "Genetic immunization with in vivo dendritic cell-targeting liposomal DNA vaccine carrier induces long-lasting antitumor immune response," *Molecular Therapy*, vol. 24, no. 2, pp. 385–397, 2015.

[13] L. J. Cruz, P. J. Tacken, I. S. Zeelenberg et al., "Tracking targeted bimodal nanovaccines: immune responses and routing in cells, tissue, and whole organism," *Molecular Pharmaceutics*, vol. 11, no. 12, pp. 4299–4313, 2014.

[14] R. Hernandez-Alcoceba, J. Poutou, M. C. Ballesteros-Briones, and C. Smerdou, "Gene therapy approaches against cancer using in vivo and ex vivo gene transfer of interleukin-12," *Immunotherapy*, vol. 8, no. 2, pp. 179–198, 2016.

[15] R. A. A. Oldham, E. M. Berinstein, and J. A. Medin, "Lentiviral vectors in cancer immunotherapy," *Immunotherapy*, vol. 7, no. 3, pp. 271–284, 2015.

[16] W. S. M. Wold and K. Toth, "Adenovirus vectors for gene therapy, vaccination and cancer gene therapy," *Current Gene Therapy*, vol. 13, no. 6, pp. 421–433, 2013.

[17] S. D. Barker, I. P. Dmitriev, D. M. Nettelbeck et al., "Combined transcriptional and transductional targeting improves the specificity and efficacy of adenoviral gene delivery to ovarian carcinoma," *Gene Therapy*, vol. 10, no. 14, pp. 1198–1204, 2003.

[18] M. F. Stein, S. Lang, T. H. Winkler et al., "Multiple interferon regulatory factor and NF-κB sites cooperate in mediating cell-type-and maturation-specific activation of the human CD83 promoter in dendritic cells," *Molecular and Cellular Biology*, vol. 33, no. 7, pp. 1331–1344, 2013.

[19] L. Vandenberk, J. Belmans, M. Van Woensel, M. Riva, and S. W. Van Gool, "Exploiting the immunogenic potential of cancer cells for improved dendritic cell vaccines," *Frontiers in Immunology*, vol. 6, article 663, 2016.

[20] S. Rohmer, A. Mainka, I. Knippertz, A. Hesse, and D. M. Nettelbeck, "Insulated hsp70B′ promoter: stringent heat-inducible activity in replication-deficient, but not replication-competent adenoviruses," *Journal of Gene Medicine*, vol. 10, no. 4, pp. 340–354, 2008.

[21] C. Rome, F. Couillaud, and C. T. W. Moonen, "Spatial and temporal control of expression of therapeutic genes using heat shock protein promoters," *Methods*, vol. 35, no. 2, pp. 188–198, 2005.

[22] R. Voellmy, "Transduction of the stress signal and mechanisms of transcriptional regulation of heat shock/stress protein gene expression in higher eukaryotes," *Critical Reviews in Eukaryotic Gene Expression*, vol. 4, no. 4, pp. 357–401, 1995.

[23] R. Baler, G. Dahl, and R. Voellmy, "Activation of human heat shock genes is accompanied by oligomerization, modification, and rapid translocation of heat shock transcription factor HSF1," *Molecular and Cellular Biology*, vol. 13, no. 4, pp. 2486–2496, 1993.

[24] A. Vihervaara and L. Sistonen, "HSF1 at a glance," *Journal of Cell Science*, vol. 127, no. 2, pp. 261–266, 2014.

[25] J. Anckar and L. Sistonen, "Regulation of HSF1 function in the heat stress response: implications in aging and disease," *Annual Review of Biochemistry*, vol. 80, pp. 1089–1115, 2011.

[26] J. Zuo, D. Rungger, and R. Voellmy, "Multiple layers of regulation of human heat shock transcription factor 1," *Molecular and Cellular Biology*, vol. 15, no. 8, pp. 4319–4330, 1995.

[27] I. Knippertz, M. F. Stein, J. Dörrie et al., "Mild hyperthermia enhances human monocyte-derived dendritic cell functions and offers potential for applications in vaccination strategies," *International Journal of Hyperthermia*, vol. 27, no. 6, pp. 591–603, 2011.

[28] I. A. Pfeiffer, E. Zinser, E. Strasser et al., "Leukoreduction system chambers are an efficient, valid, and economic source of functional monocyte-derived dendritic cells and lymphocytes," *Immunobiology*, vol. 218, no. 11, pp. 1392–1401, 2013.

[29] N. Schaft, J. Dörrie, I. Müller et al., "A new way to generate cytolytic tumor-specific T cells: electroporation of RNA coding for a T cell receptor into T lymphocytes," *Cancer Immunology, Immunotherapy*, vol. 55, no. 9, pp. 1132–1141, 2006.

[30] R. Waehler, H. Ittrich, L. Mueller, G. Krupski, D. Ameis, and F. Schnieders, "Low-dose adenoviral immunotherapy of rat hepatocellular carcinoma using single-chain interleukin-12," *Human Gene Therapy*, vol. 16, no. 3, pp. 307–317, 2005.

[31] T. C. He, "Adenoviral vectors," in *Current Protocols in Human Genetics*, chapter 12, John Wiley & Sons, New York, NY, USA, 2004.

[32] X. Liao, Y. Li, C. Bonini et al., "Transfection of RNA encoding tumor antigens following maturation of dendritic cells leads to prolonged presentation of antigen and the generation of high-affinity tumor-reactive cytotoxic T lymphocytes," *Molecular Therapy*, vol. 9, no. 5, pp. 757–764, 2004.

[33] N. Schaft, V. Wellner, C. Wohn, G. Schuler, and J. Dörrie, "$CD8^+$ T-cell priming and boosting: More antigen-presenting DC, or more antigen per DC?" *Cancer Immunology, Immunotherapy*, vol. 62, no. 12, pp. 1769–1780, 2013.

[34] R. Voellmy, A. Ahmed, P. Schiller, P. Bromley, and D. Rungger, "Isolation and functional analysis of a human 70,000-dalton heat shock protein gene segment," *Proceedings of the National Academy of Sciences of the United States of America*, vol. 82, no. 15, pp. 4949–4953, 1985.

[35] P. Schiller, J. Amin, J. Ananthan, M. E. Brown, W. A. Scott, and R. Voellmy, "Cis-acting elements involved in the regulated expression of a human hsp70 gene," *Journal of Molecular Biology*, vol. 203, no. 1, pp. 97–105, 1988.

[36] D. S. Steinwaerder and A. Lieber, "Insulation from viral transcriptional regulatory elements improves inducible transgene expression from adenovirus vectors in vitro and in vivo," *Gene Therapy*, vol. 7, no. 7, pp. 556–567, 2000.

[37] L. H. Butterfield and L. Vujanovic, "New approaches to the development of adenoviral dendritic cell vaccines in melanoma," *Current Opinion in Investigational Drugs*, vol. 11, no. 12, pp. 1399–1408, 2010.

[38] S. Bramante, J. K. Kaufmann, V. Veckman et al., "Treatment of melanoma with a serotype 5/3 chimeric oncolytic adenovirus coding for GM-CSF: results in vitro, in rodents and in humans," *International Journal of Cancer*, vol. 137, no. 7, pp. 1775–1783, 2015.

[39] S. Anguille, E. L. Smits, E. Lion, V. F. Van Tendeloo, and Z. N. Berneman, "Clinical use of dendritic cells for cancer therapy," *The Lancet Oncology*, vol. 15, no. 7, pp. e257–e267, 2014.

[40] T. K. C. Leung, M. Y. Rajendran, C. Monfries, C. Hall, and L. Lim, "The human heat-shock protein family: expression of a novel heat-inducible HSP70 (HSP70B') and isolation of its cDNA and genomic DNA," *Biochemical Journal*, vol. 267, no. 1, pp. 125–132, 1990.

[41] K.-I. Wada, A. Taniguchi, and T. Okano, "Highly sensitive detection of cytotoxicity using a modified HSP70B' promoter," *Biotechnology and Bioengineering*, vol. 97, no. 4, pp. 871–876, 2007.

[42] M. Daugaard, M. Rohde, and M. Jäättelä, "The heat shock protein 70 family: highly homologous proteins with overlapping and distinct functions," *The FEBS Letters*, vol. 581, no. 19, pp. 3702–3710, 2007.

[43] T. Ichiyanagi, T. Imai, C. Kajiwara et al., "Essential role of endogenous heat shock protein 90 of dendritic cells in antigen cross-presentation," *The Journal of Immunology*, vol. 185, no. 5, pp. 2693–2700, 2010.

[44] T. Imai, Y. Kato, C. Kajiwara et al., "Heat shock protein 90 (HSP90) contributes to cytosolic translocation of extracellular antigen for cross-presentation by dendritic cells," *Proceedings of the National Academy of Sciences of the United States of America*, vol. 108, no. 39, pp. 16363–16368, 2011.

[45] Y. Kato, C. Kajiwara, I. Ishige et al., "HSP70 and HSP90 differentially regulate translocation of extracellular antigen to the cytosol for cross-presentation," *Autoimmune Diseases*, vol. 2012, Article ID 745962, 10 pages, 2012.

[46] S. Basu, R. J. Binder, R. Suto, K. M. Anderson, and P. K. Srivastava, "Necrotic but not apoptotic cell death releases heat shock proteins, which deliver a partial maturation signal to dendritic cells and activate the NF-κB pathway," *International Immunology*, vol. 12, no. 11, pp. 1539–1546, 2000.

[47] D. G. Millar, K. M. Garza, B. Odermatt et al., "Hsp70 promotes antigen-presenting cell function and converts T-cell tolerance to autoimmunity in vivo," *Nature Medicine*, vol. 9, no. 12, pp. 1469–1476, 2003.

[48] R. P. A. Wallin, A. Lundqvist, S. H. Moré, A. Von Bonin, R. Kiessling, and H.-G. Ljunggren, "Heat-shock proteins as activators of the innate immune system," *Trends in Immunology*, vol. 23, no. 3, pp. 130–135, 2002.

[49] N. Hentze, L. Le Breton, J. Wiesner, G. Kempf, and M. P. Mayer, "Molecular mechanism of thermosensory function of human heat shock transcription factor Hsf1," *eLife*, vol. 5, article e11576, 2016.

[50] S. Jiang, K. Tu, Q. Fu et al., "Multifaceted roles of HSF1 in cancer," *Tumor Biology*, vol. 36, no. 7, pp. 4923–4931, 2015.

[51] S. Basu and P. K. Srivastava, "Fever-like temperature induces maturation of dendritic cells through induction of hsp90," *International Immunology*, vol. 15, no. 9, pp. 1053–1061, 2003.

[52] K. Matsumoto, N. Yamamoto, S. Hagiwara et al., "Optimization of hyperthermia and dendritic cell immunotherapy for squamous cell carcinoma," *Oncology Reports*, vol. 25, no. 6, pp. 1525–1532, 2011.

[53] A. Semmlinger, M. Fliesser, A. M. Waaga-Gasser et al., "Fever-range temperature modulates activation and function of human dendritic cells stimulated with the pathogenic mould

Aspergillus fumigatus," *Medical Mycology*, vol. 52, no. 4, pp. 438–444, 2014.

[54] J. R. Ostberg and E. A. Repasky, "Emerging evidence indicates that physiologically relevant thermal stress regulates dendritic cell function," *Cancer Immunology, Immunotherapy*, vol. 55, no. 3, pp. 292–298, 2006.

[55] W. Xia, R. Voellmy, and N. L. Spector, "Sensitization of tumor cells to fas killing through overexpression of heat-shock transcription factor 1," *Journal of Cellular Physiology*, vol. 183, no. 3, pp. 425–431, 2000.

[56] C. Setz, M. Friedrich, S. Hahn et al., "Just one position-independent lysine residue can direct MelanA into proteasomal degradation following N-terminal fusion of ubiquitin," *PLoS ONE*, vol. 8, no. 2, Article ID e55567, 2013.

[57] A. L. Croxford, P. Kulig, and B. Becher, "IL-12-and IL-23 in health and disease," *Cytokine and Growth Factor Reviews*, vol. 25, no. 4, pp. 415–421, 2014.

[58] M. Erdmann and B. Schuler-Thurner, "Dendritic cell vaccines in metastasized malignant melanoma," *Giornale Italiano di Dermatologia e Venereologia*, vol. 143, no. 4, pp. 235–250, 2008.

[59] R. Ross, S. Sudowe, J. Beisner et al., "Transcriptional targeting of dendritic cells for gene therapy using the promoter of the cytoskeletal protein fascin," *Gene Therapy*, vol. 10, no. 12, pp. 1035–1040, 2003.

[60] S. Sudowe, I. Ludwig-Portugall, E. Montermann, R. Ross, and A. B. Reske-Kunz, "Transcriptional targeting of dendritic cells in gene gun-mediated DNA immunization favors the induction of type 1 immune responses," *Molecular Therapy*, vol. 8, no. 4, pp. 567–575, 2003.

[61] C. Dresch, S. L. Edelmann, P. Marconi, and T. Brocker, "Lentiviral-mediated transcriptional targeting of dendritic cells for induction of T cell tolerance in vivo," *Journal of Immunology*, vol. 181, no. 7, pp. 4495–4506, 2008.

Hindawi Publishing Corporation
Journal of Immunology Research
Volume 2016, Article ID 9425172, 5 pages
http://dx.doi.org/10.1155/2016/9425172

Research Article

Overcoming the Constraints of Anti-HIV/CD89 Bispecific Antibodies That Limit Viral Inhibition

Xiaocong Yu,[1,2] Mark Duval,[1] Melissa Gawron,[1] Marshall R. Posner,[1,2] and Lisa A. Cavacini[1,2]

[1]*Department of Medicine, Beth Israel Deaconess Medical Center, Boston, MA 02215, USA*
[2]*Harvard Medical School, Boston, MA 02215, USA*

Correspondence should be addressed to Xiaocong Yu; xiaocong.yu@umassmed.edu
and Lisa A. Cavacini; lisa.cavacini@umassmed.edu

Received 30 November 2015; Revised 9 May 2016; Accepted 22 May 2016

Academic Editor: Leandro J. Carreño

Innovative strategies are necessary to maximize the clinical application of HIV neutralizing antibodies. To this end, bispecific constructs of human antibody F240, reactive with well-conserved gp41 epitope and antibody 14A8, reactive with the IgA receptor (CD89) on effector cells, were constructed. A F240 × 14A8 bispecific single chain variable region (scFv) molecule was constructed by linking two scFvs using a conventional GGGGS linker. Despite immunoreactivity with HIV gp41 and neutrophils, this bispecific scFv failed to inhibit HIV infection. This is in sharp contrast to viral inhibition using a chemical conjugate of the Fab of these two antibodies. Therefore, we constructed two novel Fab-like bispecific antibody molecules centered on fusion of the IgG1 CH1 domain or CH1-hinge domain to the C-terminus of F240scFv and fusion of the kappa chain CL domain to the C-terminus of 14A8scFv. Both Bi-Fab antibodies showed significant ADCVI activity for multiple clade B and clade C isolates by arming the neutrophils to inhibit HIV infection. The approach presented in this study is unique for HIV immunotherapy in that the impetus of neutralization is to arm and mobilize PMN to destroy HIV and HIV infected cells.

1. Introduction

Notwithstanding the isolation of broadly neutralizing anti-HIV-1 human antibodies [1], there remain a number of limitations for clinical applications, including global subtype coverage. One approach is to broadly target virus using conserved nonneutralizing domains on the HIV-1 Env and to target virus for destruction using noninfectable effector cells. It has been shown that Antibody-Dependent Cellular Cytotoxicity (ADCC) can be mediated by nonneutralizing antibodies and it has been shown to be higher in HIV controllers [2, 3].

We previously demonstrated that a bispecific antibody, constructed by chemical conjugation of the Fab regions of F240 and the anti-CD89 (IgA receptor) antibody 14A8, promotes destruction of HIV by neutrophils [4]. F240 recognizes a highly conserved extracellular epitope (residues 598 to 604) on gp41 within cluster I and reacts with primary isolates from all clades of HIV-1 [5], similar to other cluster I antibodies. The majority of clades A, B, and C isolates in the HIV-1 sequence database have an identical peptide (amino acids 592 to 606), with the exception of clade D isolates, which have a consistent L602H mutation. Our prior study supports the notion that broadly reactive, nonneutralizing antibodies, such as F240, could be used to "neutralize" HIV and might be a practicable novel therapeutic strategy for prevention and treatment of HIV infection. However, chemical conjugation for the construction of bispecific antibodies is associated with technical and large scale production issues.

To create and study different bispecific molecular constructs and promote a better production process, we have constructed bispecific antibodies using conventional linkers of scFv fragments as well as two novel Fab-like bispecific antibody structures. Further, we demonstrate that specific recombinant bispecific antibody structures effectively inhibit HIV infection. The results described here also report on the contribution of molecular structure of the bispecific antibody to maximal anti-HIV functional activity.

2. Materials and Methods

2.1. Monoclonal Antibodies, Virus, and Cell Lines. Antibody F240, generated in our laboratory, binds to a broadly conserved domain of gp41 [5]. The 14A8 is a human anti-CD89 antibody that was generated in Medarex-Mouse human Ig transgenic mice [6]. The bispecific single chain (scFv) antibody expression vector pcDNA3.1 was from Invitrogen. The vectors of pLC-HuCκ and pHC-HuCγ1 for expressing Bi-Fab antibodies were obtained from Dr. McLean [7] and were modified for expressing Fab-like bispecific antibodies. CHO-K1 cells were from American Type Culture Collection. The following reagents were obtained through the AIDS Research and Reference Reagent Program, Division of AIDS, NIAID, NIH: SF162 (R5) from Dr. Jay Levy; BaL (R5) from Dr. Suzanne Gartner, Dr. Mikulas Popovic, and Dr. Robert Gallo; 93MW960 (clade C, R5) from Dr. Robert Bollinger and the UNAIDS Network for HIV; JR-FL (R5) from Dr. Irvin Chen; TZM-bl cells from Dr. John C. Kappes, Dr. Xiaoyun Wu, and Transzyme, Inc.; isolate 67970 (CXCR4) from Dr. David Montefiori.

2.2. Construction of Antibody F240 and 14A8 scFv Molecules. Total RNA was isolated from F240 hybridoma cell line and then amplified the variable domain fragments of heavy chain (VH) and light chain (VL) using RT-PCR. The 14A8 variable domain fragments of VH and VL were directly amplified using 14A8 antibody gene plasmids as PCR template. A peptide $(GGGGS)_3$ was used as a linker to assemble VH and VL together to form the F240scFv and 14A8scFv individually by overlap PCR.

2.3. Construction of Conventional F240 × 14A8 Bis-scFv Antibody Plasmid and Establishing Stable Expressing Cell Lines. An F240 × 14A8 bispecific scFv antibody was constructed using a conventional structure. A DNA sequence that codes a short linker peptide consisting of glycine and serine residues (GGGGS) was designed to connect F240scFv and 14A8scFv by overlap PCR. The amplified Bi-scFv fragment was cloned into pcDNA3.1 vector utilizing the restriction sites of *NheI* and *HindIII*. The constructed plasmid was transfected into CHO cells with lipofectamine LTX (Invitrogen) using selection medium containing 1 mg/mL zeocin for at least two weeks. Limiting dilution at 1 cell per well was performed twice to obtain a stable cell line.

2.4. Constructing Plasmids of F240 × 14A8 Bi-Fab and Establishing Stable Expression Cell Lines. A human IgG CH1 fragment or CH1+ hinge fragment was amplified by PCR from the human IgG1 heavy chain and c-myc plus 6XHis tags was assembled into the 3′ end. The F240scFv genes (as described above with linkers) were connected directly with these amplified fragments individually by overlap extensional PCR, and the PCR products were cloned into the IgG expressing vector (Dr. McLean) to replace the human IgG1 constant domain. Meanwhile, the14A8scFv was cloned into the vector of pLC-HuCκ using *NheI*/*NotI* sites which contained human kappa chain constant. Paired purified plasmids encoding the 14A8scFv-CL versus F240scFv-CH1 or 14A8scFv-CL versus F240scFv-CH1-hinge were cotransfected into CHO-K1 cells in 6-well plates with lipofectamine LTX (Invitrogen Life Technologies). G418 (800 μg/mL) and puromycin (10 μg/mL) were used for selection of stable transfectants. The plates were screened using capture ELISA assay. The positive wells with top producing capacity were cloned by one-cell-per-well limiting dilution to establish the highest expressing cell clones. The expressed Bi-Fabs in culture supernatant were purified using protein L. Expression from the stable cell lines varied from a low expression of 1 μg/mL to 50 μg/mL depending on the tissue culture vessel used. Recovery of antibody following purification was similar to what we see using protein G columns and IgG and efficiency was proportional to the amount of antibody applied to the column up to capacity.

2.5. Immunoreactivity of F240 and CD89 Components of Bi-Fab Antibodies. To detect F240 reactivity, microplates were coated with recombinant gp41 (ectodomain aa 546–682 of HxB2 strain, Meridian) at 2 μg/mL in PBS overnight at 4°C followed by blocking with BSA blocking buffer plus 0.01%-tween at room temperature for 2 hours. Bi-Fab samples were added at 1 μg/mL and serial dilutions were performed. Samples were incubated for 30 minutes followed by washing and incubation with HRP-conjugated protein L (Pierce). The human monoclonal F240 was run as a standard to determine relative reactivity of the F240-14A8 Bi-Fabs. After washing, 100 μL of TMB substrate was added and incubated for 5 minutes. Reaction was stopped with 100 μL of 1 M phosphoric acid and plate was read on a plate reader at 450 nm.

Immunoreactivity of 14A8 with CD89 was determined by flow cytometry. Neutrophils were isolated from peripheral blood of HIV seronegative donors using Ficoll-Hypaque gradient centrifugation and dextran sedimentation. PMNs were washed twice with PBS and resuspended at a concentration of 1×10^7 c/mL in HBSS containing 2.5% FBS. 100 μL of PMNs was mixed with 100 μL of serial diluted Bi-Fab antibodies and incubated on ice for 30 minutes. Cells were washed twice with PBS followed by 30-minute incubation with FITC-labeled Goat anti-human Ig Kappa (Southern Biotechnology Associates). PMNs were washed and fixed in 1% paraformaldehyde and samples were acquired and analyzed using Guava 8HT and Incyte software. Live cells were gated based on forward and side scatter.

2.6. Antibody-Dependent Cell-Mediated Viral Inhibition (ADCVI). The ability of the antibody to arm neutrophils to inhibit HIV infection was measured as ADCVI activity of constructed bispecific antibodies using HIV grown in PHA stimulated PBMC [8, 9]. Bispecific antibodies were tittered in 96-well plates with 50 μL media. Neutrophils (5×10^6 cells/well) were added and incubated with antibody for 10 minutes. PBMC productively infected with HIV-1 four days earlier were used as target cells and 5×10^5 infected cells were added to the antibody/effector cell mixture resulting in an E : T ratio of 10 : 1. The 10 : 1 E : T ratio was selected as the concentration of neutrophils that does not result in nonspecific inhibition of HIV by the neutrophils. After incubation for 4 hours, PHA stimulated PBMC (2×10^6/well)

were added as indicator cells for measuring the surviving infectious virus and incubated for seven days in the presence of IL-2 and p24 quantitated by ELISA [10]. Linear regression analysis was used to determine IC_{50} values and Student's t-test was used to detect significance. Control wells included absent antibody, absent effector cells, and absent target cells to determine background release of virus, maximal production of virus, and whether PMN alone were infected, respectively. Experiments were repeated three times.

3. Results

A bispecific single chain antibody was made using a G4S peptide to link the F240 scFv with the 14A8 scFv. The bispecific scFv was found to bind to both gp41 (ELISA) and CD89 on neutrophils (flow cytometry). However, in contrast to our results using a chemical conjugate of Fab fragments of F240 and 14A8[4], the F240 × 14A8 biscFv antibody demonstrated limited ADCVI activity. At 10 μg/mL, F240 × 14A8 biscFv only inhibited 21–23% for JR-FL or 89.6 and failed to inhibit 93MW960 (data not shown). At this concentration, the chemical conjugate of F240 and 14A8 inhibited more than 50% for the isolates tested above. To ensure that this was not due to a donor specific neutrophil defect, the experiment was repeated on four separate occasions using different donor neutrophils. While the biscFv antibody failed to mediate ADCVI, a positive control anti-HIV b12 IgA or A1g8-IgA antibody known to mediate ADCVI inhibited infection (>40% at 10 μg/mL), in the presence of neutrophil effectors as previously reported [10]. Furthermore, failure of the bispecific scFv to mediate ADCVI was not related to immunoreactivity of the anti-gp41 F240 component as the sequence of the epitope on gp41 recognized by this antibody is identical in all isolates used in this study.

In reviewing the structure of the chemically conjugated versus biscFv bispecific antibodies, we hypothesized that failure of the biscFv to mediate ADCVI yet retain immunoreactivity may be a function of the structural constraints of the smaller and less flexible biscFv as compared to the Fab. The longer Fab fragment with the first Fc constant domain (CH1) and light chain constant (CL) may allow for more flexibility in bridging between the neutrophils and the infected cells. Therefore, we performed an innovative design to construct Fab-like bispecific antibodies. A dimeric or a tetrameric bispecific antibody was formed through the interchain disulfide bond between CH1 and CL or the CH1-hinge part and CL, respectively. The dimeric F240-CH1/14A8-CL is designated as F240 × 14A8 Bi-Fab-A and the tetrameric F240-CH1-hinge/14A8-CL as F240 × 14A8 Bi-Fab-B and as depicted in Figure 1. Immunoreactivity of the F240 × 14A8 Bi-Fab antibodies with HIV gp41 was determined by ELISA using F240 IgG1 antibody as the standard (Figure 2). Given that the epitope recognized by F240 is extremely conserved, it is expected that the Bi-Fab would react with the majority of isolates, with the exception of clade D. Both F240 × 14A8Bi-Fab antibodies react with gp41 and due to bivalency for gp41 binding, higher level binding is seen with Bi-Fab-B and the F240 IgG1, as compared to Bi-Fab-A. Immunoreactivity of the 14A8 component of Bi-Fab antibodies with CD89 is evident in Figure 3 using neutrophils from uninfected donors. Binding of both Bi-Fab antibodies occurs in a dose dependent manner and, similar to immunoreactivity with gp41, means that fluorescent intensity of Bi-Fab-B was greater than that seen for Bi-Fab-A.

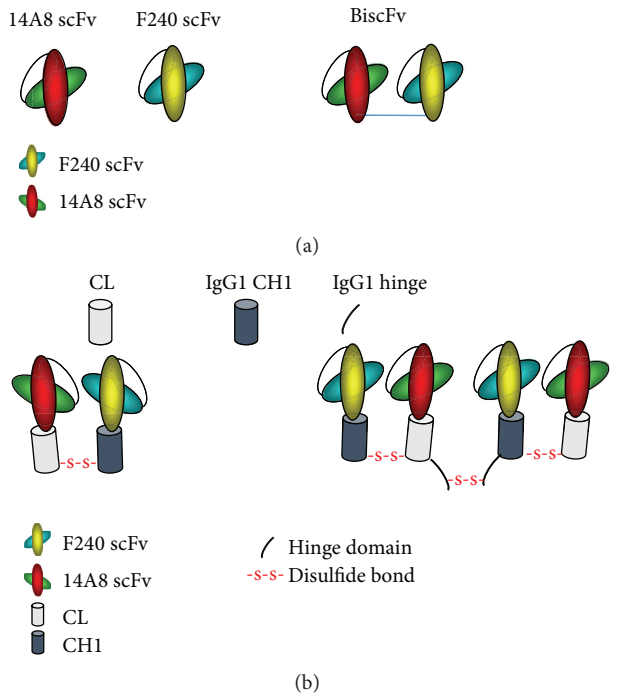

Figure 1: Schematic diagram of F240 × 14A8 Bi-Fab construction. The structure of the bispecific single chain antibody (biscFv) is depicted in (a) with the VH as either the green oval (14A8) or blue oval (F240) and the VL as the red oval (14A8) or yellow oval (F240). (b) represents the organization of the Bi-Fab.

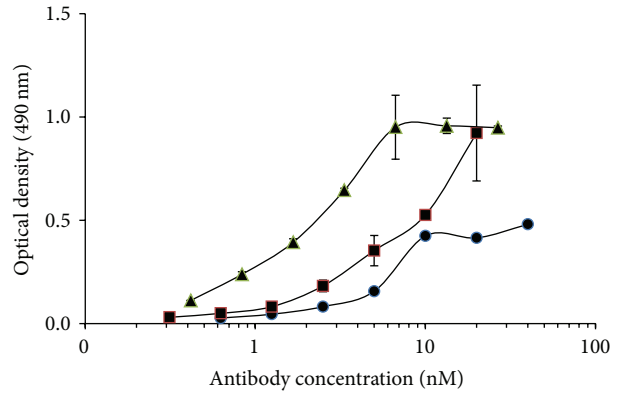

Figure 2: Immunoreaction of F240 × 14A8 Bi-Fab with gp41. Immunoreactivity of Bi-Fab antibody constructs with HIV antigen gp41. Antigen gp41 was coated at 2 μg/mL in PBS; the serial dilutions of Bi-Fab antibodies (Bi-Fab A, ●, and Bi-Fab B, ■) compared to that of serial dilutions of F240 antibody (▲); the reaction was developed by HRP-conjugated protein L (1 : 20,000) and measured by optical density at 490 nm. Results are representative of three different experiments and each experimental point is the mean ± standard deviation of triplicate wells.

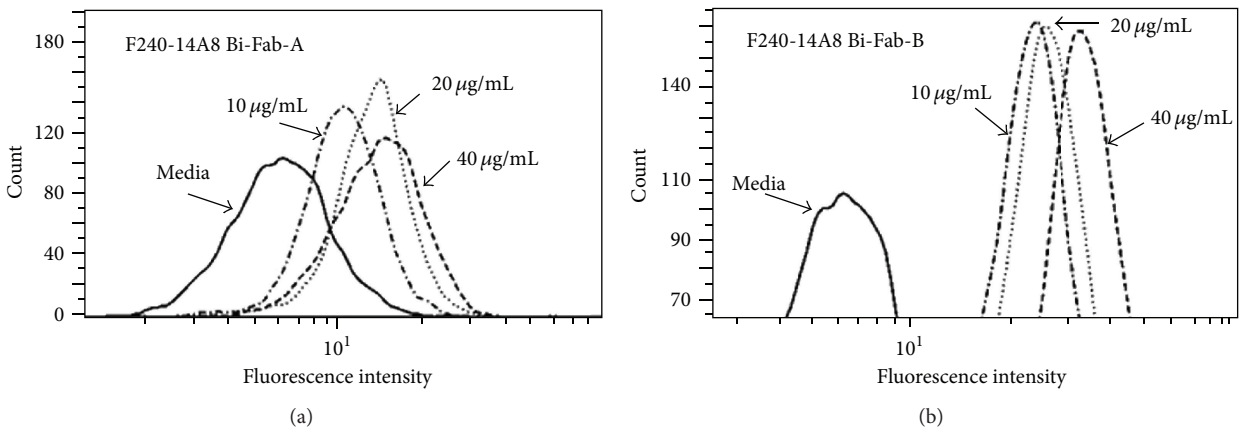

Figure 3: Binding affinity of F240 × 14A8 Bi-Fab with neutrophil through CD89. Neutrophils were washed twice with PBS and resuspended at a concentration of 1×10^7 c/mL in HBSS containing 2.5% FBS. 100 μL of neutrophils was mixed with 100 μL of serial diluted Bi-Fab antibodies with Bi-Fab A in (a) and Bi-Fab B in (b). Cells were incubated with FITC-labeled goat anti-human Ig Kappa for 30 minutes. Neutrophils were fixed in 1% paraformaldehyde. Results are representative of four different neutrophil donors.

Table 1: ADCVI activity of HIV-1 by F240 Bi-Fab antibody constructs.

	IC_{50} (μg/mL)[a]			
	BaL	JR-FL	93MW960	SF162
	Clade B, R5	Clade B, R5	Clade C R5	Clade B, R5
Bi-Fab-A	3.38 ± 2.39	0.04 ± 0.04	27.50 ± 7.78	15.69 ± 5.49
Bi-Fab-B	4.43 ± 0.16	35.85 ± 5.87	1.93 ± 2.65	0.22 ± 0.04
	$p = 0.60$[b]	$p = 0.01$	$p = 0.05$	$p = 0.06$
Chemical bispecific[c]	4.35 ± 1.2	NT[d]	10.4 ± 7.7	10.7 ± 2.9

[a]The ADCVI activity was determined by IC_{50} that represents concentration (μg/mL) of Bi-Fab antibody constructs required for 50% inhibition of HIV. Results are from three separate experiments.
[b]The p value reflects the comparison of Bi-Fab-A versus Bi-Fab-B.
[c]Chemical conjugation of Fab fragments of F240 and 14A8 as described in [4].
[d]NT: not tested.

Importantly, both Bi-Fab antibodies showed significant ADCVI activity for three clade B isolates and a clade C isolate (Table 1). There are significant differences in ADCVI activity among the virus isolates and between the different Bi-Fab constructs which is not necessarily explained by differences in the immunoreactivity with gp41 and neutrophils by the Bi-Fab molecules. Whereas both molecules were effective at inhibiting BaL (similar to the chemical conjugate of antibody Fabs), F240 × 14A8 Bi-Fab-A was more effective at ADCVI than F240 × 14A8 Bi-Fab-B for JR-FL. In contrast, the F240 × 14A8 Bi-Fab-B showed much higher ADCVI activity than Bi-Fab-A against 93MW960 and SF162 with the activity of the chemical conjugate intermediate between both of them. These differences may represent a number of mechanistic effects of the structure of both the antibody and the virus. Neither Bi-Fab construct neutralized HIV directly (data not shown).

4. Discussion

Building on our previous report of a chemically constructed bispecific antibody directing destruction of HIV[4], we have produced molecular HIV specific bispecific antibody molecules incorporating the HIV gp41 specific antibody, F240, and an IgA receptor specific antibody, 14A8. A conventional design was used to link two scFvs for expression as a bispecific scFv. Despite immunoreactivity with HIV (gp41) and neutrophils, this bispecific scFv failed to mediate ADCVI activity. In retrospect, failure of the conventional F240 × 14A8 biscFv may be predicted by the structure of the biscFv. We hypothesized that failure of the biscFv to mediate ADCVI yet retain immunoreactivity with both HIV and neutrophils may be a function of the structural constraints of the scFv as compared to the Fab. The longer antibody Fab fragment with the first constant domain of Fc part may allow for more flexibility in bridging the neutrophils and the infected cells.

Viral isolates vary in quaternary structure such that env trimers may range from open to closed. Additional factors include differences in the spatial arrangement of envelope or the glycosylation pattern of viral isolates or the contribution of other membrane components as these studies were performed with HIV infected PBMC. Further studies using mutated viral isolates and crystallography are being designed to explore this. It is also evident that the structure of the bispecific antibody directly impacts function. Consistent with what was observed previously, the heavy chain CH1 domain can affect antibody binding affinity and fine specificity [11]. A larger, flexible structure conferred by the CH1 and CL domains significantly contributes to the action of the bispecific antibodies in inhibiting HIV. Whereas the single chain construct failed to function although it did bind HIV and PMN, a flexible Bi-Fab molecule was able to confer function. Interestingly, the activity of the chemical conjugate of the Fab of antibodies F240 and 14A8 is similar to both Bi-Fabs for BaL but intermediate between Bi-Fab A

and Bi-Fab B for two other isolates (93MW960 and SF162). This would suggest that the structure or conformation of the variable regions (e.g., natural Fab versus scFv) also impacts function. Finally, it is clearly shown that cross-linking CD89, which occurs outside of the IgA binding site, is active even if CD89 is occupied by IgA and is a viable option to activate PMN to "inhibit" HIV. There is considerable research demonstrating that cross-linking of FcαR (CD89) using bispecific antibodies can induce tumor cytotoxicity [12–15], as well as target pathogens, such as *Streptococcus pneumonia* [16], *Porphyromonas gingivalis* [17], and *Bordetella pertussis* [18]. The approach presented in this study is unique for HIV immunotherapy in that the impetus for "neutralization" is to arm and mobilize neutrophils, which do not get infected, to globally destroy HIV and HIV infected cells.

5. Conclusions

These results demonstrate that recombinant Fab-like bispecific antibody constructs effectively inhibit HIV. Moreover, the molecular bispecific antibody construct profoundly affects the functional activity of the antibody. The approach presented in this study is unique for HIV immunotherapy in that the impetus of neutralization is to arm and mobilize PMN to destroy HIV and HIV infected cells.

Disclosure

Current address of Mark Duval, Melissa Gawron, and Lisa A. Cavacini is as follows: MassBiologics, University of Massachusetts Medical School, Boston, MA, USA. Current address of Marshall R. Posner is as follows: The Tisch Cancer Institute, Icahn School of Medicine at Mount Sinai, New York, NY, USA.

Competing Interests

The authors declare that there are no competing interests related to the publication of this paper.

Acknowledgments

This work was supported by Public Health Service Grant R01AI076138 from the National Institute of Health.

References

[1] P. D. Kwong and J. R. Mascola, "Human antibodies that neutralize HIV-1: identification, structures, and B cell ontogenies," *Immunity*, vol. 37, no. 3, pp. 412–425, 2012.

[2] O. Lambotte, G. Ferrari, C. Moog et al., "Heterogeneous neutralizing antibody and antibody-dependent cell cytotoxicity responses in HIV-1 elite controllers," *AIDS*, vol. 23, no. 8, pp. 897–906, 2009.

[3] J. Thèze, L. A. Chakrabarti, B. Vingert, F. Porichis, and D. E. Kaufmann, "HIV controllers: a multifactorial phenotype of spontaneous viral suppression," *Clinical Immunology*, vol. 141, no. 1, pp. 15–30, 2011.

[4] M. Duval, M. R. Posner, and L. A. Cavacini, "A bispecific antibody composed of a nonneutralizing antibody to the gp41 immunodominant region and an anti-CD89 antibody directs broad human immunodeficiency virus destruction by neutrophils," *Journal of Virology*, vol. 82, no. 9, pp. 4671–4674, 2008.

[5] L. A. Cavacini, C. L. Emes, A. V. Wisnewski et al., "Functional and molecular characterization of human monoclonal antibody reactive with the immunodominant region of HIV type 1 glycoprotein 41," *AIDS Research and Human Retroviruses*, vol. 14, no. 14, pp. 1271–1280, 2009.

[6] D. M. Fishwild, S. L. O'Donnell, T. Bengoechea et al., "High-avidity human IgGκ monoclonal antibodies from a novel strain of minilocus transgenic mice," *Nature Biotechnology*, vol. 14, no. 7, pp. 845–851, 1996.

[7] G. R. McLean, A. Nakouzi, A. Casadevall, and N. S. Green, "Human and murine immunoglobulin expression vector cassettes," *Molecular Immunology*, vol. 37, no. 14, pp. 837–845, 2001.

[8] L. A. Cavacini, J. E. Peterson, E. Nappi et al., "Minimal incidence of serum antibodies reactive with intact primary isolate virions in human immunodeficiency virus type 1-infected individuals," *Journal of Virology*, vol. 73, no. 11, pp. 9638–9641, 1999.

[9] L. R. Miranda, M. Duval, H. Doherty, M. S. Seaman, M. R. Posner, and L. A. Cavacini, "The neutralization properties of a HIV-specific antibody are markedly altered by glycosylation events outside the antigen-binding domain," *Journal of Immunology*, vol. 178, no. 11, pp. 7132–7138, 2007.

[10] X. Yu, M. Duval, C. Lewis et al., "Impact of IgA constant domain on HIV-1 neutralizing function of monoclonal antibody F425A1g8," *Journal of Immunology*, vol. 190, no. 1, pp. 205–210, 2013.

[11] D. Tudor, H. Yu, J. Maupetit et al., "Isotype modulates epitope specificity, affinity, and antiviral activities of anti-HIV-1 human broadly neutralizing 2F5 antibody," *Proceedings of the National Academy of Sciences of the United States of America*, vol. 109, no. 31, pp. 12680–12685, 2012.

[12] Y. M. Deo, K. Sundarapandiyan, T. Keler, P. K. Wallace, and R. F. Graziano, "Bispecific molecules directed to the Fc receptor for IgA (FcαRI, CD89) and tumor antigens efficiently promote cell-mediated cytotoxicity of tumor targets in whole blood," *Journal of Immunology*, vol. 160, no. 4, pp. 1677–1686, 1998.

[13] K. Sundarapandiyan, T. Keler, D. Behnke et al., "Bispecific antibody-mediated destruction of Hodgkin's lymphoma cells," *Journal of Immunological Methods*, vol. 248, no. 1-2, pp. 113–123, 2001.

[14] B. Stockmeyer, M. Dechant, M. van Egmond et al., "Triggering FCα-receptor I (CD89) recruits neutrophils as effector cells for CD20-directed antibody therapy," *Journal of Immunology*, vol. 165, no. 10, pp. 5954–5961, 2000.

[15] F. J. Hernandez-Ilizaliturri, V. Jupudy, J. Ostberg et al., "Neutrophils contribute to the biological antitumor activity of rituximab in a non-hodgkin's lymphoma severe combined immunodeficiency mouse model," *Clinical Cancer Research*, vol. 9, no. 16 I, pp. 5866–5873, 2003.

[16] W.-L. Van der Pol, G. Vidarsson, H. A. Vile, J. G. J. Van de Winkel, and M. E. Rodriguez, "Pneumococcal capsular polysaccharide-specific IgA triggers efficient neutrophil effector functions via FcαRI (CD89)," *Journal of Infectious Diseases*, vol. 182, no. 4, pp. 1139–1145, 2000.

[17] T. Kobayashi, A. Takauchi, A. B. V. Spriel et al., "Targeting of *Porphyromonas gingivalis* with a bispecific antibody directed to FcαRI (CD89) improves in vitro clearance by gingival crevicular neutrophils," *Vaccine*, vol. 23, no. 5, pp. 585–594, 2004.

[18] S. M. M. Hellwig, A. B. Van Spriel, J. F. P. Schellekens, F. R. Mooi, and J. G. J. Van de Winkel, "Immunoglobulin A-mediated protection against *Bordetella pertussis* infection," *Infection and Immunity*, vol. 69, no. 8, pp. 4846–4850, 2001.

Hindawi Publishing Corporation
Journal of Immunology Research
Volume 2016, Article ID 4156456, 8 pages
http://dx.doi.org/10.1155/2016/4156456

Research Article

A Fusion Protein Consisting of the Vaccine Adjuvant Monophosphoryl Lipid A and the Allergen Ovalbumin Boosts Allergen-Specific Th1, Th2, and Th17 Responses *In Vitro*

Stefan Schülke,[1] Lothar Vogel,[2] Ann-Christine Junker,[1] Kay-Martin Hanschmann,[3] Adam Flaczyk,[1] Stefan Vieths,[1] and Stephan Scheurer[1]

[1]*Vice President's Research Group 1: Molecular Allergology, Paul-Ehrlich-Institut, Langen, Hessen, Germany*
[2]*Division of Allergology, Paul-Ehrlich-Institut, 63225 Langen, Germany*
[3]*Division of Microbiology, Paul-Ehrlich-Institut, 63225 Langen, Germany*

Correspondence should be addressed to Stefan Schülke; stefan.schuelke@pei.de

Received 7 March 2016; Revised 25 April 2016; Accepted 17 May 2016

Academic Editor: Leandro J. Carreño

Background. The detoxified TLR4-ligand Monophosphoryl Lipid A (MPLA) is the first approved TLR-agonist used as adjuvant in licensed vaccines but has not yet been explored as part of conjugated vaccines. *Objective*. To investigate the immune-modulating properties of a fusion protein consisting of MPLA and Ovalbumin (MPLA : Ova). *Results*. MPLA and Ova were chemically coupled by stable carbamate linkage. MPLA : Ova was highly pure without detectable product-related impurities by either noncoupled MPLA or Ova. Light scattering analysis revealed MPLA : Ova to be aggregated. Stimulation of mDC and mDC : DO11.10 $CD4^+$ TC cocultures showed a stronger activation of both mDC and Ova-specific DO11.10 $CD4^+$ TC by MPLA : Ova compared to the mixture of both components. MPLA : Ova induced both strong proinflammatory (IL-1β, IL-6, and TNF-α) and anti-inflammatory (IL-10) cytokine responses from mDCs while also boosting allergen-specific Th1, Th2, and Th17 cytokine secretion. *Conclusion*. Conjugation of MPLA and antigen enhanced the immune response compared to the mixture of both components. Due to the nonbiased boost of Ova-specific Th2 and Th17 responses while also inducing Th1 responses, this fusion protein may not be a suitable vaccine candidate for allergy treatment but may hold potential for the treatment of other diseases that require a strong stimulation of the host's immune system (e.g., cancer).

1. Introduction

Currently, conventional allergen immunotherapy (AIT) with allergen extracts is not convenient for patients due to a multiyear treatment regimen [1]. For some allergies, AIT is only partially efficacious and can be hampered by unwanted side effects. To improve AIT, novel vaccine candidates and accompanying adjuvants that increase efficacy while decreasing unwanted adverse-effects are needed [2].

In this context, the discovery of TLR-ligands with their intrinsic ability to induce robust innate immune responses was thought to hold great potential for the discovery and development of novel adjuvants. One of the best-characterized TLR-ligands is lipopolysaccharide (LPS), a cell wall component of Gram-negative bacteria that activates TLR4. Despite its strong immune-stimulatory potential, its use as an adjuvant is strongly limited due to its inherent toxicity [3]. Accordingly, nucleic acid-based TLR-ligands, such as CpG (TLR9), R848 (TLR7/8), or Poly I:C (TLR3), are good immune activators but are hampered in their clinical efficacy due to problems with both toxicity and stability *in vivo* [3].

To be able to take advantage of the strong immune-activating properties of TLR-ligands without the inherent toxicity, variants of TLR-ligands were generated by chemical modification which should retain most of their immune-stimulating properties [4]. One such adjuvant is the TLR4-ligand Monophosphoryl Lipid A (MPLA), a detoxified LPS-derivative. MPLA was derived from the LPS of *Salmonella minnesota* R595 by a series of organic extractions followed by

mild acid and alkaline treatments [4]. This resulted in three distinct modifications compared to the parent molecule: (1) the removal of the core polysaccharide containing the O-antigen, (2) the removal of one phosphate group, and (3) one fatty acid chain [4].

Up to now, MPLA is the only TLR-ligand used as an adjuvant in licensed vaccines. Several vaccines including Fendrix® (hepatitis B), Cervarix® (human papillomavirus-16 and papillomavirus-18), RTS,S® (malaria) [5–7], and the allergen product Pollinex® Quattro (pollen allergies) [8] which contain MPLA as one component of more complex adjuvant systems have been licensed or are undergoing phase III clinical trials. Immunologically, MPLA has been repeatedly shown to induce a predominantly Th1-biased immune response [9]. The application of allergen therapeutics containing MPLA leads to isotype switching from allergen-specific IgE antibodies towards IgG_1- and IgG_4-dominated humoral immune response in humans [10].

While MPLA was reported to be less toxic and pyrogenic than LPS [11], the recent approval of several vaccine formulations adjuvanted with MPLA prompted us to initiate further detailed investigations of its adjuvant potential. In a previous study we showed that, in direct comparison to LPS, MPLA-stimulation induced similar but attenuated immune responses in several important immune cell types such as mouse epithelial cells, myeloid dendritic cells (mDCs), B and T cells, and human *ex vivo* isolated monocytes. Interestingly, MPLA was not able to activate either human or mouse mast cells [12].

After initially characterizing MPLA's immune-activating potential [12] we wanted to determine its potential as an integral part of an adjuvant : allergen fusion protein. In several experimental allergy models, such conjugates, for example, incorporating TLR5-, TLR7/8-, and TLR9-ligands, have been described to have beneficial immune-modulating properties by promoting Th1- and appropriate regulatory responses [13–16].

To this end, we chemically coupled MPLA to the model allergen Ovalbumin (Ova) and characterized the conjugate by SDS-PAGE and light scattering analysis. Subsequently, the immune-modulating properties of this MPLA : Ova fusion protein were investigated using mouse bone marrow-derived mDC and a coculture system of mDC and allergen-specific DO11.10 $CD4^+$ T cells (mDC : DO11.10 $CD4^+$ TC) *ex vivo* to directly compare what effect fusion of MPLA to Ova would have on the initiated immune response.

2. Methods

2.1. Coupling of MPLA and Ova. To activate MPLA (InvivoGen, Toulouse, France), it was dissolved in dried dioxane (Sigma) at a concentration of 50 mM and subsequently incubated at 37°C. 1,1′-Carbonyldiimidazole (CDI, Sigma, Steinheim, Germany) was added to a final concentration of 0.5 M and the mixture was incubated for 2 h at 37°C with stirring. Finally, dioxane was removed by the addition of diethyl ether and evaporation overnight. To couple the allergen to CDI-activated MPLA, EndoGrade Ovalbumin (Hyglos, Bernried, Germany) was dissolved in 10 mM sodium borate (pH 8.5) at 2.5 mg/mL and was subsequently used to dissolve the CDI-activated MPLA. After incubation for 48 h at 4°C with stirring, unconjugated MPLA was removed by extensive dialysis against PBS at 4°C for two days. The resulting MPLA : Ova fusion protein was characterized by SDS-PAGE and dynamic light scattering analysis.

2.2. SDS-PAGE. Chemically conjugated MPLA : Ova was compared to EndoGrade Ovalbumin (Hyglos) by SDS-PAGE according to the method described by Laemmli (cross linker C = 5%, total bis/acrylamide 15%) [17] under reducing conditions.

2.3. Dynamic Light Scattering Analysis. Dynamic light scattering analysis was performed using a Zetasizer Nano ZS (Malvern, Herrenberg, Germany). For light scattering analysis, 70 μL of MPLA (1 mg/mL), MPLA : Ova (0.6 mg/mL), LPS (1 mg/mL), or Ova (1 mg/mL) in PBS was analyzed at room temperature. Three individual measurements per sample were performed and the mean frequencies (calculated as relative % in class) of hydrodynamic radii (r_H) in nm were plotted.

2.4. In Vitro Generation of Mouse Bone Marrow-Derived Dendritic Cells. Mouse myeloid dendritic cells (mDCs) were generated as described previously [18]. Briefly, bone marrow cells (BMCs) were isolated from femur and tibia of BALB/c, mice and differentiated into mDCs using GM-CSF (R&D Systems, Minneapolis, USA). On day eight, mDCs were harvested for experiments.

2.5. Preparation and Stimulation of mDC and mDC : DO11.10 $CD4^+$ T Cell Cocultures. Splenic $CD4^+$ T cells were isolated from Ova-TCR transgenic DO11.10 mice using the $CD4^+$ T Cell Isolation Kit (Miltenyi Biotec, Bergisch Gladbach, Germany). BALB/c mDCs (3.2×10^5 cells/mL) were cultured alone or in combination with DO11.10 $CD4^+$ T cells (8.0×10^5 cells/mL, >95% purity) and stimulated with equimolar amounts of Ova, MPLA, MPLA mixed with Ova (MPLA + Ova), or MPLA : Ova (fusion protein) for 72 h. Subsequently, concentrations of IL-1β, IL-2, IL-5, IL-6, IL-9, IL-10, IL-12p70, IL-13, IL-17A, TNF-α, and IFN-γ in the supernatants were measured by BD OptEIA ELISA (BD Biosciences, Heidelberg, Germany) or Ready-SET-Go! ELISA Sets (eBiosciences, Frankfurt, Germany).

2.6. Statistical Analysis. The hypothesis of a significant higher cytokine secretion among all three concentrations used for stimulation was tested with a two-factorial analysis of variance (ANOVA) with factors stimulus (0.2, 1.0, and 5.0) and group ("MPLA + OVA" or "MPLA : OVA"). For statistical significant results the following convention was used: $^*p$ value < 0.05, $^{**}p$ value < 0.01, and $^{***}p$ value < 0.001. The statistical analysis was performed with SAS/STAT software, version 9.4, SAS System for Windows.

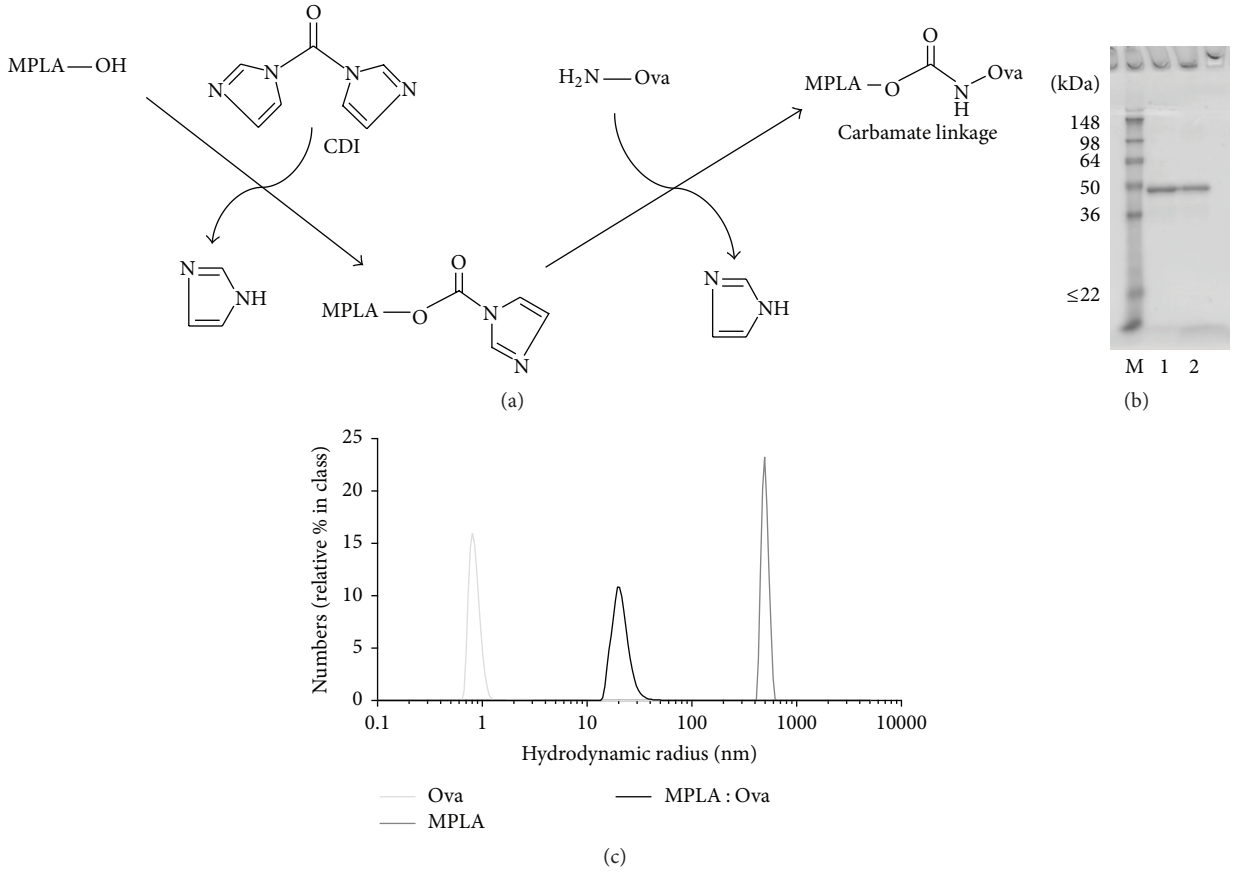

Figure 1: Generation of MPLA : Ova fusion protein. Applied chemical coupling strategy (a). Analysis of MPLA : Ova by reducing SDS-PAGE (b, M: molecular weight marker, 1: EndoGrade Ova, and 2: MPLA : Ova) and dynamic light scattering (c). For light scattering analysis, 70 μL of MPLA (1 mg/mL), MPLA : Ova (0.6 mg/mL), LPS (1 mg/mL), or Ova (1 mg/mL) in PBS was analyzed at room temperature. Three individual measurements per sample were performed and the mean frequencies (calculated as relative % in class) of hydrodynamic radii (r_H) in nm were plotted.

3. Results

3.1. A Fusion Protein of MPLA and Ova Shows Noncovalent Aggregation. For the generation of the MPLA : Ova fusion protein, MPLA was conjugated to EndoGrade Ova using a carbonyldiimidazole linker in order to generate a stable carbamate linkage between both molecules (Figure 1(a)). Noncoupled MPLA was removed by extensive dialysis. The resulting MPLA : Ova fusion protein was characterized by SDS-PAGE and displayed a distinct band with an apparent molecular mass of 47 kDa (Figure 1(b)). Compared to Ova (apparent molecular mass of 45 kDa) this moderate shift of approximately 2 kDa suggests a coupling rate of one molecule of MPLA (molecular mass: 1.7 kDa) per molecule of Ova (Figure 1(b)).

Dynamic light scattering analysis determined the hydrodynamic radius of MPLA (r_H = 496 nm) to be larger than the radius of Ova (r_H = 0.9 nm, Figure 1(c)). This finding suggests aggregation in the MPLA preparation which is likely explained by the formation of micelle-like structures by the fatty acid chains of MPLA [19]. Here, the size of aggregates was reduced for the MPLA : Ova fusion protein (r_H = 20 nm), likely due to steric hindrance of micelle-formation induced by the fusion of Ova to MPLA (Figure 1(c)). However, compared to Ova alone, the hydrodynamic radius of the MPLA : Ova fusion protein was 22-fold enhanced in size, and no molecules with the hydrodynamic radius of either Ova or MPLA were detected in the MPLA : Ova preparation (Figure 1(c)). Taken together, these findings suggest both a complete coupling of the two molecules at a one-to-one ratio for the fusion protein and a complete removal of noncoupled MPLA by dialysis, resulting in a pure fusion protein preparation.

3.2. MPLA : Ova Boosts mDC-Derived Cytokine Secretion Compared to the Mixture of Both Components. To investigate the potential immune-modulating properties of the fusion protein compared to both components alone or as a mixture we performed stimulation experiments using both myeloid dendritic cells (mDCs) alone (Figure 2(a)) and in coculture experiments with Ova-T cell receptor transgenic DO11.10 $CD4^+$ T cells (Figures 2(b) and 3).

In mDC cultures, stimulated with the different constructs, application of the MPLA : Ova fusion protein resulted in increased secretion of IL-1β, IL-6, IL-10, and TNF-α (Figure 2(a), IL-1β: MPLA : Ova versus MPLA + Ova p = 0.0241,

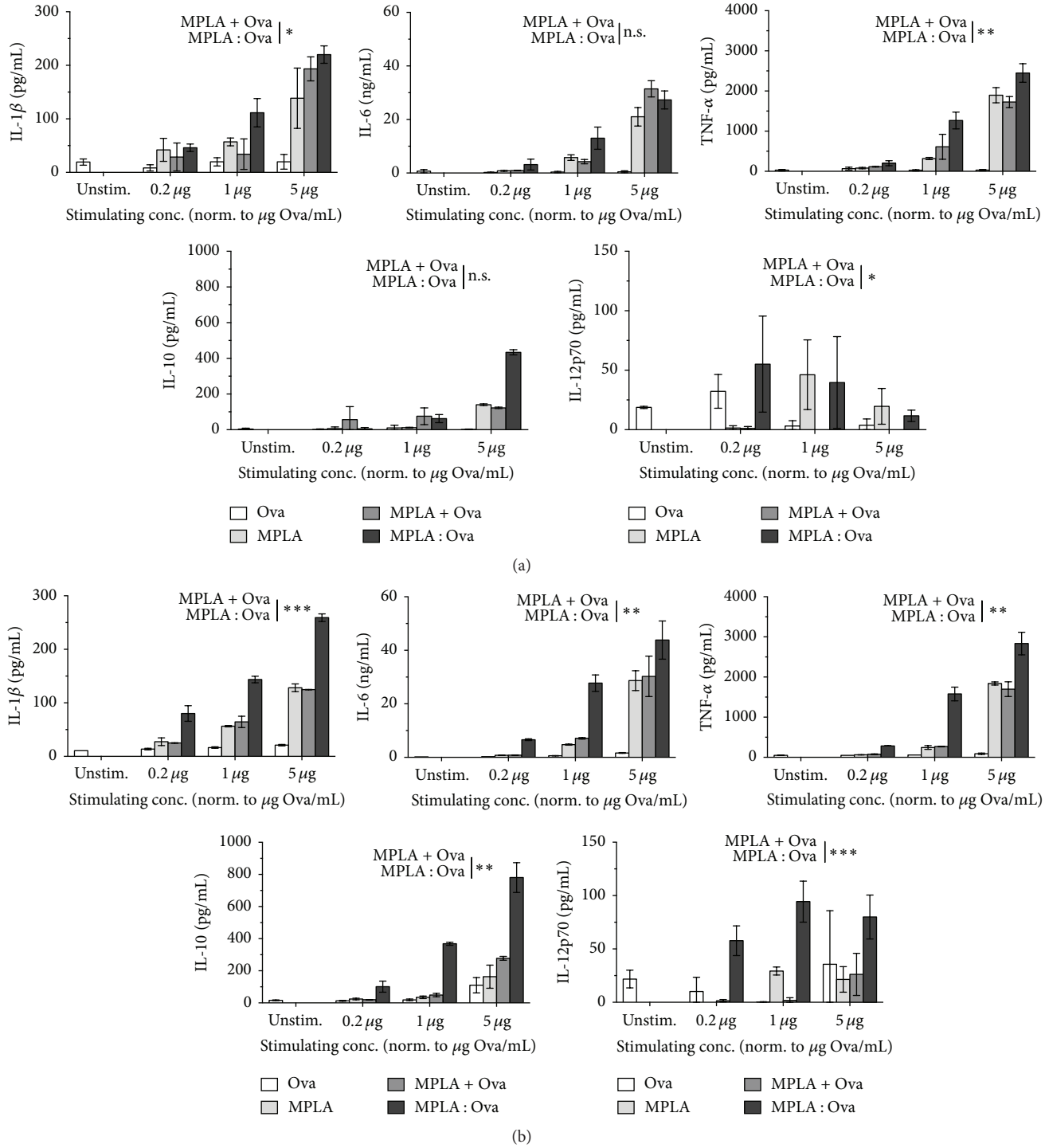

Figure 2: The MPLA : Ova fusion protein boosts mDC-derived cytokine secretion compared to the mixture of both components. Cytokine secretion determined from either BALB/c mDC (3.2×10^5 cells/mL, a) or BALB/c mDC (3.2×10^5 cells/mL) plus DO11.10 $CD4^+$ T cell (8.0×10^5 cells/mL, >95% purity) cocultures (b) stimulated with equimolar amounts of Ova (white bars), MPLA (light grey bars), MPLA + Ova (dark grey bars), and the MPLA : Ova fusion protein (black bars) for 72 h and analyzed by ELISA. ELISAs were performed using either BD OptEIA™ ELISA (BD Biosciences) or Ready-SET-Go! ELISA Sets (eBiosciences). Data are mean results of two independent experiments ± SD. The hypothesis of a significant higher cytokine secretion among all three concentrations used for stimulation was tested with a two-factorial analysis of variance (ANOVA) with factors stimulus (0.2, 1.0, and 5.0) and group ("MPLA + OVA" or "MPLA : OVA"). For statistical significant results the following convention was used: $^*p$ value < 0.05, $^{**}p$ value < 0.01, and $^{***}p$ value < 0.001. The statistical analysis was performed with SAS®/STAT software, version 9.4, SAS System for Windows.

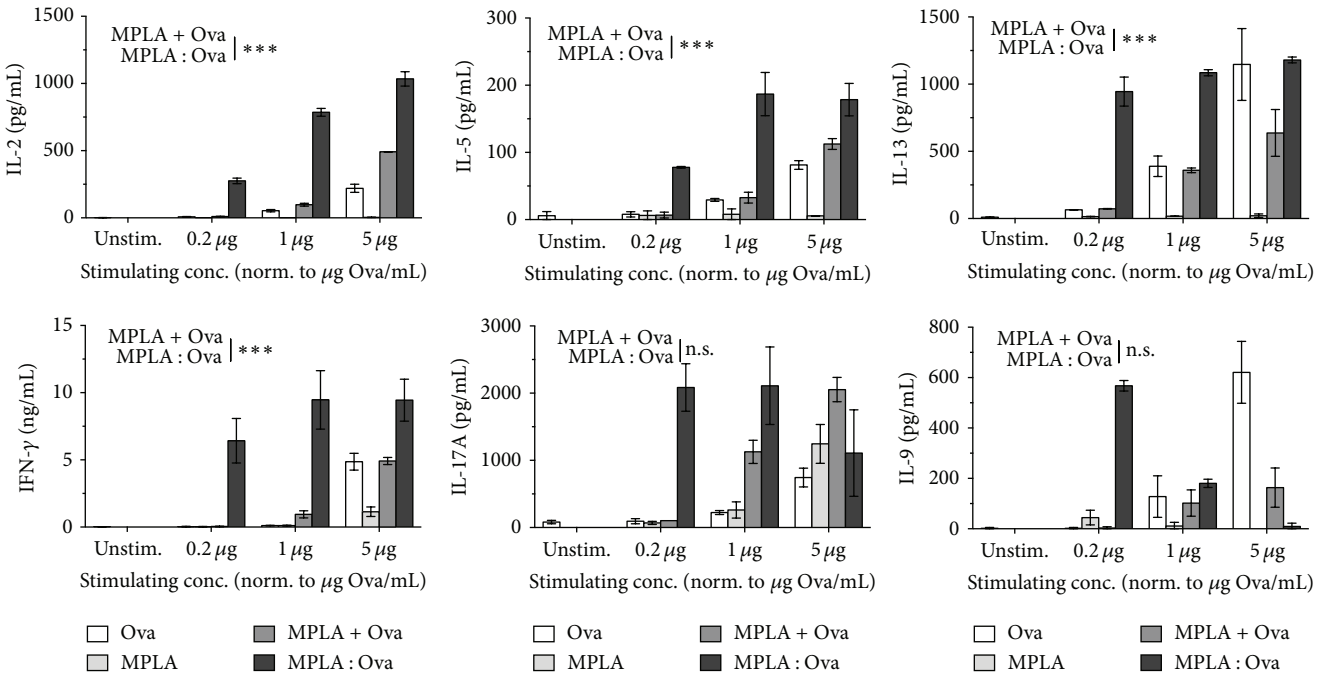

FIGURE 3: The MPLA : Ova fusion protein nonspecifically boosts Th1, Th2, and Th17 cytokine secretion from Ova-specific T cells. Cytokine secretion from BALB/c mDC (3.2×10^5 cells/mL) and DO11.10 $CD4^+$ T cell (8.0×10^5 cells/mL, >95% purity) cocultures stimulated with Ova (white bars), MPLA (light grey bars), MPLA + Ova (dark grey bars), or MPLA : Ova (black bars) for either 24 h (IL-2) or 72 h (all other cytokines). ELISAs were performed using either BD OptEIA ELISA (BD Biosciences) or Ready-SET-Go! ELISA Sets (eBiosciences). Data are mean results of two independent experiments ± SD. Statistical analysis was performed according to Figure 2.

IL-6: $p = 0.3447$, IL-10: $p = 0.2114$, TNF-α: $p = 0.0078$). In contrast, stimulation with MPLA : Ova resulted in a dose-dependent decrease of IL-12p70 secretion, which was not observed for either component alone or the mixture of MPLA and Ova (Figure 2(a) IL-12p70: MPLA : Ova versus MPLA + Ova $p = 0.0272$).

Compared to the results obtained when stimulating mDCs alone, the levels of MPLA : Ova-induced cytokine secretion observed upon stimulation of mDC : DO11.10 $CD4^+$ T cell cultures were either unchanged (TNF-α and IL-1β) or further increased (IL-6, IL-10, and IL-12p70, Figure 2(a) versus 2(b)). Therefore, when MPLA : Ova was added to mDC : DO11.10 $CD4^+$ T cell cultures, the fusion protein induced a significantly higher cytokine secretion than equimolar amounts of either component alone or the mixture of MPLA and Ova (Figure 2(b)). Here, in direct comparison to the mixture of both components, the MPLA : Ova fusion protein significantly boosted both proinflammatory (IL-1β: MPLA : Ova versus MPLA + Ova $p < 0.0001$, IL-6: $p = 0.0026$, IL-12: $p = 0.0001$, TNF-α: $p = 0.0015$) and anti-inflammatory (IL-10: $p = 0.0016$) cytokine secretion.

Moreover, for the concentration corresponding to 1 μg Ova per mL, MPLA : Ova induced 4-fold higher IL-1β, 4-fold higher IL-6, 6-fold higher TNF-α, 8-fold higher IL-10, and 53-fold higher IL-12p70 levels compared to the noncoupled mixture of MPLA + Ova (Figure 2(b)).

3.3. MPLA : Ova Boosts Th1, Th2, and Th17 Cytokine Secretion from Ova-Specific T Cells in a Nonbiased Way. In the next step we investigated the effect of MPLA : Ova-mediated mDC activation on the differentiation of Ova-specific $CD4^+$ T cells (Figure 3). In addition to the significantly increased mDC-derived cytokine secretion (Figure 2), induced by the fusion protein compared to the controls, we observed the same effect for enhanced T cell-derived cytokine secretion in the applied coculture system (Figure 3).

In accordance with the results shown in Figure 2, at a stimulating concentration corresponding to 1 μg Ova per mL, MPLA : Ova induced an 8-fold higher IL-2, 6-fold higher IL-5, 3-fold higher IL-13, 10-fold higher IFN-γ, 2-fold higher IL-17A, and 2-fold higher IL-9 secretion than the equimolar mixture of both components (Figure 3). Here, neither IL-2, IL-5, IL-13, IFN-γ, and IL-17A nor IL-9 secretion was detectable when mDCs were stimulated in the absence of Ova-specific $CD4^+$ T cells (data not shown). Remarkably, at low concentrations (equivalent to 0.2 μg/mL Ova) MPLA : Ova induced a 20-fold higher production of IL-17A in comparison to the equimolar mixture of MPLA and Ova, whereas at the highest applied concentration there was no difference between the different stimuli (Figure 3).

Of note, this effect was reversed for MPLA : Ova-induced IL-9 production, where stimulation with increasing amounts of MPLA : Ova resulted in a dose-dependent decrease in IL-9 secretion, while Ova alone dose-dependently induced IL-9 secretion (Figure 3, IL-9: MPLA : Ova versus MPLA + Ova $p = 0.1691$).

Finally, the MPLA : Ova fusion protein boosted Th1 (IFN-γ: MPLA : Ova versus MPLA + Ova $p < 0.0001$ and IL-2: $p < 0.0001$), Th2 (IL-5: $p = 0.0004$ and IL-13: $p < 0.0001$), and Th17 cytokine secretion (IL-17A, $p = 0.1920$ Figure 3) from

allergen-specific T cells without skewing the overall immune response in any particular direction.

4. Discussion

Herein we describe the generation and immunological characterization of a novel vaccine candidate consisting of the adjuvant MPLA and the model allergen Ovalbumin.

Adjuvant : allergen conjugates have several advantages over simple nonconjugated mixtures of both components: (1) they target the conjugate to the respective immune cells by binding to specific immune receptors (in this case TLR4 which may mediate both proinflammatory signaling and uptake). Upon binding to the target cell they (2) deliver the conjugated allergen to the immune cell in the context of the adjuvant-mediated immune cell activation which may influence allergen uptake, processing, and presentation [20]. Moreover, (3) adjuvant and allergen are simultaneously delivered to the same cell in a fixed molecular ratio, thereby preventing potentially detrimental bystander activation.

For this purpose, MPLA and Ovalbumin were coupled chemically via a stable carbamate linkage and the resulting fusion protein was characterized by SDS-PAGE and light scattering analysis. In SDS-PAGE, MPLA : Ova displayed a slight shift in molecular weight from approximately 45 kDa observed for Ova to approximately 47 kDa observed for MPLA : Ova. This moderate shift of approximately 2 kDa indicates a coupling rate of one molecule of MPLA (molecular mass: 1.7 kDa) per molecule of Ova.

Successful coupling of both molecules was further confirmed by light scattering analysis. With this assay we were able to demonstrate that the resulting MPLA : Ova fusion protein showed a single peak with a hydrodynamic radius of approximately 20 nm, which represents a 22-fold increase in size compared to nonconjugated Ova. Additionally, no molecules with the hydrodynamic radius of MPLA or Ova were detected within the MPLA : Ova preparation, demonstrating a complete removal of noncoupled MPLA by dialysis after coupling.

Previous studies investigating the effects of adjuvant : allergen fusion proteins, including TLR5-, TLR7-, and TLR9-ligands, on the modulation of allergen-specific immune responses demonstrated the potential for such conjugate vaccines to improve allergy treatment [13–16]. Studies by Kastenmüller et al. [15] and Filí et al. [16] describe allergen fusion proteins with TLR7- and TLR7/8-ligands as adjuvants.

Kastenmüller and colleagues reported a conjugate vaccine of a TLR7/8-ligand and Ova and showed this conjugate to elicit potent Th1-biased $CD4^+$ and $CD8^+$ T cell responses by activation and recruitment of dendritic cells to draining lymph nodes and the subsequent induction of type I interferon production [15]. In line with these results, Filí and coauthors described that the mite allergen nDer p 2 conjugated to a TLR7-ligand (4-(6-amino-9-benzyl-8-hydroxy-9H-purin-2-ylsulfanyl-)-butyric acid succinimidyl ester) stimulated IL-12 and IFN-γ production from monocytes and plasmacytoid DC and reduced allergic symptoms, while inducing allergen-specific IgG_{2A} antibodies in mice [16]. In this context, no induction of autoantibodies or Th17 cells was observed [16].

Moreover, Tighe and colleagues described the conjugation of a 22-mer CpG-motif, acting as a TLR9-ligand, to the major short ragweed allergen Amb a 1 [14]. In accordance with the results from the other adjuvant : allergen fusion proteins, this conjugate was shown to both induce Th1-biased immune responses in both naïve and sensitized mice and suppress IgE-induction after allergen-challenge [14].

In our own preliminary work we could show that prophylactic and therapeutic vaccination with a recombinant conjugate of the TLR5 agonist flagellin A (FlaA) from *Listeria monocytogenes* and Ova (rFlaA : Ova) was able to diminish Th2 responses in a mouse model of Ova-induced intestinal allergy [13]. Cocultures of mouse bone marrow-derived mDCs and $CD4^+$ DO11.10 T cells demonstrated an IL-10-dependent reduction of Th2 and Th1 cytokine production upon stimulation with rFlaA : Ova but not with rOva and FlaA provided as a mixture [21].

When stimulating mDC with MPLA : Ova and the respective controls we observed an increased secretion of both proinflammatory (IL-1β, IL-6, and TNF-α) and anti-inflammatory (IL-10) cytokines. Here, in direct comparison of mDC stimulations with mDC : $CD4^+$ TC coculture stimulations, overall levels of MPLA : Ova-induced cytokines were further increased in cocultures compared to the respective stimulation of mDCs alone. These results suggest that the mDC : TC interaction in the cocultures either further increased mDC-derived secretion (possibly by licensing effects of $CD4^+$ T cells via mechanisms such as CD40-CD40L interaction) or induced additional production of the respective cytokines from Ova-specific T cells.

Unexpectedly in mDC : DO11.10 $CD4^+$ T cell cocultures, when chemically fusing the TLR4 agonist MPLA to Ova, we observed a boost of Th2 cytokine (IL-5 and IL-13) production in such mDC : DO11.10 $CD4^+$ T cell cocultures compared to equimolar amounts of MPLA + Ova. In addition, we observed an upregulation of both Th1 and Th17 cytokines IFN-γ and IL-17A as well as mDC-derived proinflammatory (IL-1β, IL-6, and TNF-α) and anti-inflammatory (IL-10) cytokines. Such strong APC activation and TC-derived cytokine boosts without distinct bias towards a defined T cell subtype (e.g., Th1-cells) are likely detrimental and can have significant consequences for both vaccine development and safety.

In contrast to this pattern, we observed a dose-dependent decrease of IL-9 secretion upon stimulation with the MPLA : Ova fusion protein while Ova alone or the mixture of MPLA + Ova dose-dependently induced IL-9 secretion. IL-9 stimulates cell growth and prevents apoptosis [21]; therefore, we believe that the observed reduction of IL-9 secretion upon stimulation with higher doses of MPLA : Ova represents a countermeasure to limit excessive cell activation and its potentially detrimental effects by this fusion protein. In line with our results the available literature describes the suppression of TC-derived IL-9 secretion by differentially activated DC: Rampal and colleagues reported that retinoic acid-monocyte-derived dendritic cells in the presence of TGF-β1 and IL-4 inhibited IL-9 and induced IFN-γ expression [22]. Concordantly, IFN-γ secretion was shown

to inhibit Th9-differentiation [23]. Taking into account these results, the dose-dependent decrease of IL-9 secretion upon stimulation with the MPLA : Ova fusion protein may also be explained by the strong induction of other cytokines such as IFN-γ in higher stimulation concentrations. However, further investigations of this phenomenon and physiological relevance of MPLA : Ova-induced IL-9 secretion will need to be addressed in further *in vivo* studies.

In contrast to the strongly Th1-promoting TLR7 or TLR9 ligands, LPS was described to induce both Th1 and Th2 responses depending on either the applied dose [24] or the genetic background of the used organism [25]. The influence of genetic background on the capacity of LPS to induce either Th1 or Th2 responses was, for example, investigated by Soudi and colleagues [25]. They found that (in line with the well-described tendency of C57BL/6 and BALB/c to induce Th1 and Th2 responses, resp.) macrophages isolated from thioglycolate stimulated C57BL/6 mice produced more IL-17, IL-10, and IFN-γ, while BALB/c macrophages produced more TGF-β 1 and IL-4 when stimulated with LPS [25].

In our own previous work, when directly comparing LPS and MPLA for their capacity to skew Ova-induced T helper cell differentiation in BALB/c mDC : DO11.10 $CD4^+$ TC coculture experiments we have demonstrated that MPLA was able to boost Ova-induced Th2-cytokine (IL-4, IL-5, and IL-13) secretion [12]. Interestingly, this effect was not observed upon coapplication of LPS and Ova [12]. Here, further studies are necessary to more clearly define the adjuvant capacity of MPLA in comparison to its parent molecule LPS. Also, while MPLA was shown to induce an immune deviation in favor of Th1 responses in grass pollen allergic donors [26] the differences in MPLAs adjuvant capacity in men versus mice are not yet fully clear and need further investigation. In line with this, the question whether the results obtained for the MPLA : Ova fusion protein in this study can be transferred to human DC : TC cocultures needs to be addressed in further studies.

In summary, we successfully generated a novel fusion protein consisting of the vaccine adjuvant MPLA and the model allergen Ova by chemical linkage. The generated fusion protein displayed a suggested coupling ratio of one molecule MPLA per molecule of Ova and was shown to aggregate, possibly mediated by the formation of micelle-like structures by the fatty chains of MPLA. Immunologically we observed that, compared to both components alone or as a mixture, the fusion protein boosted both mDC-cytokines as well as TC-derived Th1, Th2, and Th17 cytokine secretion without skewing the induced TC-differentiation in any particular direction.

Although the generated MPLA : Ova fusion protein may not be a suitable vaccine candidate for allergy treatment, due to the nonbiased boost of allergen-specific Th1, Th2, and Th17 responses, these findings open many new avenues for future research in the field of adjuvant biology, allergy, and immunology. Here, MPLA : antigen fusion proteins might hold potential for the treatment of other diseases which require a strong stimulation of the hosts immune system (e.g., cancer).

5. Conclusions

(i) A fusion protein of the TLR4-ligand MPLA and Ovalbumin (MPLA : Ova) was generated in a highly pure form with a coupling ratio of one molecule MPLA per molecule of Ova and without contaminations by either noncoupled MPLA or Ova.

(ii) Immunologically, in mDC : DO11.10 $CD4^+$ TC cocultures MPLA : Ova induced both stronger innate (mDC) and adaptive (Ova-specific TC) immune responses compared to the mixture of both components, boosting Th1, Th2, and Th17 TC-derived cytokine secretion.

Disclosure

Adam Flaczy current address is School of Medicine and Medical Science, University College Dublin, Belfield, Dublin, Ireland.

Competing Interests

In the past 3 years Stefan Vieths has received speakers honoraria by the Swiss Society of Allergy and Clinical Immunology, the German Society of Dermatology, and by the "Ärzteverband Deutscher Allergologen," which may be perceived as potential conflict of interests. All other authors have no conflict of interests to declare.

Acknowledgments

The authors would like to thank Maren Krause, Paul-Ehrlich-Institut, for breeding of DO11.10 mice. This work was funded in part by the German Research Foundation (SCHE637/3).

References

[1] J. L. Justicia, V. Cardona, P. Guardia et al., "Validation of the first treatment-specific questionnaire for the assessment of patient satisfaction with allergen-specific immunotherapy in allergic patients: the ESPIA questionnaire," *Journal of Allergy and Clinical Immunology*, vol. 131, no. 6, pp. 1539–1546.e2, 2013.

[2] R. Valenta, "The future of antigen-specific immunotherapy of allergy," *Nature Reviews Immunology*, vol. 2, pp. 446–453, 2002.

[3] D. Toussi and P. Massari, "Immune adjuvant effect of molecularly-defined toll-like receptor ligands," *Vaccines*, vol. 2, no. 2, pp. 323–353, 2014.

[4] J. T. Ulrich and K. R. Myers, "Monophosphoryl lipid A as an adjuvant. Past experiences and new directions," *Pharmaceutical Biotechnology*, vol. 6, pp. 495–524, 1995.

[5] M. Kundi, "New hepatitis B vaccine formulated with an improved adjuvant system," *Expert Review of Vaccines*, vol. 6, no. 2, pp. 133–140, 2007.

[6] S. T. Agnandji, B. Lell, S. S. Soulanoudjingar et al., "First results of phase 3 trial of RTS,S/AS01 malaria vaccine in African children," *The New England Journal of Medicine*, vol. 365, pp. 1863–1875, 2011.

[7] B. Romanowski, P. C. de Borba, P. S. Naud et al., "Sustained efficacy and immunogenicity of the human papillomavirus (HPV)-16/18 AS04-adjuvanted vaccine: analysis of a randomised placebo-controlled trial up to 6.4 years," *The Lancet*, vol. 374, no. 9706, pp. 1975–1985, 2009.

[8] P. Patel and A. M. F. Salapatek, "Pollinex® quattro: a novel and well-tolerated, ultra short-course allergy vaccine," *Expert Review of Vaccines*, vol. 5, no. 5, pp. 617–629, 2006.

[9] C. R. Casella and T. C. Mitchell, "Putting endotoxin to work for us: monophosphoryl lipid a as a safe and effective vaccine adjuvant," *Cellular and Molecular Life Sciences*, vol. 65, no. 20, pp. 3231–3240, 2008.

[10] N. Mothes, M. Heinzkill, K. J. Drachenberg et al., "Allergen-specific immunotherapy with a monophosphoryl lipid A-adjuvanted vaccine: Reduced seasonally boosted immunoglobulin E production and inhibition of basophil histamine release by therapy-induced blocking antibodies," *Clinical and Experimental Allergy*, vol. 33, no. 9, pp. 1198–1208, 2003.

[11] P. Baldrick, D. Richardson, G. Elliott, and A. W. Wheeler, "Safety evaluation of monophosphoryl lipid A (MPL): an immunostimulatory adjuvant," *Regulatory Toxicology and Pharmacology*, vol. 35, no. 3, pp. 398–413, 2002.

[12] S. Schülke, A. Flaczyk, L. Vogel et al., "MPLA shows attenuated pro-inflammatory properties and diminished capacity to activate mast cells in comparison with LPS," *Allergy: European Journal of Allergy and Clinical Immunology*, vol. 70, no. 10, pp. 1259–1268, 2015.

[13] S. Schülke, M. Burggraf, Z. Waibler et al., "A fusion protein of flagellin and ovalbumin suppresses the TH2 response and prevents murine intestinal allergy," *Journal of Allergy and Clinical Immunology*, vol. 128, no. 6, pp. 1340.e12–1348.e12, 2011.

[14] H. Tighe, K. Takabayashi, D. Schwartz et al., "Conjugation of immunostimulatory DNA to the short ragweed allergen Amb a 1 enhances its immunogenicity and reduces its allergenicity," *Journal of Allergy and Clinical Immunology*, vol. 106, no. 1 I, pp. 124–134, 2000.

[15] K. Kastenmüller, U. Wille-Reece, R. W. B. Lindsay et al., "Protective T cell immunity in mice following protein-TLR7/8 agonist-conjugate immunization requires aggregation, type I IFN, and multiple DC subsets," *The Journal of Clinical Investigation*, vol. 121, no. 5, pp. 1782–1796, 2011.

[16] L. Filí, A. Vultaggio, E. Cardilicchia et al., "A novel allergen-adjuvant conjugate suitable for specific immunotherapy of respiratory allergy," *Journal of Allergy and Clinical Immunology*, vol. 132, no. 1, pp. 84–92, 2013.

[17] U. K. Laemmli, "Cleavage of structural proteins during the assembly of the head of bacteriophage T4," *Nature*, vol. 227, no. 5259, pp. 680–685, 1970.

[18] S. Schülke, Z. Waibler, M.-S. Mende et al., "Fusion protein of TLR5-ligand and allergen potentiates activation and IL-10 secretion in murine myeloid DC," *Molecular Immunology*, vol. 48, no. 1–3, pp. 341–350, 2010.

[19] P. N. Domadia, A. Bhunia, A. Ramamoorthy, and S. Bhattacharjya, "Structure, interactions, and antibacterial activities of MSI-594 derived mutant peptide MSI-594F5A in lipopolysaccharide micelles: role of the helical hairpin conformation in outer-membrane permeabilization," *Journal of the American Chemical Society*, vol. 132, no. 51, pp. 18417–18428, 2010.

[20] S. Khan, M. S. Bijker, J. J. Weterings et al., "Distinct uptake mechanisms but similar intracellular processing of two different toll-like receptor ligand-peptide conjugates in dendritic cells," *The Journal of Biological Chemistry*, vol. 282, no. 29, pp. 21145–21159, 2007.

[21] L. Knoops and J.-C. Renauld, "IL-9 and its receptor: from signal transduction to tumorigenesis," *Growth Factors*, vol. 22, no. 4, pp. 207–215, 2004.

[22] R. Rampal, A. Awasthi, and V. Ahuja, "Retinoic acid-primed human dendritic cells inhibit Th9 cells and induce Th1/Th17 cell differentiation," *Journal of Leukocyte Biology*, 2016.

[23] G. Murugaiyan, V. Beynon, A. P. Da Cunha, N. Joller, and H. L. Weiner, "IFN-γ limits Th9-mediated autoimmune inflammation through dendritic cell modulation of IL-27," *The Journal of Immunology*, vol. 189, no. 11, pp. 5277–5283, 2012.

[24] J. D. de Boer, J. J. T. H. Roelofs, A. F. de Vos et al., "Lipopolysaccharide inhibits Th2 lung inflammation induced by house dust mite allergens in mice," *American Journal of Respiratory Cell and Molecular Biology*, vol. 48, no. 3, pp. 382–389, 2013.

[25] S. Soudi, A. Zavaran-Hosseini, Z. M. Hassan, M. Soleimani, F. J. Adegani, and S. M. Hashemi, "Comparative study of the effect of LPS on the function of BALB/c and C57BL/6 peritoneal macrophages," *Cell Journal*, vol. 15, no. 1, pp. 45–54, 2013.

[26] F. Puggioni, S. R. Durham, and J. N. Francis, "Monophosphoryl lipid A (MPL®)* promotes allergen-induced immune deviation in favour of Th1 responses," *Allergy: European Journal of Allergy and Clinical Immunology*, vol. 60, no. 5, pp. 678–684, 2005.